From kinetic theory to hydrodynamisation: The onset of fluid behaviour in relativistic heavy ion collisions

By

Reghukrishnan Gangadharan

Enrolment No: PHYS11202104016

**National Institute of Science Education and Research,
Bhubaneswar**

A thesis submitted to the

Board of Studies in Physical Sciences

(as applicable)

In partial fulfillment of requirements

for the Degree of

DOCTOR OF PHILOSOPHY

of

HOMI BHABHA NATIONAL INSTITUTE

November, 2025

Homi Bhabha National Institute

Recommendations of the Viva Voce Committee

As members of the Viva Voce Committee, we certify that we have read the dissertation prepared by Reghukrishnan Gangadharan entitled "*From kinetic theory to hydrodynamisation: The onset of fluid behaviour in relativistic heavy ion collisions* " and recommend that it may be accepted as fulfilling the thesis requirement for the award of Degree of Doctor of Philosophy.

Chairman - Bedangadas Mohanthy	4/5/2026
Guide / Convener - Victor Roy	04/05/2026
External Examiner - Chitrasen Jena	4/5/2026
Member 1 - Amresh Jaiswal	4/5/2026
Member 2 - Najmul Haque	04.05.2026
External Member - Santosh Kumar Das	4/5/26

Final approval and acceptance of this thesis is contingent upon the candidate's submission of the final copies of the thesis to HBNI.
I/We hereby certify that I/we have read this thesis prepared under my/our direction and recommend that it may be accepted as fulfilling the thesis requirement.

Date : 04/05/2026

Place : NISER, Bhubaneswar.

Signature
Co-guide (if any)

Signature
Guide

PhD Viva-Voce Examination

(Attendance Sheet)

1.	**Name of the Student**	**: Reghukrishnan Gangadharan**
2.	**Name of the CI/OCC**	**: NISER, Bhubaneshwar**
3.	**Discipline**	**: Physical Sciences**
4.	**Enrolment Number**	**: PHYS11202104016**
5.	**Date and time of viva-voce**	**: 04-05-2026**
6.	**Venue**	**: SPS Seminar Hall, NISER**

S. No.	Name	Affiliation	Signature or indicate	In-Person/ Online
1	Chairman: Bedangadas Mohanty	NISER	Bedangadas	In person
2	Guide: Victor Roy	NISER	Victor Roy	In person
3	Co-guide: Name			
4	External examiner: Chitrasen Jena	IISER Tirupati	Gene	In-person
5	Member-I: Amresh Jaiswal	NISER	Amresh	In-person
6	Member-II: Najmul Haque	NISER	Haque	In-person
7	Member-III: Santosh Kumar Das			
8				
9	Krishanu Sengupta	NISER	Krish	In-person
10	Tanmay Mondal	NISER	Tanmay Mondal	In-person
11	Srijan Volety	NISER	Srijan	In-person
12	Soham Banerjee	NISER	Soham Banerjee	In-person.
13	Syed Jaffri	NISER	Syed Jaffri	In-person
14	Ayan R	NISER		In-person
15	Pratyush P Patra	NISER	Pratyush	In-person
16	Milan Ghorai	NISER	Milan Ghorai	In. person.
17	Neharika Varma	NISER	Neharika	In person
18	Ravi Pandey	NISER	Ravi Pandey	In person
19				
20				
21				
22				

23				
24				
25				
26				
27				
28				
29				
30				

(Signature of Guide)

Note: Number is only indicative; more sheets can be added if required.

STATEMENT BY AUTHOR

This dissertation has been submitted in partial fulfillment of requirements for an advanced degree at Homi Bhabha National Institute (HBNI) and is deposited in the Library to be made available to borrowers under rules of the HBNI.

Brief quotations from this dissertation are allowable without special permission, provided that accurate acknowledgement of source is made. Requests for permission for extended quotation from or reproduction of this manuscript in whole or in part may be granted by the Competent Authority of HBNI when in his or her judgment the proposed use of the material is in the interests of scholarship. In all other instances, however, permission must be obtained from the author.

Reghukrishnan Gangadharan

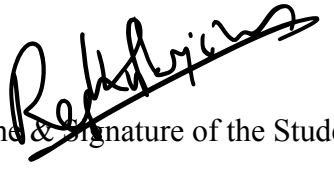

Name & Signature of the Student

DECLARATION

I hereby declare that I am the sole author of this thesis in partial fulfillment of the requirements for a postgraduate degree from National Institute of Science Education and Research (NISER). I authorize NISER to lend this thesis to other institutions or individuals for the purpose of scholarly research.

Reghukrishnan Gangadharan

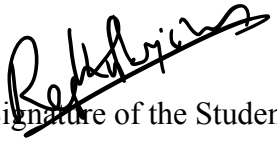

Name & Signature of the Student

List of Publications arising from the thesis

Journal Publications related to the thesis

1. **Study of early time attractor with longitudinal forces with Bjorken symmetry**
   R. Gangadharan (NISER, Jatni), A. K. Panda (NISER, Jatni), V. Roy (NISER, Jatni)
   Physical Review D **109** (2024) 7, 074020
   Published: November 17, 2023
   DOI: 10.1103/PhysRevD.109.074020

2. **Convergence problem of gradient expansion in the relaxation-time approximation**
   R. Gangadharan (NISER, Jatni), V. Roy (NISER, Jatni)
   Physical Review D **111** (2025) 7, L071901
   Published: May 17, 2024

3. **On the Approach Towards Equilibrium Through Momentum-Dependent Relaxation: Insights from Evolution of the Moments in Kinetic Theory**
   R. Gangadharan (NISER, Jatni), S. Mitra (NISER, Jatni), V. Roy (NISER, Jatni)
   Physical Review D **112** (2025) 9, 096019
   Published: June 14, 2025

4. **Validity of relativistic hydrodynamics beyond local equilibrium**
   R. Gangadharan (NISER, Jatni) [Accepted in Physical Review D]
   arXiv:2508.17543 [nucl-th]

Journal Publications not related to the thesis

5. **Investigating the role of electric fields on flow harmonics in heavy-ion collisions**
   A. K. Panda (NISER, Jatni), **R. Gangadharan** (NISER, Jatni), V. Roy (NISER, Jatni)
   Journal of Physics G: Nuclear and Particle Physics, **50** (2023) 7, 075102

Published: January 2, 2023

Conference / Symposium Presentations

- **ATHIC** (13–16 January 2025)
  Title: *On the convergence of the gradient expansion of the Boltzmann equation*

Posters

- **DAE Conclave** (22–26 October 2024)
  Title: *On The Convergence of RTA Gradient Expansion*
- **ATHIC** (13–16 January 2025)
  Title: *On The Convergence of RTA Gradient Expansion*

Conference Proceedings

1. **Convergence of the gradient expansion of Boltzmann equation in the relaxation time approximation**
   R. Gangadharan (NISER, Jatni), V. Roy (NISER, Jatni)
   Journal of Subatomic Particles and Cosmology, Volume 4, December 2025

Reghukrishnan Gangadharan
Name & Signature of the Student

To my grandmother.

ACKNOWLEDGEMENTS

I would like to take this opportunity to express my deepest gratitude to everyone who has supported and guided me throughout my doctoral journey. First and foremost, I offer my sincere thanks to my supervisor, **Dr. Victor Roy**. I am grateful for his patience and kindness throughout my PhD, and for his consistent encouragement. His guidance strikes a remarkable balance between pragmatic decision-making and uncompromising academic rigour, which greatly strengthened my research. His thoughtful guidance and well-timed support were invaluable in keeping my work on track and ensuring the timely completion of this thesis.

I also extend my sincere appreciation to the members of my thesis committee—**Prof. Bedangadas Mohanty, Dr. Amaresh Jaiswal, Dr. Najmul Haque, and Dr. Santosh Kumar Das**—for their constructive feedback, thoughtful suggestions, and constant encouragement. My sincere thanks go to **NISER** and **DAE** for providing the academic environment, financial support, and research facilities that made this work possible.

I am deeply thankful to my colleagues, collaborators, and fellow researchers at NISER. Their camaraderie, wide-ranging discussions—both academic and otherwise—and steady encouragement have made this journey both fulfilling and enjoyable. I am especially grateful to **Ankit Kumar Panda**, whose insight and friendship enriched my academic life well beyond the scope of this thesis; as my senior, his guidance was invaluable when I began my research. I also wish to thank **Dr. Sukanya Mitra** for our collaboration and for co-authoring a paper that forms an integral part of this thesis. My thanks further go to **Kishanu Sengupta**, whose infectious passion for physics made our many wide-ranging discussions particularly enjoyable, even though we met only later in my PhD journey.

Above all, I owe my deepest gratitude to my family—my amma **Jalajakumari B**, my achan **K. Reghu**, **Chinchi** , **Nidi** annan, **Sruthi** akka, **Swarnnamachi**, and **Vakkelachan** —for their unconditional love, encouragement, and understanding. I wish to offer special thanks to **Ponny Hadid** for her constant guidance, thoughtful criticism, and unfailing support. I am grateful as well to my friends and batchmates—**Mahesh Gandikota**, **Amudhan K. U.**, **Palash Dubey**, **Jobin Sebastian**, **Kirubi**, **Srijan Volety**, and **Neharika Varma**—for their support, companionship, and for making this journey memorable.

Although it is impossible to acknowledge everyone who has contributed to this journey individually, I am sincerely thankful to each person who has supported, encouraged, or inspired me along the way. This achievement is as much theirs as it is mine.

ABSTRACT

This thesis examines the microscopic foundations of relativistic hydrodynamics in far-from-equilibrium systems, focusing on the quark–gluon plasma created in ultrarelativistic heavy-ion collisions. Experiments show that the quark–gluon plasma exhibits strong collective flow and behaves as an almost perfect fluid despite large initial anisotropies and rapid expansion, raising the question of why hydrodynamics applies when local equilibrium is not yet established.

Using the relativistic Boltzmann equation in the relaxation-time approximation, the thesis develops exact solutions for boost-invariant systems, analyses hydrodynamic attractors, and identifies the role of non-hydrodynamic modes in driving universal behaviour. A complete gradient expansion is constructed, its asymptotic character is demonstrated, and an operator-based decomposition is introduced to separate hydrodynamic and transient sectors. This leads to time-dependent, renormalised transport coefficients that encode far-from-equilibrium dynamics.

A central insight is the distinction between the Chapman–Enskog gradient expansion and fully relativistic causal hydrodynamics. The gradient expansion captures only long-wavelength perturbative contributions and is intrinsically acausal, whereas causal theories such as Israel–Stewart hydrodynamics promote dissipative quantities to independent dynamical fields with finite relaxation times. This promotion incorporates the fast transient modes already present in the Boltzmann equation, producing a consistent, stable, and causal macroscopic evolution. Hydrodynamics, therefore, emerges as a resummed effective theory that includes both long-lived collective behaviour and transient microscopic dynamics

Contents

Summary

Ultrarelativistic heavy-ion collisions create short-lived systems of deconfined quarks and gluons known as the quark–gluon plasma (QGP). Experimental signatures—including strong collective flow, elliptic anisotropy, and mass-ordered hadron spectra—show that the QGP behaves as a nearly perfect fluid despite being initially far from equilibrium. Hydrodynamic modelling reproduces these observables with remarkable accuracy, but doing so requires initialization at very early times, when the system exhibits strong momentum anisotropies and large gradients. This raises the central theoretical question addressed in this thesis: why does hydrodynamics remain valid when the QGP is far from local equilibrium?

To investigate this, the thesis employs relativistic kinetic theory based on the Boltzmann equation. Starting from the Bogoliubov–Born–Green–Kirkwood–Yvon (BBGKY) hierarchy, the Boltzmann equation provides a microscopic evolution equation for the single-particle distribution function $f(x^\mu, p^\mu)$. In practical applications the full collision integral is often replaced by the Anderson–Witting relaxation-time approximation (AW-RTA),

$$C[f, f] \approx -\frac{f - f_{\text{eq}}}{\tau_R},$$

where $f_{\text{eq}}(T, \mu)$ is the local equilibrium distribution and τ_R is the characteristic relaxation time. Hydrodynamic quantities follow from moments of f, establishing a direct connection between microscopic dynamics and macroscopic evolution.

The thesis adopts both numerical and analytical approaches. Numerical solutions of the AW-RTA Boltzmann equation—first in highly symmetric $(0+1)$D systems and then with symmetry-breaking perturbations—are used to study thermalisation and hydrodynamic attractor behaviour. Introducing external forces or finite particle masses significantly modifies early-time attractors, leaving only late-time universal behaviour. Extending the analysis to momentum-dependent relaxation times reveals that realistic momentum scaling introduces an additional physical scale, couples different energy moments, and delays thermalisation. A momentum-dependent ansatz,

$$\tau_R = \tau_R^0 \, p^\Lambda, \qquad \Lambda \in [0, 1),$$

leads to multiple relaxation times and enhanced anisotropy at intermediate stages. To preserve conservation laws in such cases, the thesis employs the Novel relaxation time approximation (NRTA) kernel, which maintains the Landau matching conditions for arbitrary $\tau_R(p)$.

Building on these numerical observations, the thesis undertakes an analytical study of the hydrodynamic gradient expansion. The Chapman–Enskog expansion expresses the distribution function as a gradient series controlled by the Knudsen number Kn. However, this gradient series is asymptotic and ultimately divergent. By analysing a representative singular-perturbation model,

$$\delta \frac{df}{dt} = -\big(f(t) - g(t)\big),$$

and its exact solution,

$$f(t) = e^{-t/\delta} f(0) + \int_0^t \frac{dt'}{\delta}\, e^{-(t-t')/\delta}\, g(t'),$$

the thesis illustrates how perturbative gradient terms and non-perturbative transient (exponential) contributions coexist. This structure also appears in the exact integral solution of the AW-RTA Boltzmann equation.

Using the exact AW-RTA solution, the gradient expansion of f is constructed explicitly. The resulting series is shown to be asymptotic but resummable, containing both traditional hydrodynamic gradient terms and exponentially decaying transient contributions. These transient contributions can be absorbed into renormalised, time-dependent transport coefficients, which extend the validity of hydrodynamics far into the non-equilibrium regime. For the $(0+1)$D system, exact moment equations demonstrate that incorporating these renormalised coefficients yields a convergent hydrodynamic description that correctly reduces to free-streaming in the appropriate limit.

A key conclusion of this work is the distinction between the Chapman–Enskog gradient expansion and modern relativistic hydrodynamics. The gradient expansion captures only slow, long-wavelength perturbations and is intrinsically acausal in relativistic systems. Causal formulations such as Israel–Stewart theory address this by promoting dissipative quantities to independent dynamical fields with finite relaxation times, which incorporate the fast transient modes naturally present in the Boltzmann equation. These “non-

hydrodynamic" modes are therefore not external to hydrodynamics but essential to any consistent relativistic fluid theory.

Overall, the thesis shows that relativistic hydrodynamics is an emergent, analytic limit of microscopic Boltzmann dynamics, in which both long-lived collective modes and fast transient modes must be included. Hydrodynamics succeeds so widely because its structure closely mirrors that of exact kinetic-theory evolution, even far from equilibrium. While the relaxation-time approximation has limitations, the central conclusions regarding hydrodynamisation and the emergence of effective transport coefficients remain robust.

List of Figures

List of Tables

Chapter 1

Introduction

The behaviour of the universe is governed by the interplay of four fundamental forces: gravity, electromagnetism (EM), the strong interaction, and the weak interaction. Gravity and electromagnetism dominates phenomena ranging from atomic processes (10^{-10}m) to planetary motion (10^{7}m), while at the nuclear scale (10^{-15}m) the strong and weak interactions emerge as dominant players. Among these, the strong interaction plays a crucial role in binding quarks and gluons into protons, neutrons, and ultimately atomic nuclei, thereby determining the structure and stability of matter at its most fundamental level. The theoretical framework describing this force is Quantum Chromodynamics (QCD), which encapsulates the dynamics of quarks and gluons, which carry colour charge. A detailed understanding of QCD is essential for explaining phenomena such as hadron masses, nuclear binding energies, and the emergence of collective behaviour in strongly interacting systems. However, due to the non-perturbative nature of QCD at low energies, many of its predictions are challenging to test directly.

Relativistic heavy-ion-collisions provide a unique experimental avenue to probe QCD at high temperature and density. In relativistic heavy-ion collisions, heavy nuclei such as gold (Au) and lead (Pb) are collided at extremely high energies, up to $\sqrt{s_{NN}} = 5.36$ TeV [1] at the Relativistic Heavy Ion Collider (RHIC) and the Large Hadron Collider (LHC). Under such extreme conditions, quarks and gluons, normally confined within hadrons, can become liberated in a state known as the quark-gluon plasma (QGP) [2, 3, 4, 5]. These collisions thus allow the study of deconfinement, phase transitions, and the emergent collective properties of strongly interacting matter, offering invaluable insights into understanding QCD

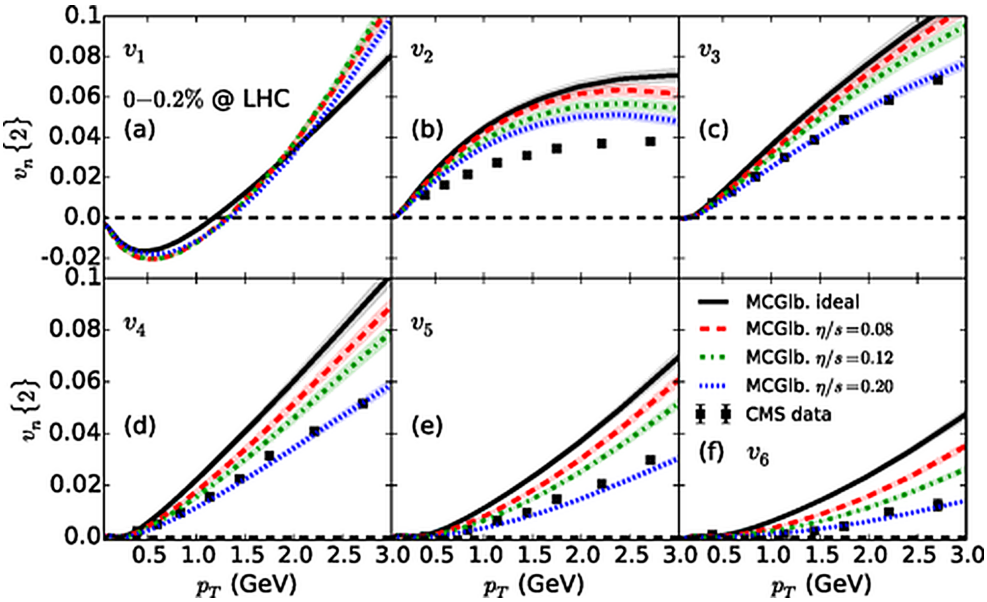

Figure 1.1: Comparison of p_T dependence of $v_n\{2\}$(two-particle cumulant $n \in [1-6]$) of charged hadrons $Pb-Pb$ collisions at $\sqrt{s_{\rm NN}} = 2.76$ TeV with CMS data [25]. Figure taken from [26]

matter. The QGP is initially highly anisotropic and far from local equilibrium, but as the system expands and cools, it gradually approaches a near-equilibrium state. Experimental observations at RHIC and the LHC have revealed that the QGP behaves as an almost perfect fluid [6, 7, 8, 9, 10, 11, 12] with an extremely small shear-viscosity-to-entropy ratio ($\eta/s \sim 1/4\pi$) [13, 14, 15, 16], indicating strongly collective behaviour.

Although the early, far-from-equilibrium dynamics of the QGP remain incompletely understood, relativistic viscous hydrodynamics has proven remarkably effective in describing its subsequent near-equilibrium evolution. In particular, hydrodynamic simulations quantitatively reproduce the anisotropic flow coefficients, including elliptic flow (v_2) and higher harmonics [17, 18, 19], across a broad range of beam energies and collision systems [20, 21, 22, 23, 24]. Figure 1.1 presents the two-particle cumulant $v_n\{2\}(p_T)$ for $n \in [1-6]$ as a function of the transverse momentum p_T, together with model predictions that provide a good description of the data. The framework also accounts for the transverse-momentum

spectra of identified hadrons, naturally capturing the characteristic mass ordering driven by radial flow [27]. Furthermore, hydrodynamics successfully describes the centrality and pseudorapidity dependence of particle yields, as well as event-by-event fluctuations that generate higher-order flow components. Notably, signatures of collective behaviour persist even in small systems such as p–Pb and high-multiplicity p–p collisions, where the system size and lifetime are significantly reduced [28, 29, 30, 31, 32].

1.1 The hydrodynamisation problem

The robustness of hydrodynamic predictions in these environments challenges traditional assumptions linking fluid-like behaviour to near-local-equilibrium conditions and short relaxation time. Collectively, these observations motivate a deeper theoretical understanding of why hydrodynamics remains applicable in regimes featuring large gradients. Traditional hydrodynamic descriptions assume local thermal equilibrium and rely on a clear separation of time scales: microscopic interactions rapidly drive the system toward equilibrium, while macroscopic gradients evolve on much longer scales. In the relativistic context, this separation becomes subtle, as expanding systems (such as those created in heavy-ion collisions) undergo rapid expansion and position-space and momentum-space anisotropies in the early stages. Traditional viscous hydrodynamics (e.g., second-order theories) extend the ideal framework but still implicitly hinge on near-equilibrium assumptions. Theoretical studies, however, indicate that at such early times the system exhibits large anisotropies and deviations from equilibrium, challenging the conventional assumption that hydrodynamics is applicable only close to local thermal equilibrium.

To reproduce experimental data, hydrodynamic simulations typically assume a hydrodynamisation time of $\tau_{\text{hydro}} \sim 0.1$–$1$ fm at LHC energies [33, 34, 35, 36]. This implies that fluid-dynamical behaviour sets in at extremely early stages, well before local thermal

equilibrium is established. One possible remedy is to employ higher-order or anisotropic hydrodynamic formulations, but these expansions are known to be divergent and asymptotic, limiting their validity to small deviations from equilibrium. Consequently, despite the empirical success of hydrodynamic modeling, fundamental questions remain as to why and under what conditions a hydrodynamic description accurately captures the evolution of a system that is far from equilibrium.

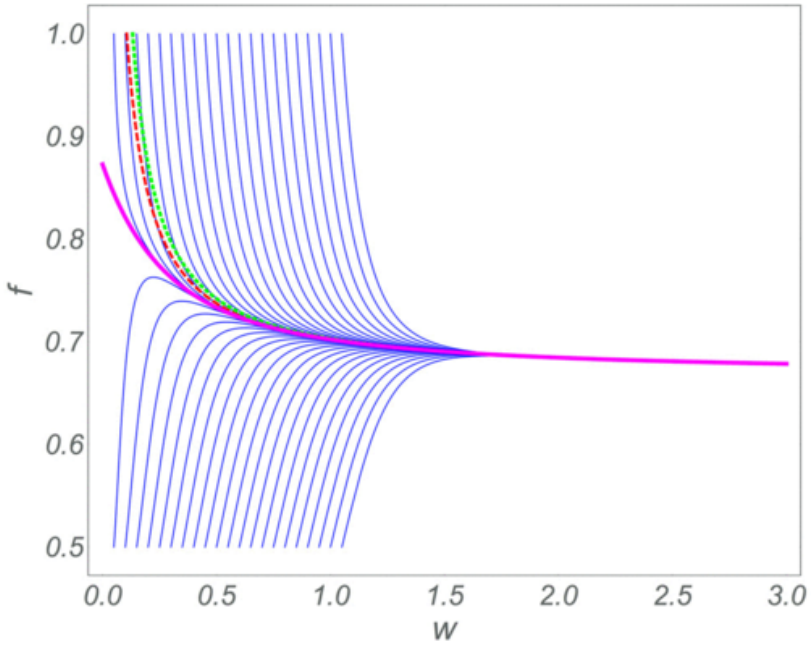

Figure 1.2: $w = \tau\varepsilon^{1/4}$ is a dimensionless scaled time and $f(w) = \tau\partial_\tau \log w$ is a measure of the anisotropy in the system. Hydrodynamic attractor for $0 + 1$D Bjorken flow shown in magenta. The blue shows $f(w)$ in Muller–Israel–Stewart hydrodynamics for various initial conditions. The red and green dashed lines are first and second-order hydrodynamics solutions, respectively. Figure taken from [37]

Two complementary explanations have emerged to understand the unexpected success of relativistic hydrodynamics: the existence of *hydrodynamic attractors* [38, 39, 37, 40, 41, 42, 43, 44] and the renormalisation (or resummation) of hydrodynamic transport coefficients [45, 46]. Hydrodynamic attractors correspond to special solutions of the underlying evolution equations toward which a broad class of initial conditions rapidly converge. As

a result, macroscopic observables exhibit universal behaviour largely insensitive to microscopic details. In conformal systems undergoing Bjorken expansion, for example, quantities such as the pressure anisotropy approach a universal attractor curve (Fig. 1.2) well before isotropisation, suggesting that hydrodynamisation can occur long before isotropization.

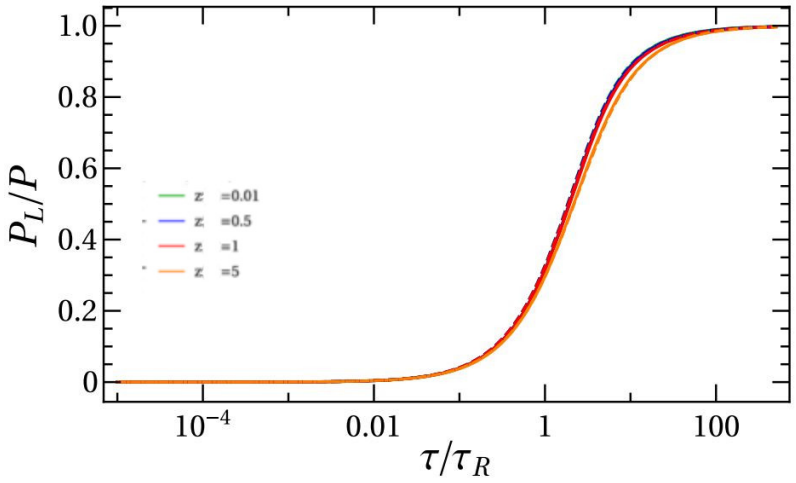

Figure 1.3: The evolution of P_L/P as a function of scaled time for various initial $z = m/T$. Solid lines represent exact kinetic theory solutions, dashed lines for the three-moment truncation of the moment equations with renormalised transport coefficients. The solutions almost overlap. Figure taken from [47]

A complementary perspective, developed by Blaizot, Yan, and collaborators [45, 46, 48, 49, 47], interprets this behaviour through the renormalisation of transport coefficients. In this framework, the success of the gradient expansion is attributed to the influence of non-hydrodynamic modes, whose transient effects can be resummed into *effective*, time-dependent transport coefficients that reproduce non-equilibrium evolution Fig. 1.3. These rescaled coefficients evolve toward their equilibrium values and encode non-equilibrium corrections to the constitutive relations. Together, these viewpoints indicate that the robustness of hydrodynamics in such regimes is rooted in transient microscopic dynamics and the effective dressing of transport data by short-lived non-hydrodynamic modes.

1.2 Objectives and methodology

Building upon these insights, the present thesis seeks to deepen the theoretical understanding of how hydrodynamics emerges and remains valid in far-from-equilibrium regimes. While previous studies have revealed the existence of hydrodynamic attractors and suggested that the apparent applicability of hydrodynamics may arise from the effective resummation of transient microscopic effects, a comprehensive, analytical framework connecting these phenomena to the underlying kinetic theory remains incomplete. In this work, we extend these foundational ideas by examining the microscopic emergence of hydrodynamic behaviour, the structure and divergence of the gradient expansion, and the emergence of time-dependent, renormalised transport coefficients in relativistic systems undergoing expansion.

The primary aim of this thesis is to establish a systematic and analytical account of how relativistic hydrodynamics arises from kinetic theory, and to delineate the boundaries of its applicability beyond near-equilibrium assumptions. The first part of the study focuses on understanding hydrodynamisation and attractor behaviour in both conformal and non-conformal systems, analysing how macroscopic quantities such as pressure anisotropy approach universal attractor curves across different dynamical settings, specifically in the presence of external forces. The subsequent part investigates the role of perturbations due to momentum-dependent relaxation times in shaping hydrodynamisation dynamics. By introducing departures from the simple kinetic relaxation time models, we assess how such factors influence the approach to equilibrium.

A central component of this work involves developing a complete gradient expansion and its trans-series representation for the relativistic Boltzmann equation within the relaxation-time approximation. This analytical construction enables a clear identification of the divergent structure of the gradient series and its decomposition into hydrodynamic

(slow) and non-hydrodynamic (transient) sectors. Through asymptotic and operator-based analysis, we demonstrate how these transient contributions yield effective, time-dependent transport coefficients that smoothly interpolate between far-from-equilibrium and near-equilibrium regimes.

Finally, the operator-based kinetic formulation introduced in this thesis is extended from simplified $(0+1)$D models to more general $(3+1)$D frameworks. This generalisation allows for a systematic exploration of gradient resummation and hydrodynamisation in realistic systems. On this basis, we derive a quantitative criterion that delineates the validity regime of hydrodynamic descriptions, thereby providing a unified theoretical understanding of how macroscopic fluid dynamics can faithfully describe the evolution of systems far from equilibrium.

Collectively, these investigations aim to bridge the conceptual gap between microscopic kinetic theory and macroscopic fluid dynamics, clarifying the dynamical processes that enable the apparent universality and resilience of hydrodynamic behaviour in rapidly evolving relativistic systems.

Throughout this thesis, we work in natural units, setting $c = \hbar = k_{\mathrm{B}} = 1$. In this convention, space and time share the same units, and energy, momentum, temperature, and inverse length are all expressed in units of energy, typically GeV. As a result, quantities such as relaxation time, mean free path, and proper time are written in inverse-energy units (for example, $\mathrm{fm}/c \equiv \mathrm{fm}$), while thermodynamic variables scale with appropriate powers of energy. This choice simplifies the relativistic equations and ensures that all expressions remain dimensionally consistent.

1.3 Organisation of the Thesis

The remainder of this thesis is organised as follows. Chapter 2 introduces the theoretical framework underlying the analyses presented in this work. It reviews relativistic viscous hydrodynamics, develops the kinetic description based on the Boltzmann equation, and formulates the moment hierarchy within the relaxation-time approximation. An exact (0+1)D integral solution is constructed, together with the machinery required for evaluating macroscopic observables.

In Chapter 3, we investigate equilibration in the presence of external forces. By incorporating a force term into the Boltzmann equation, we analyse how the additional scale modifies the approach to equilibrium and suppresses early-time attractor behaviour, especially in non-conformal settings. Numerical implementations, force parametrisations, and representative observables are presented.

Chapter 4 extends this analysis to collision models with momentum-dependent relaxation times. The resulting moment equations require regularisation of the collision kernel, and the evolution of selected moments is used to quantify hydrodynamisation. We examine how different microscopic relaxation channels influence attractor-like behaviour and derive conditions under which universality persists.

In Chapter 5, we derive the exact gradient expansion of the Boltzmann equation, elucidating the asymptotic nature of the Chapman–Enskog series. The structure of the expansion is presented in closed form, allowing us to characterise its divergence, identify non-perturbative transient contributions, and assess the regime of validity of hydrodynamic truncations.

Chapter 6 develops a formal operator-based solution to relativistic hydrodynamics beyond local equilibrium. Working within $0+1$D and subsequently extending to the general $3+1$D case, we decompose the dynamics into gradient and non-perturbative parts, identify

the hydrodynamic generator, and formulate a quantitative validity criterion for hydrodynamics in expanding systems.

Finally, Chapter 7 summarises the main results and outlines potential directions for future work, including applications to more realistic collision kernels, additional conserved charges, and generalised flows relevant to heavy-ion phenomenology.

Chapter 2

Theoretical Framework

This chapter presents the theoretical framework that underpins the analyses carried out in this thesis. Our goal is to provide a self-contained account of both macroscopic and microscopic descriptions of relativistic fluids, with particular emphasis on the connection between kinetic theory and viscous relativistic hydrodynamics. We begin with a concise review of equilibrium and viscous relativistic hydrodynamics, highlighting the conservation laws, constitutive relations, and the limitations of first-order (Navier–Stokes) formulations. We then introduce modern second-order approaches, such as the Israel–Stewart (IS) and Denicol–Niemi–Molnár–Rischke (DNMR) formalisms, which render relativistic hydrodynamics causal and stable by promoting dissipative fluxes to dynamical variables. This hydrodynamic overview establishes the theoretical framework and defines the key hydrodynamic variables—such as the energy density, pressure, and viscous stresses—that are employed throughout the thesis.

To place hydrodynamics on a microscopic foundation, the chapter develops the essentials of relativistic kinetic theory. We describe the derivation of the Boltzmann equation from the Bogoliubov–Born–Green–Kirkwood–Yvon (BBGKY) hierarchy [50] under the molecular-chaos assumption and discuss its role as the basic equation for out-of-equilibrium evolution. The Anderson–Witting relaxation-time approximation (AW-RTA) is introduced as a pragmatic linearization of the collision integral that captures the dominant relaxation dynamics while remaining analytically tractable. We describe Landau matching and the extraction of macroscopic fields from moments of the single-particle distribution, thereby showing how kinetic theory yields hydrodynamic variables and transport coefficients.

Building on these foundations, we present generalisations relevant to this thesis. A constant relaxation time cannot represent the energy dependence of microscopic scattering and lead to violations of exact energy–momentum conservation in multi-scale systems. To address this, we describe a generalised (momentum-dependent) relaxation-time kernel developed in the literature that preserves conservation laws while capturing realistic spectral dependence. We then derive the exact integral solution of the AW-RTA Boltzmann equation in boost-invariant $(0 + 1)$D Bjorken flow using the method of characteristics. The integral solution, consisting of a damped free-streaming term and a history integral over an equilibrium source, provides insight into memory effects, collisional relaxation, and the emergence of hydrodynamic behaviour. We explain how anisotropic initial conditions, represented by the Romatschke–Strickland form [51, 52, 53, 54, 55], are implemented and how the integral solution is used to compute the energy–momentum tensor and its longitudinal and transverse pressure components.

2.1 Relativistic Hydrodynamics

Hydrodynamics is an effective macroscopic theory that describes the collective behaviour of many-particle systems in terms of conserved quantities such as energy, momentum, and charge. Instead of tracking individual microscopic degrees of freedom, hydrodynamics employs fields like energy density, pressure, fluid velocity, and conserved currents to capture the long-wavelength, low-frequency dynamics of matter. The fundamental equations governing hydrodynamics arise from local conservation laws, supplemented by an equation of state that encodes the microscopic physics. Depending on the level of description, hydrodynamics may include dissipative effects such as viscosity and diffusion, which account for deviations from local equilibrium.

2.1.1 Ideal Hydrodynamics

The simplest realisation of a hydrodynamic system is one in local thermal equilibrium, meaning that within each infinitesimal fluid element, microscopic interactions rapidly drive the single-particle distribution toward an equilibrium form characterised by well-defined temperature, chemical potential, and flow velocity. In this regime, local entropy production is zero, and the usual thermodynamic relations and equations of state are locally valid.

This assumption relies on a clear separation of time scales: a short microscopic scale, over which collisions establish equilibrium, and a much longer macroscopic scale, over which gradients of hydrodynamic fields drive collective evolution. Such a separation typically holds in dense, strongly interacting systems with short mean free paths, for example, liquids or the quark–gluon plasma near hadronisation. It breaks down in dilute or weakly interacting systems with long mean free paths, such as rarefied gases or systems undergoing rapid expansion, where collisions are too infrequent to maintain equilibrium. Because microscopic interactions act on much shorter time scales than the macroscopic dynamics, this equilibrium form is continuously maintained as the system evolves. In this regime, each fluid element can be parameterised by equilibrium thermodynamic variables such as energy density, pressure, temperature, and chemical potential, which vary smoothly in space and time.

For a single-component fluid with one conserved charge, the ideal hydrodynamic description is formulated in terms of the energy–momentum tensor $T^{\mu\nu}$ and the conserved charge current n^{μ}. In local thermal equilibrium, the system has six independent degrees of freedom: the energy density ε, the number density n, the fluid four-velocity u^{μ}, and the isotropic pressure P. The conserved fields are then written as

$$T^{\mu\nu}_{\text{ideal}} = \varepsilon\, u^{\mu} u^{\nu} + P\, \Delta^{\mu\nu}\,, \tag{2.1}$$

$$\mathrm{n}^{\mu}_{\text{ideal}} = \mathrm{n}\, u^{\mu}\,, \tag{2.2}$$

where $\Delta^{\mu\nu} = g^{\mu\nu} - u^\mu u^\nu$ projects onto spatial directions orthogonal to the flow velocity. The metric tensor $g^{\mu\nu}$ is a symmetric rank-two object that encodes spacetime intervals and is used to raise and lower Lorentz indices. In the mostly negative convention its components are $g^{\mu\nu} = \mathrm{diag}(+1, -1, -1, -1)$. It specifies the underlying spacetime geometry, and with this metric, the four-velocity satisfies $u^\mu u_\mu = 1$. The conservation laws give five dynamical equations,

$$\partial_\mu T^{\mu\nu} = 0\,, \qquad\qquad \partial_\mu \mathrm{n}^\mu = 0\,, \tag{2.3}$$

which, together with an equation of state $\varepsilon = \varepsilon(n, P)$ and specified initial or boundary conditions, determine the ideal hydrodynamic evolution of the system.

2.1.2 Viscous Hydrodynamics

Real systems have finite viscosities, and when gradients of temperature, velocity, or chemical potential are present, the single-particle distribution deviates from its equilibrium form and additional fluxes appear. Therefore, ideal hydrodynamics based on perfect local equilibrium is only approximate. These fluxes through dissipative effects drive entropy production and relax the system toward equilibrium. In relativistic many-body systems, such as those created in heavy-ion collisions, large gradients make dissipative corrections essential.

To account for these effects, viscous hydrodynamics extends the ideal description by adding non-equilibrium corrections to the energy–momentum tensor and conserved current,

$$T^{\mu\nu} = T^{\mu\nu}_{\mathrm{eq}} + \Pi^{\mu\nu}\,, \tag{2.4}$$

$$\mathrm{n}^\mu = \mathrm{n}^\mu_{\mathrm{eq}} + V^\mu\,. \tag{2.5}$$

The most general first-order decomposition in a single-component fluid is

$$T^{\mu\nu} = \varepsilon\, u^\mu u^\nu + (P + \Pi)\,\Delta^{\mu\nu} + \pi^{\mu\nu} + u^\mu q^\nu + u^\nu q^\mu\,, \tag{2.6}$$

$$\mathrm{n}^\mu = \mathrm{n}\, u^\mu + V^\mu\,, \tag{2.7}$$

where u^μ is the fluid four-velocity, the trace of the non-equilibrium correction is the bulk viscous pressure Π, $\pi^{\mu\nu}$ is the traceless shear-stress tensor, q^μ is the heat-flow four-vector, and V^μ is the charge-diffusion current. These dissipative quantities satisfy

$$u_\mu \pi^{\mu\nu} = 0, \qquad \pi^\mu{}_\mu = 0, \qquad u_\mu q^\mu = 0, \qquad u_\mu V^\mu = 0\,,$$

ensuring they are spatial in the local rest frame. The above decomposition is not unique until a convention for u^μ is chosen. Two standard frame choices remove this ambiguity:

Landau frame:

$$T^{\mu\nu} u_\nu = \varepsilon\, u^\mu\,.$$

This defines the flow velocity as the timelike eigenvector of $T^{\mu\nu}$ and enforces $q^\mu = 0$, eliminating heat flow by construction.

Eckart frame:

$$\mathrm{n}^\mu = n\, u^\mu\,.$$

Here u^μ is aligned with the conserved charge current, which sets $V^\mu = 0$ but allows $q^\mu \neq 0$.

In this thesis, the Landau frame is used, so $q^\mu = 0$. The resulting decompositions are

$$T^{\mu\nu} = \varepsilon\, u^\mu u^\nu + (P + \Pi)\, \Delta^{\mu\nu} + \pi^{\mu\nu}\,, \tag{2.8}$$

$$\mathrm{n}^\mu = \mathrm{n}\, u^\mu + V^\mu\,. \tag{2.9}$$

In the ideal limit, all dissipative quantities vanish, reducing the system to a perfect fluid.

Hydrodynamic gradient expansion

The hydrodynamic gradient expansion is an ordering scheme in which one systematically includes all terms allowed by symmetries, organised by the number of spacetime derivatives acting on the hydrodynamic fields. At zeroth order there are no gradients and the system behaves as an ideal fluid. First-order terms involve a single derivative and produce the Navier–Stokes constitutive relations. Higher orders include products of gradients

and capture nonlinear and memory effects. The expansion is controlled when gradients are small compared to the microscopic relaxation scale. The non-equilibrium contributions in viscous hydrodynamics—shear stress $\pi^{\mu\nu}$, bulk viscous pressure Π, and diffusion current V^{μ}—can be expressed in terms of gradients of the hydrodynamic fields

In the first-order (Navier–Stokes) approximation, these quantities are assumed to respond instantaneously to local gradients:

$$\pi^{\mu\nu} = 2\eta\, \nabla^{\langle\mu} u^{\nu\rangle}, \tag{2.10}$$

$$\Pi = -\zeta\, \nabla_{\alpha} u^{\alpha}, \tag{2.11}$$

$$V^{\mu} = \kappa\, \nabla^{\mu} \frac{\mu}{T}, \tag{2.12}$$

where η and ζ are the shear and bulk viscosities, κ is the thermal conductivity (or charge diffusion coefficient), and $\nabla^{\langle\mu} u^{\nu\rangle}$ denotes the symmetric, traceless, and transverse velocity gradient. The relevant differential operators are defined by separating temporal and spatial derivatives with respect to the fluid four-velocity: the comoving (material) derivative $D \equiv u^{\alpha}\partial_{\alpha}$ and the spatial gradient $\nabla^{\alpha} \equiv \Delta^{\alpha\beta}\partial_{\beta}$. The symmetric, traceless, transverse velocity-gradient tensor is given by

$$\nabla^{\langle\mu} u^{\nu\rangle} = \frac{1}{2}\left(\nabla^{\mu} u^{\nu} + \nabla^{\nu} u^{\mu}\right) - \frac{1}{3}\Delta^{\mu\nu}\left(\nabla_{\alpha} u^{\alpha}\right),$$

and satisfies the transversality condition $u_{\mu}\nabla^{\langle\mu} u^{\nu\rangle} = 0$.

Non-equilibrium corrections describe fluxes proportional to gradients. These fluxes (shear stress, bulk pressure, heat flow) irreversibly convert ordered energy into internal energy. The result is entropy production and damping of gradients. This loss of macroscopic order is dissipation.

However, the relativistic Navier–Stokes theory suffers from acausality and numerical instabilities. The viscous terms introduce second-order spatial gradients but no corresponding time derivatives. Information then propagates with infinite speed. Small short-wavelength perturbations grow instead of damping because the equations do not provide

intrinsic relaxation. Linear stability analysis shows modes with positive imaginary frequency at finite wave number. In discretised form these modes amplify numerical noise [56, 57].

To resolve the issues of acausality and instability present in first-order relativistic hydrodynamics, Israel and Stewart [58, 59] developed a second-order theory in which the dissipative fluxes—shear stress $\pi^{\mu\nu}$, bulk viscous pressure Π, and diffusion current q^{μ}—are promoted to independent dynamical variables.

To resolve the issues of acausality and instability present in first-order relativistic hydrodynamics, Israel and Stewart [58, 59] developed a second-order theory in which the dissipative fluxes—shear stress $\pi^{\mu\nu}$, bulk viscous pressure Π, and diffusion current q^{μ}—are promoted to independent dynamical variables. Rather than being instantaneously tied to local gradients, these quantities relax toward their first-order (Navier–Stokes) limits over finite relaxation times. The construction begins with the relativistic first law of thermodynamics, expressing the entropy current in terms of the energy–momentum tensor and the charge current,

$$s^{\mu} = P\beta^{\mu} + \beta^{\nu}T^{\mu}_{\nu} - \frac{\mu}{T}n^{\mu} \tag{2.13}$$

where $\beta^{\mu} = u^{\mu}/T$.

The most general extension of the entropy current is then obtained by including contributions quadratic in the dissipative fields, achieved by expanding $T^{\mu\nu}$ and n^{μ} to second order in deviations from equilibrium. Imposing the second law of thermodynamics, $\partial_{\mu}s^{\mu} \geq 0$, enforces non-negative entropy production and constrains the allowed evolution equations.

Sketch proof: quadratic corrections to the entropy current

We start with the local-equilibrium entropy current

$$s^{\mu}_{\mathrm{eq}} = s\,u^{\mu}, \tag{2.14}$$

By the Israel–Stewart anzatz [58, 59, 60, 61, 62, 63], we add the lowest-order (in deviations) non-equilibrium corrections that are quadratic in the dissipative fields. The most general allowed ansatz (up to second order) is

$$s^\mu = s\,u^\mu - \frac{\beta_0}{2}\,\Pi^2\,u^\mu - \frac{\beta_1}{2}\,q_\alpha q^\alpha\,u^\mu - \frac{\beta_2}{2}\,\pi_{\alpha\beta}\pi^{\alpha\beta}\,u^\mu + \mathcal{O}(\text{cubic}), \tag{2.15}$$

where β_i are phenomenological (positive) coefficients. By computing the divergence $\partial_\mu s^\mu$ and using the conservation laws

$$\partial_\mu T^{\mu\nu} = 0, \qquad \partial_\mu \mathrm{n}^\mu = 0,$$

and the first law relations to get the derivatives of equilibrium quantities. Keeping only terms up to second order in the dissipative fields (linear in their gradients). and projecting along and orthogonal to u^μ,

$$\partial_\mu s^\mu = -\Pi\left(\theta + \beta_0\dot{\Pi} + \cdots\right) - V^\mu\left(\nabla_\mu\alpha + \beta_1\dot{q}_\mu + \cdots\right) - \pi^{\mu\nu}\left(\sigma_{\mu\nu} + \beta_2\dot{\pi}_{\mu\nu} + \cdots\right), \tag{2.16}$$

Now the second law $\partial_\mu s^\mu \geq 0$ is imposed for arbitrary small dissipative fields by choosing linear constitutive (relaxation) relations that make the right-hand side a manifest sum of positive products. The simplest choice is to require the terms inside each parenthesis to be proportional to the corresponding dissipative field with a positive coefficient. This procedure leads to constitutive relations in which the dissipative quantities obey relaxation-type dynamics. In Israel–Stewart theory, these take schematic forms such as

$$\tau_\Pi\dot{\Pi} + \Pi = -\zeta\,\theta + \mathcal{O}(\text{second order}), \tag{2.17}$$

$$\tau_V\dot{V}^{\langle\mu\rangle} + V^\mu = -\kappa\,\nabla^\mu T + \mathcal{O}(\text{second order}), \tag{2.18}$$

$$\tau_\pi\dot{\pi}^{\langle\mu\nu\rangle} + \pi^{\mu\nu} = 2\eta\,\sigma^{\mu\nu} + \mathcal{O}(\text{second order}), \tag{2.19}$$

with positive transport coefficients $\zeta, \kappa, \eta > 0$ and relaxation times related to the β_i coefficients, e.g.

$$\tau_\Pi = \zeta\,\beta_0, \qquad \tau_V = \kappa\,\beta_1, \qquad \tau_\pi = 2\eta\,\beta_2. \tag{2.20}$$

With these signs the entropy production becomes

$$\partial_\mu s^\mu = \frac{\Pi^2}{\zeta} + \frac{V_\alpha V^\alpha}{\kappa T} + \frac{\pi_{\alpha\beta}\pi^{\alpha\beta}}{2\eta} + \cdots \geq 0,$$

which is manifestly non-negative to quadratic order. The relaxation times τ_π, τ_Π, and τ_q control the rate at which the system approaches equilibrium, ensuring that relaxation occurs over finite timescales. This renders the evolution equations hyperbolic, allowing for causal signal propagation and stable dynamics, thereby resolving the pathologies of first-order relativistic hydrodynamics.

A key drawback of the Israel–Stewart construction is that it is fundamentally built on an equilibrium thermodynamic foundation. The derivation begins with the equilibrium form of the entropy current and then extends it by adding quadratic terms in the dissipative quantities. This procedure assumes that deviations from equilibrium remain small, so that equilibrium thermodynamic relations continue to hold locally. As a result, the framework lacks a systematic microscopic justification: it cannot, on its own, capture strongly out-of-equilibrium dynamics or provide a first-principles determination of transport coefficients and relaxation times. Instead, many of these coefficients must be supplied externally from kinetic theory or effective field theory calculations.

To overcome these limitations, several modern frameworks have been developed. For instance, the Denicol–Niemi–Molnár–Rischke (DNMR) formalism [62, 64] systematically derives second-order hydrodynamics from kinetic theory using the 14-moment approximation of the Boltzmann equation. Similarly, gradient expansion methods within the AW-RTA [65, 66, 67, 68] provide a controlled expansion in terms of the Knudsen number (Kn) and inverse Reynolds (Rn) numbers, yielding evolution equations for dissipative currents with transport coefficients directly linked to microscopic dynamics. In addition, effective field theory approaches formulate hydrodynamics as a low-energy, long-wavelength effective theory constrained by symmetries and the second law of thermodynamics, allowing

for a systematic classification of higher-order corrections. Collectively, these modern approaches overcome the equilibrium-based limitations of Israel–Stewart theory and offer a more robust framework for describing strongly out-of-equilibrium dynamics, such as those encountered in relativistic heavy-ion collisions.

2.2 Kinetic Theory

Boltzmann kinetic theory provides a microscopic framework for describing the evolution of a many-particle system out of equilibrium. It can be viewed as a truncation of the BBGKY hierarchy, which offers a systematic description of an N-particle system in terms of *reduced distribution functions*. In this formalism, the complete statistical state of the system is described by the N-particle distribution function $f^{(N)}(x_1, p_1, \ldots, x_N, p_N)$, defined over the full $6N$-dimensional phase space. The s-particle or *reduced distribution function* $f^{(s)}(x_1, p_1, \ldots, x_s, p_s)$ is obtained by integrating the full distribution function over the remaining $(N - s)$ particle coordinates and momenta,

$$f^{(s)}(x_1, p_1, \ldots, x_s, p_s) = \int \prod_{i=s+1}^{N} d^3x_i \, d^3p_i \; f^{(N)}(x_1, p_1, \ldots, x_N, p_N). \tag{2.21}$$

This marginalisation procedure effectively "coarse-grains" over microscopic degrees of freedom, allowing macroscopic observables to be expressed in terms of a few reduced distributions.

The BBGKY hierarchy expresses the evolution of each s-particle distribution function in terms of the next higher one, $f^{(s+1)}$, producing an infinite chain of coupled equations that encode all inter-particle correlations. To obtain a closed kinetic equation for the single-particle distribution function $f^{(1)}(x, p) \equiv f(x, p)$, one must introduce approximations. The Boltzmann equation emerges when the assumption of *molecular chaos* (Stosszahlansatz) is invoked, factorizing the two-particle distribution function before collisions as

$$f^{(2)}(x_1, p_1, x_2, p_2) \approx f^{(1)}(x_1, p_1) \, f^{(1)}(x_2, p_2), \tag{2.22}$$

thereby neglecting correlations between incoming particles. This approximation closes the hierarchy at the single-particle level and forms the foundation of kinetic theory and its hydrodynamic limits. This truncation allows one to write a closed equation for $f(x,p)$ with a collision integral $C[f,f]$, providing a practical and tractable kinetic description. The system is then described in terms of the single-particle phase-space distribution function $f(x,p)$. In relativistic kinetic theory one treats spacetime position x^μ and four-momentum p^μ as independent coordinates on phase space. The single-particle distribution function $f(x,p)$ is defined such that

$$f(x,p)\, d^3x\, \frac{d^3p}{(2\pi)^3\, p^0}\,,$$

gives the expected number of particles in the spatial volume element d^3x around x with three-momentum in d^3p around p, where $p^0 = \sqrt{\mathbf{p}^2 + m^2}$ and d^3p/p^0 is the Lorentz-invariant momentum-space measure. Here, $d^3x\, d^3p/p^0$ is the invariant phase space volume element.

2.2.1 The Boltzmann equation

The evolution of $f(x,p)$ is governed by the Boltzmann equation [69]:

$$\left(p^\mu \frac{\partial}{\partial x^\mu} + m\, K^\mu \frac{\partial}{\partial p^\mu} - \Gamma^\sigma_{\mu\nu} p^\mu p^\nu \frac{\partial}{\partial p^\sigma}\right) f(x^\mu, p^\mu) = C[f,f]\,, \tag{2.23}$$

where K^μ represents an external four-force, and $\Gamma^\sigma_{\mu\nu}$ are the Christoffel symbols accounting for spacetime curvature and the four-momentum p^μ obeys the on-shell condition $g_{\mu\nu}p^\mu p^\nu = m^2$ with the force term obeying $g_{\mu\nu}p^\mu K^\nu/p^0 = 0$. The collision integral $C[f,f]$ is given by,

$$C[f,f] = \int dP_1\, dP'\, dP'_1\, W(p,p_1 \mid p',p'_1)\,[f'f'_1 - ff_1]\,, \tag{2.24}$$

where $W(p,p_1 \mid p',p'_1)$ is the Lorentz invariant transition rate for the process $p{+}p_1 \to p'{+}p'_1$ and $dP = d^3p/[(2\pi)^3 2p^0]$, and the bracketed term represents gain and loss due to collisions.

The condition $C[f_{\text{eq}}, f_{\text{eq}}] = 0$ defines the local thermal equilibrium distribution:

$$f_{\text{eq}} = \frac{1}{e^{(u\cdot p-\mu)/T} + r}, \tag{2.25}$$

where r takes values $-1, 0, 1$ corresponding to Bose-Einstein, Maxwell-Juttner, and Fermi-Dirac statistics, respectively.

Moments of the single-particle distribution function $f(x, p)$ provide a direct link between the microscopic dynamics encoded in the Boltzmann equation and macroscopic hydrodynamic quantities. In particular, the energy–momentum tensor and the particle four current are expressed as

$$T^{\mu\nu}(x) = \int dP\, p^\mu p^\nu f(x, p), \quad \text{n}^\mu(x) = \int dP\, p^\mu f(x, p)\,. \tag{2.26}$$

These quantities satisfy the conservation laws Eq.(2.3), when collisions respect energy-momentum and particle number conservation. By taking successive moments of the Boltzmann equation and performing controlled approximations—such as the AW-RTA and Chapman–Enskog[70] expansion—one can derive hydrodynamic equations that include viscous corrections, transport coefficients, and dissipative fluxes. This procedure provides a systematic, microscopic foundation for relativistic hydrodynamics.

2.2.2 The Anderson-Witting Kernel

The full relativistic Boltzmann equation contains a nonlinear collision integral $C[f, f]$, which accounts for all possible microscopic interactions between particles. This collision term is generally highly complex, as it depends on the detailed scattering process, phase-space distributions of incoming and outgoing particles, and can involve both elastic and inelastic processes. Solving the Boltzmann equation with the full collision integral is therefore computationally demanding, and often analytically intractable. The Anderson–Witting (AW) kernel provides a significant simplification by replacing the full collision integral with

a AW-RTA [71]:

$$C[f,f] \longrightarrow C_{\text{AW}}[f] = -u \cdot p \frac{(f - f_{\text{eq}})}{\tau_R}, \tag{2.27}$$

where f_{eq} is the local equilibrium distribution and τ_R is the characteristic relaxation time. This approximation assumes that the distribution function relaxes exponentially toward equilibrium over a single timescale, capturing the essential dissipative physics without requiring detailed knowledge of microscopic scattering processes. The introduction of the $u \cdot p$ factor is a key improvement over Marle's earlier model, which fails in the massless limit, $\frac{m}{\tau_R}(f - f_{\text{eq}})$. Replacing m with $u \cdot p$ gives the correct non-relativistic limit and extends the model to massless particles. Furthermore, this makes the relaxation model compatible with Landau matching when energy–momentum conservation is imposed. Moreover, in relativistic regimes the $u \cdot p$ term yields transport coefficients in both the classical and ultrarelativistic limits that agree with those obtained from Grad's method applied to the full relativistic Boltzmann collision kernel.

From a formal kinetic theory perspective, the linearized collision operator $\hat{\mathbf{L}}$, defined via

$$C[f,f] \approx -\hat{\mathbf{L}}[\delta f] + \mathcal{O}(\delta f^2), \quad \delta f = f - f_{\text{eq}}, \tag{2.28}$$

possesses a spectrum of eigenvalues and eigen functions corresponding to different modes of relaxation. Each eigenmode of $\hat{\mathbf{L}}$ decays exponentially with a characteristic timescale $\tau_i = 1/\lambda_i$, where λ_i is the corresponding eigenvalue [72]. The eigenfunctions associated with conserved quantities (particle number, momentum, energy) have zero eigenvalue ($\lambda_i = 0$) due to the conservation laws; these correspond to hydrodynamic modes. All other modes, sometimes called non-hydrodynamic modes, have finite positive eigenvalues, corresponding to decaying microscopic excitations.

In general, the eigen-spectrum spans a wide range of relaxation timescales, reflecting the fact that different momentum components and different microscopic processes equilibrate

at different rates. For example, high-momentum particles or short-wavelength modes may relax faster than low-momentum or long-wavelength modes.

From this linearisation, Boltzmann equation can be modeled with a collision kernel that has the linear structure of the linearised Boltzmann collision kernel:

$$\left(p^\mu \frac{\partial}{\partial x^\mu} + mK^\mu \frac{\partial}{\partial p^\mu} - \Gamma^\sigma_{\mu\nu} p^\mu p^\nu \frac{\partial}{\partial p^\sigma}\right) f(x^\mu, p^\mu) = -\hat{\mathbf{L}}[\delta f]\,. \tag{2.29}$$

However, this formulation is not strictly linear in the distribution function f. Although the collision term on the right-hand side involves the linear operator $-\hat{\mathbf{L}}[\delta f]$, the equilibrium distribution $f_{\text{eq}}(T, \mu, u^\mu)$—around which the system is linearized—depends on the local hydrodynamic variables: the temperature $T(x)$, chemical potential $\mu(x)$, and flow velocity $u^\mu(x)$.

These quantities are not fixed externally but are instead determined self-consistently from the full distribution function f through matching conditions. A common choice, for example, is the Landau or Eckart matching condition, which requires that the conserved quantities computed from f (such as energy density, particle number, and momentum) match those of the local equilibrium distribution:

$$\int dP\,\{1,\, p^\mu,\, p^\mu p^\nu\}\, f(x,p) = \int dP\,\{1,\, p^\mu,\, p^\mu p^\nu\}\, f_{\text{eq}}\big(T(x), \mu(x), u^\mu(x)\big)\,. \tag{2.30}$$

Because f_{eq} thus depends on f through these relations, the overall kinetic equation remains nonlinear in f, even though the collision operator itself has a formally linearised structure. In essence, the apparent linearity of the model is broken by the fact that the local equilibrium parameters evolve dynamically with the distribution function itself.

The Anderson–Witting kernel effectively selects the slowest nonzero relaxation mode by replacing the full spectrum with a single relaxation time τ_R:

$$\hat{\mathbf{L}}[\delta f] \;\longrightarrow\; \frac{u \cdot p}{\tau_R} \delta f \tag{2.31}$$

Here, τ_R is in general a function of x^μ and p^μ and is typically chosen to correspond to the dominant timescale controlling the approach to equilibrium, which is often the lowest nonzero eigenvalue of $\hat{\mathbf{L}}$. This approximation captures the essential dissipative dynamics relevant for hydrodynamic behavior, while ignoring the faster-decaying modes that relax quickly.

Conservation laws and matching conditions

To ensure that the Anderson–Witting relaxation-time approximation respects fundamental conservation laws, it is necessary to impose Landau matching conditions. These conditions require that the energy density and number density calculated from the non-equilibrium distribution $f(x,p)$ match those of the local equilibrium distribution $f_{\text{eq}}(x,p)$ in the local rest frame of the fluid:

$$u_\nu T^{\mu\nu} = u_\nu T^{\mu\nu}_{\text{eq}} = \varepsilon_{\text{eq}} u^\mu \,, \tag{2.32}$$

$$u_\mu \mathrm{n}^\mu = u_\mu n^\mu_{\text{eq}} = \mathrm{n}_{\text{eq}} \,, \tag{2.33}$$

where u^μ is the fluid four-velocity. These conditions ensures the energy-momentum and number conservation via,

$$\int dP\; p^\nu p^\mu \partial_\mu f = \partial_\mu T^{\mu\nu} = \int dP\; u_\mu p^\mu p^\nu \frac{(f - f_{\text{eq}})}{\tau_R} = \frac{1}{\tau_R} u_\mu (T^{\mu\nu} - T^{\mu\nu}_{\text{eq}}) = 0 \,, \tag{2.34}$$

$$\int dP\; p^\mu \partial_\mu f = \partial_\mu n^\mu = \int dP u_\mu p^\mu \frac{(f - f_{\text{eq}})}{\tau_R} = \frac{1}{\tau_R} u_\mu (\mathrm{n}^\mu - \mathrm{n}^\mu_{\text{eq}}) = 0 \,, \tag{2.35}$$

provided that the relaxation time τ_R does not depend on momenta. The Landau matching procedure thus serves as the definition for the parameters of $f_{\text{eq}}(x,p,T,\mu,u^\mu)$ (temperature, chemical potential, and flow velocity) in such a way that the AW-RTA collision term conserves total energy and momentum, making the Anderson–Witting kernel consistent with the macroscopic conservation laws.

However, when the relaxation time depends on momentum, the standard Landau matching conditions (2.32) no longer guarantee the conservation of energy and charge. This is because the factors of $1/\tau_R(p)$ cannot be pulled out of the momentum integrals in (2.34) and (2.35). To consistently account for a momentum-dependent relaxation time while preserving both conservation laws and the Landau conditions (2.32) that define the local thermodynamic variables, a modified form of the collision kernel must be introduced.

2.2.3 Generalized Relaxation Time Kernel

A generalised relaxation time model [73, 74] can be constructed by modifying the Anderson–Witting kernel to consistently incorporate momentum-dependent relaxation times while preserving conservation laws. The procedure begins by recognising that the collision operator must annihilate the conserved hydrodynamic modes, namely particle number and energy–momentum, corresponding to the invariants 1 and p^μ. To enforce this, the deviation from equilibrium $\delta f = f - f_{\text{eq}}$ is decomposed into two parts: a hydrodynamic contribution lying within the subspace spanned by the collision invariants, and a purely dissipative part orthogonal to it. A projector is then built using the inner product weighted by $(u \cdot p)/\tau_R(p)$, such that the hydrodynamic part is exactly subtracted from the relaxation dynamics. The resulting kernel takes the form [72, 73]

$$C[f] = -\frac{u \cdot p}{\tau_R(x^\mu, p^\mu)} \Big[\delta f - \mathcal{P}[\delta f]\Big], \tag{2.36}$$

where $\mathcal{P}[\delta f]$ is the projection of the deviation δf on the hydrodynamic subspace. This ensures that the collision term relaxes only the non-hydrodynamic modes. This guarantees exact conservation of energy–momentum and charge, even with momentum-dependent τ_R, while leaving the Landau matching conditions intact.

Accordingly, while considering the collision term for a momentum-dependent relaxation time, we use the novel relaxation time collision operator that conserves both particle

number and energy-momentum irrespective of the momentum-dependence considered in $\tau_R(p)$ and the hydrodynamic frame chosen. Explicitly the collision kernel has the form [73, 74],

$$\mathcal{L}[\phi_p] = -\frac{E}{\tau_R} f^{eq} \left[\phi_p - P_0 \frac{\langle \frac{E}{\tau_R} P_0 \phi_p \rangle_{eq}}{\langle \frac{E}{\tau_R} P_0 P_0 \rangle_{eq}} - P_1 \frac{\langle \frac{E}{\tau_R} P_1 \phi_p \rangle_{eq}}{\langle \frac{E}{\tau_R} P_1 P_1 \rangle_{eq}} - p^{\langle \mu \rangle} \frac{\langle \frac{E}{\tau_R} p_{\langle \mu \rangle} \phi_p \rangle_{eq}}{\frac{1}{3} \langle \frac{E}{\tau_R} p_{\langle \nu \rangle} p^{\langle \nu \rangle} \rangle_{eq}} \right] , \quad (2.37)$$

with $E = u \cdot p$, $P_0 = 1$, $P_1 = 1 - p \langle \frac{p}{\tau_R} \rangle_{eq} / \langle \frac{p^2}{\tau_R} \rangle_{eq}$ and $p^{\langle \mu \rangle} = \Delta^{\mu\nu} p_\nu$. The notation $\langle \cdots \rangle_{eq}$ reads, $\langle \cdots \rangle_{eq} = \int dP f_p^{eq} (\cdots)$.

Explicit demonstration of number current conservation

Integrating the collision kernel over momentum gives zero, which ensures particle number conservation.

Proof. Define the weighted equilibrium average

$$\langle X \rangle_{eq} = \int dP \, f^{eq} \, X, \quad (2.38)$$

and use $E = u \cdot p$ in the collision kernel definition,

$$\int dP \, \mathcal{L}[\phi_p] = - \int dP \, \frac{E}{\tau_R} f^{eq} \left[\phi_p - P_0 \frac{\langle \frac{E}{\tau_R} P_0 \phi_p \rangle_{eq}}{\langle \frac{E}{\tau_R} P_0 P_0 \rangle_{eq}} - P_1 \frac{\langle \frac{E}{\tau_R} P_1 \phi_p \rangle_{eq}}{\langle \frac{E}{\tau_R} P_1 P_1 \rangle_{eq}} - p^{\langle \mu \rangle} \frac{\langle \frac{E}{\tau_R} p_{\langle \mu \rangle} \phi_p \rangle_{eq}}{\frac{1}{3} \langle \frac{E}{\tau_R} p_{\langle \nu \rangle} p^{\langle \nu \rangle} \rangle_{eq}} \right]. \quad (2.39)$$

Evaluating term by term, the first two pieces combine to

$$-\left\langle \frac{E}{\tau_R} \phi_p \right\rangle_{eq} + \left\langle \frac{E}{\tau_R} P_0 \right\rangle_{eq} \frac{\langle \frac{E}{\tau_R} P_0 \phi_p \rangle_{eq}}{\langle \frac{E}{\tau_R} P_0 P_0 \rangle_{eq}} = -\left\langle \frac{E}{\tau_R} \phi_p \right\rangle_{eq} + \left\langle \frac{E}{\tau_R} \phi_p \right\rangle_{eq} = 0, \quad (2.40)$$

since $P_0 = 1$ and $\langle \frac{E}{\tau_R} P_0 P_0 \rangle_{eq} = \langle \frac{E}{\tau_R} P_0 \rangle_{eq}$.

The remaining projector terms vanish because they are orthogonal to the constant mode under the $\langle \frac{E}{\tau_R} \cdot \rangle_{eq}$ inner product:

$$\left\langle \frac{E}{\tau_R} P_1 \right\rangle_{eq} = 0, \qquad \left\langle \frac{E}{\tau_R} p^{\langle \mu \rangle} \right\rangle_{eq} = 0. \quad (2.41)$$

The first relation follows from the definition of P_1 (constructed to be orthogonal to P_0), and the second from the isotropy of the equilibrium distribution.
Therefore,

$$\int dP\, \mathcal{L}[\phi_p] = 0, \tag{2.42}$$

which shows that the collision operator does not alter the total particle number. Hence, number conservation is automatic in the generalised relaxation-time kernel.

With the kinetic foundation in place, one can now systematically connect microscopic transport dynamics to macroscopic fluid behaviour. This is achieved through the Chapman–Enskog expansion, which provides an explicit procedure to derive hydrodynamic equations and transport coefficients from the Boltzmann equation by expanding around local equilibrium. The following section develops this expansion in detail and briefly reviews how hydrodynamic equations emerge from the order-by-order derivative expansion of the distribution function around its local equilibrium form.

2.3 The Chapman–Enskog Expansion

The hydrodynamic gradient expansion can be systematically derived from the relativistic Boltzmann equation using the Chapman–Enskog procedure. This formalism provides a controlled bridge between microscopic kinetic theory and macroscopic hydrodynamics by expanding the single-particle distribution function around its local equilibrium form. In this approach, the distribution function is expressed as

$$f(x,p) = f_{\text{eq}}(x,p) + \delta f(x,p), \tag{2.43}$$

where f_{eq} denotes the local equilibrium (Maxwell–Jüttner) distribution, and δf encodes deviations induced by gradients of the hydrodynamic fields such as temperature, chemical potential, and velocity. The magnitude of δf is assumed to be small when the system is

close to local equilibrium, such that the macroscopic gradients of thermodynamic variables evolve on timescales much longer than the microscopic mean free path.

The starting point is the Boltzmann equation, which governs the evolution of the distribution function,

$$p^\mu \partial_\mu f = C[f, f], \tag{2.44}$$

where $C[f]$ is the collision integral. In the Anderson–Witting relaxation-time approximation (AW-RTA) [71], the collision term is replaced by a simple linear relaxation form,

$$C[f, f] = -\frac{u \cdot p}{\tau_R} \left(f - f_{\text{eq}}\right), \tag{2.45}$$

where τ_R is the microscopic relaxation time and u^μ is the local fluid four-velocity satisfying $u^\mu u_\mu = 1$. The AW-RTA equation is linear in f but effectively nonlinear in the hydrodynamic variables (T, μ, u^μ), which determine f_{eq} through Landau matching conditions ensuring energy–momentum and charge conservation.

2.3.1 Gradient Expansion of the Distribution Function

To connect kinetic theory with hydrodynamics, one expands the distribution function in powers of a small parameter, the *Knudsen number* Kn, which measures the ratio of the microscopic mean free path λ to a characteristic macroscopic length scale L:

$$\text{Kn} \sim \frac{\lambda}{L} \sim \frac{\tau_R}{\tau_{\text{hydro}}} \ll 1. \tag{2.46}$$

The distribution function and its corresponding moments can then be written as

$$f = f^{(0)} + \text{Kn}\, f^{(1)} + (\text{Kn})^2 f^{(2)} + \cdots, \tag{2.47}$$

$$\rho_n = \rho_n^{(0)} + \text{Kn}\, \rho_n^{(1)} + (\text{Kn})^2 \rho_n^{(2)} + \cdots, \tag{2.48}$$

where ρ_n denotes the n-th moment of the distribution function. Substituting this expansion into the Boltzmann equation and equating terms of the same order in Kn generates an infinite hierarchy of equations that can be solved iteratively.

At zeroth order, the system is in local equilibrium, satisfying $C[f^{(0)}, f^{(0)}] = 0$, which gives $f^{(0)} = f_{\text{eq}}$. At first order, the Boltzmann equation yields

$$p^\mu \partial_\mu f^{(0)} = -\frac{u \cdot p}{\tau_R} f^{(1)}. \tag{2.49}$$

Solving for $f^{(1)}$ gives

$$f^{(1)} = -\frac{\tau_R}{u \cdot p} p^\mu \partial_\mu f_{\text{eq}}. \tag{2.50}$$

Iteratively applying this procedure yields the formal series solution

$$f = f_{\text{eq}} + \sum_{k=1}^{\infty} \left[-\frac{\tau_R}{u \cdot p} p^\mu \partial_\mu \right]^k f_{\text{eq}}, \tag{2.51}$$

which expresses f entirely in terms of f_{eq} and gradients of hydrodynamic fields. This expansion provides a microscopic foundation for the hydrodynamic gradient series.

2.3.2 Hydrodynamic Moments and Constitutive Relations

Macroscopic observables such as the energy–momentum tensor and the conserved charge current are obtained as moments of the single-particle distribution function. Substituting $f = f_{\text{eq}} + \delta f$ and expanding, we separate each quantity into an equilibrium and a non-equilibrium part,

$$T^{\mu\nu} = T^{\mu\nu}_{\text{eq}} + \delta T^{\mu\nu}, \qquad n^\mu = n^\mu_{\text{eq}} + \delta n^\mu, \tag{2.52}$$

with

$$\delta T^{\mu\nu} = \int dP\, p^\mu p^\nu\, \delta f, \tag{2.53}$$

$$\delta n^\mu = \int dP\, p^\mu\, \delta f. \tag{2.54}$$

The equilibrium parts yield the ideal hydrodynamic quantities in Eq.(2.1).

Non-equilibrium corrections from $\delta f^{(1)}$.

At first order in the Chapman–Enskog expansion, deviations from local equilibrium are

given by

$$\delta f^{(1)} = -\frac{\tau_R}{u \cdot p}\, p^\alpha \partial_\alpha f_{\text{eq}}. \tag{2.55}$$

This term encodes how gradients of the hydrodynamic fields (temperature, chemical potential, and velocity) drive the system away from equilibrium. Substituting Eq. (2.55) into the definitions of $\delta T^{\mu\nu}$ and δn^μ provides explicit expressions for the non-equilibrium corrections to the macroscopic quantities:

$$\delta T^{\mu\nu} = -\int dP\, \frac{\tau_R}{u \cdot p}\, p^\mu p^\nu p^\alpha \partial_\alpha f_{\text{eq}}, \tag{2.56}$$

$$\delta n^\mu = -\int dP\, \frac{\tau_R}{u \cdot p}\, p^\mu p^\alpha \partial_\alpha f_{\text{eq}}. \tag{2.57}$$

Performing the momentum integrations and projecting these expressions along and orthogonal to the flow velocity allows us to identify the dissipative contributions to the energy–momentum tensor:

$$\delta T^{\mu\nu} = \pi^{\mu\nu} + \Pi\, \Delta^{\mu\nu}, \tag{2.58}$$

where $\pi^{\mu\nu}$ is the traceless shear-stress tensor and Π the scalar bulk viscous pressure. Similarly, the correction to the number current can be decomposed as

$$\delta n^\mu = q^\mu, \tag{2.59}$$

where q^μ represents the heat flux (or particle diffusion current).

To evaluate the integrals in Eqs. (2.56)–(2.57), one substitutes the explicit form of f_{eq},

$$f_{\text{eq}} = \frac{1}{\exp[(u \cdot p - \mu)/T] + r}, \tag{2.60}$$

and expands the derivatives $\partial_\alpha f_{\text{eq}}$ in terms of the hydrodynamic gradients:

$$\partial_\alpha f_{\text{eq}} = f_{\text{eq}} \left[\frac{p^\beta}{T} \nabla_\alpha u_\beta - \frac{u \cdot p - \mu}{T^2}\, \partial_\alpha T - \frac{1}{T}\, \partial_\alpha \mu \right]. \tag{2.61}$$

Integrating over momentum then yields constitutive relations for the dissipative quantities:

$$\pi^{\mu\nu} = 2\eta\,\nabla^{\langle\mu}u^{\nu\rangle}, \tag{2.62}$$

$$\Pi = -\zeta\,\nabla_\alpha u^\alpha, \tag{2.63}$$

$$q^\mu = \kappa\,\nabla^\mu\left(\frac{\mu}{T}\right), \tag{2.64}$$

where η, ζ, and κ are the shear viscosity, bulk viscosity, and thermal conductivity, respectively. These transport coefficients are determined by the microscopic properties of the medium through momentum integrals weighted by τ_R, p^μ, and f_{eq}.

Hence, the first-order correction $\delta f^{(1)}$ provides the microscopic origin of the viscous terms in relativistic hydrodynamics. Inserting these corrections into the conservation laws $\partial_\mu T^{\mu\nu} = 0$ and $\partial_\mu n^\mu = 0$ yields the Navier–Stokes equations, which describe dissipative evolution in the near-equilibrium regime.

2.3.3 Higher-Order Corrections and Causality

While the first-order (Navier–Stokes) theory captures dissipative effects, it suffers from acausality and instabilities in the relativistic regime, since the equations are parabolic and permit instantaneous signal propagation. These issues are resolved by extending the Chapman–Enskog expansion to second order in Kn, introducing additional time-derivative (relaxation). For the theory to be causal, the relaxation time must be finite. However, this is not a sufficient condition. Causality imposes stronger constraints on IS theory. In the case of sheer viscosity only, the relaxation time must obey the inequality [75],

$$\frac{\tau_\pi}{\eta/(\varepsilon + P)} \geq \frac{4}{3(1 - c_s^2)} \tag{2.65}$$

where c_s is the speed of sound in the medium. This condition ensures that the propagation speed of linear perturbations in the fluid remains subluminal, thereby preserving causality and stability of the hydrodynamic evolution. In particular, if the relaxation time τ_π is smaller

than this bound, perturbations can propagate faster than the speed of light, leading to acausal behavior

At second order, the evolution equations for the dissipative quantities take the generic Israel–Stewart form [58, 59, 62]:

$$\dot{\pi}^{\langle\mu\nu\rangle} = -\frac{1}{\tau_\pi}\,\pi^{\mu\nu} + \frac{2\eta}{\tau_\pi}\,\sigma^{\mu\nu} + \frac{\lambda_{\pi\Pi}}{\tau_\pi}\,\Pi\,\sigma^{\mu\nu} + \cdots\,, \tag{2.66}$$

$$\dot{\Pi} = -\frac{1}{\tau_\Pi}\,\Pi - \frac{\zeta}{\tau_\Pi}\,\theta + \frac{\delta_{\Pi\Pi}}{\tau_\Pi}\,\Pi\,\theta + \frac{\lambda_{\Pi\pi}}{\tau_\Pi}\,\pi^{\mu\nu}\sigma_{\mu\nu} + \cdots\,, \tag{2.67}$$

$$\dot{q}^{\langle\mu\rangle} = -\frac{1}{\tau_q}\,q^\mu + \frac{\kappa}{\tau_q}\,\nabla^\mu\!\left(\frac{\mu}{T}\right) + \cdots\,. \tag{2.68}$$

where τ_π, τ_Π, and τ_q are relaxation times for the shear stress, bulk pressure, and heat flux, respectively. The additional coefficients $\lambda_{\pi\Pi}$, $\lambda_{\Pi\pi}$, $\delta_{\Pi\Pi}$, etc., encode nonlinear couplings between gradients and dissipative quantities, and can be computed directly from kinetic theory.

2.3.4 Asymptotic Nature of the Gradient Series

It is important to note that the Chapman–Enskog expansion generates an *asymptotic* rather than convergent series. This reflects the fact that the hydrodynamic gradient expansion cannot capture the full far-from-equilibrium behaviour of the system, as higher-order terms eventually diverge due to the factorial growth of coefficients. Nevertheless, the asymptotic nature of the series reveals the existence of a hydrodynamic *attractor*—a universal solution toward which the system relaxes regardless of its initial state [37, 76].

In this sense, the Chapman–Enskog method provides a controlled microscopic derivation of hydrodynamics and its regime of validity. While it fails to describe non-perturbative far-from-equilibrium dynamics, it establishes a clear connection between kinetic theory and macroscopic transport equations, elucidating how dissipative and relaxation phenomena emerge from microscopic scattering processes.

2.4 Exact solution in 0+1 D System

We now present how to obtain a formal integral solution to the $(0+1)$D AW-RTA Boltzmann equation in Bjorken flow. Here $(0+1)$D denotes a system with one temporal dimension and no spatial dependence, appropriate for boost-invariant longitudinal expansion in which the transverse plane is taken to be homogeneous. This integral formulation is particularly relevant because it provides an exact and self-consistent description of the microscopic evolution of a relativistic system undergoing boost-invariant longitudinal expansion. Unlike approximate moment-based or gradient-expansion approaches, the integral solution captures the full time dependence of the distribution function and therefore allows one to study the system's behaviour across the entire evolution-from the far-from-equilibrium regime to the onset of hydrodynamics. It also naturally incorporates memory effects through the damping function that governs the relaxation toward equilibrium, offering a clear interpretation of how different initial conditions influence the approach to isotropy and thermalisation. This framework serves as the foundation for exploring non-equilibrium phenomena such as hydrodynamic attractors, the effects of conformal symmetry breaking, and the role of external forces, connecting kinetic theory with macroscopic hydrodynamic behaviour in the context of heavy-ion collisions.

Bjorken flow and Milne coordinates

Consider a system with rotational and translational symmetry in the x–y plane and boost invariance along the z-axis. It is then convenient to work in the following **Milne coordinate** system,

$$\begin{aligned} \tau &= \sqrt{t^2 - z^2} \ ; \quad \eta = \tanh^{-1}(z/t) \ ; \\ r &= \sqrt{x^2 + y^2} \ ; \quad \theta = \tan^{-1}(y/x) \, . \end{aligned} \tag{2.69}$$

In these coordinates the metric takes the form $ds^2 = d\tau^2 - dx^2 - dy^2 - \tau^2 d\eta_s^2$, with $g_{\mu\nu} = \text{diag}(1, -1, -1, -\tau^2)$.

The flow velocity consistent with boost invariance is the **Bjorken flow** profile [77], $u^\mu = (1, 0, 0, 0)$ in Milne coordinates, which in Cartesian coordinates corresponds to $u^\mu = (t/\sqrt{t^2 - z^2},\ 0,\ 0,\ z/\sqrt{t^2 - z^2})$, describing a longitudinal expansion where the fluid velocity grows linearly with position, $v_z = z/t$. The symmetries of the system—**longitudinal boost invariance**, **translational invariance** in the transverse plane, and **rotational invariance** in the azimuthal angle—imply that all hydrodynamic fields such as energy density and pressure depend only on the proper time τ. This high degree of symmetry makes Bjorken flow an analytically tractable model that captures the essential longitudinal expansion dynamics of the quark–gluon plasma in heavy-ion collisions.

In Milne coordinates, the Boltzmann Equation with these symmetries under Bjorken flow profile takes the simplified form, [78],

$$\left(\frac{\partial}{\partial\tau} - \frac{p_\eta}{\tau}\frac{\partial}{\partial p_\eta}\right) f(\tau, p_T, p_\eta) \;=\; -\frac{1}{\tau_R(\tau)}\big(f(\tau, p_T, p_\eta) - f_{\text{eq}}(\tau, p_T, p_\eta)\big), \tag{2.70}$$

where $p_T = \sqrt{p_x^2 + p_y^2}$ and p_z is the longitudinal momentum (all momenta are on-shell).

Change of variables (method of characteristics). Introduce the *comoving longitudinal momentum* (a characteristic variable)

$$w \equiv \tau\, p_z.$$

Holding (w, p_T) fixed gives the combination appearing on the left of (2.70). Indeed, using $p_z = w/\tau$ [78],

$$\left.\frac{d}{d\tau}\right|_{w,p_T} f(\tau, p_T, p_z) = \frac{\partial f}{\partial\tau} + \frac{\partial f}{\partial p_z}\left.\frac{dp_z}{d\tau}\right|_w = \frac{\partial f}{\partial\tau} - \frac{p_z}{\tau}\frac{\partial f}{\partial p_z},$$

since $dp_z/d\tau|_w = -w/\tau^2 = -p_z/\tau$. Hence the left-hand side of (2.70) is exactly the total derivative of f along curves of constant (w, p_T). Denoting $f(\tau, w, p_T) \equiv f(\tau, p_T, p_z = w/\tau)$, the kinetic equation becomes an ordinary differential equation along characteristics:

$$\frac{d}{d\tau} f(\tau, w, p_T) = -\frac{1}{\tau_R(\tau)}\big(f(\tau, w, p_T) - f_{\text{eq}}(\tau, w, p_T)\big). \tag{2.71}$$

Solving the ODE with an integrating factor. Eq. (2.71) is linear in f. Define the damping (integrating-factor) function

$$D(\tau,\tau') \equiv \exp\Big[-\int_{\tau'}^{\tau} \frac{d\bar{\tau}}{\tau_R(\bar{\tau})}\Big], \qquad D(\tau,\tau) = 1,$$

so that $\frac{d}{d\tau}D(\tau,\tau') = -D(\tau,\tau')/\tau_R(\tau)$. Multiplying (2.71) by $D(\tau,\tau_0)$ and integrating from τ_0 to τ yields

$$\frac{d}{d\tau}\Big[D(\tau,\tau_0)\, f(\tau,w,p_T)\Big] = D(\tau,\tau_0)\,\frac{f_{\rm eq}(\tau,w,p_T)}{\tau_R(\tau)}.$$

Integrating both sides from τ_0 to τ and using $D(\tau_0,\tau_0) = 1$ gives the standard integral solution

$$f(\tau,w,p_T) = D(\tau,\tau_0)\, f(\tau_0,w,p_T) + \int_{\tau_0}^{\tau} d\tau'\, D(\tau,\tau')\,\frac{f_{\rm eq}(\tau',w,p_T)}{\tau_R(\tau')}\,. \tag{2.72}$$

The integral solution in Eq. (2.72) provides a transparent physical interpretation of the microscopic evolution of the system. The first term represents the *free-streaming contribution*, which carries information about the initial distribution function $f(\tau_0,w,p_T)$. This contribution is exponentially damped by the factor $D(\tau,\tau_0)$, signifying the progressive loss of memory of the initial state as the system evolves in time. The second term corresponds to the *equilibrium source term*, which accounts for the cumulative effect of collisions driving the system toward local equilibrium. Each past proper time τ' contributes to the current distribution with a weight given by the damping function $D(\tau,\tau')$, which encodes the probability that a particle retains its nonequilibrium character between τ' and τ. Together, these two terms describe the competition between microscopic collisions and macroscopic expansion in determining the approach to equilibrium.

The local-equilibrium distribution $f_{\rm eq}(\tau',w,p_T)$ depends implicitly on the hydrodynamic fields—such as the temperature $T(\tau')$, chemical potential $\mu(\tau')$, and the fluid four-velocity $u^\mu(\tau')$. These quantities are not known *a priori* but are determined self-consistently

through the energy–momentum tensor, obtained by taking momentum moments of the distribution function. The matching conditions, commonly referred to as *Landau matching*, ensure that the energy density calculated from the microscopic distribution equals the macroscopic hydrodynamic energy density, thereby maintaining thermodynamic consistency throughout the evolution. For an isotropic equilibrium gas of massless particles, the equilibrium relation reduces to the familiar conformal form, with the energy density ε and equilibrium pressure P_{eq} given by,

$$\varepsilon_{\text{eq}}(T) = \frac{3}{\pi^2}\, T^4, \qquad P_{\text{eq}}(T) = \frac{1}{\pi^2}\, T^4 .$$

Then the Landau-matched temperature satisfies $\varepsilon(\tau) = 3T^4(\tau)/\pi^2$.

For a constant relaxation time τ_R, the damping function simplifies to an exponential form, $D(\tau, \tau') = \exp[-(\tau - \tau')/\tau_R]$. However, when the relaxation time depends on temperature or proper time, the integral $\int_{\tau'}^{\tau} d\bar{\tau}/\tau_R(\bar{\tau})$ must be evaluated numerically. This flexibility allows the formalism to incorporate physically motivated temperature-dependent relaxation mechanisms, such as those relevant for the quark–gluon plasma, where the microscopic scattering rate changes with temperature.

Once the distribution function $f(\tau, w, p_T)$ is obtained, macroscopic observables can be evaluated by taking moments over the phase-space distribution. The energy–momentum tensor is given by

$$T^{\mu\nu}(\tau) = \int dP\, p^\mu p^\nu\, f(\tau, w, p_T), \tag{2.73}$$

where dP denotes the Lorentz-invariant phase-space measure in Milne coordinates. From $T^{\mu\nu}$, one can extract the energy density, pressure components, and viscous corrections, which describe the system's hydrodynamic evolution.

The initial distribution: The initial distribution function in the integral solution can be taken to be the *Romatschke–Strickland* (RS) form, which provides a convenient parametrization of momentum-space anisotropy in a longitudinally expanding system. The RS distri-

bution is expressed as

$$f_{\mathrm{RS}}(p_T, p_z; \Lambda_0, \Sigma_0) = \frac{2}{(2\pi)^3 N_0} \exp\left[-\frac{\sqrt{p_T^2 + (1+\Sigma_0)p_z^2}}{\Lambda_0}\right], \tag{2.74}$$

where Λ_0 is a transverse momentum scale analogous to an effective temperature, Σ_0 is the anisotropy parameter and N_0 is a normalization factor that allows the RS ansatz to reproduce the correct initial macroscopic quantities (energy density, particle number, or entropy). For $\Sigma_0 = 0$, the distribution reduces to an isotropic equilibrium form with temperature Λ_0, while $\Sigma_0 > 0$ corresponds to an oblate momentum-space deformation ($P_L < P_T$) expected in the early stages of Bjorken expansion. This anisotropic distribution serves as the initial condition $f(\tau_0, p_T, p_z) = f_{\mathrm{RS}}$ in the integral solution of the Boltzmann equation. Substituting this form into the first term of Eqs. (2.75)–(2.77) provides the initial contribution to the energy density and pressure components. The parameters Λ_0 and Σ_0 are then fixed by matching the initial energy density $\varepsilon(\tau_0)$ to a chosen value or by ensuring that the initial moments of the distribution satisfy a given anisotropy ratio P_L/P_T. This procedure allows the RS form to capture the essential early-time momentum anisotropy of the system while preserving a simple analytical structure suitable for numerical evolution.

2.4.1 Evolution of macroscopic observables

The energy density and the transverse/longitudinal pressures obtained from the integral solution of the AW-RTA Boltzmann equation can be written in the form: [79]

$$\varepsilon(\tau) = D(\tau,\tau_0)\,\frac{\Lambda_0^4}{4\pi^2\alpha_0}\,\widetilde{H}_\varepsilon\!\left[\frac{\tau_0}{\tau}\sqrt{1+\Sigma_0}\,,\,\frac{m}{\Lambda_0}\right] + \frac{1}{4\pi^2}\int_{\tau_0}^{\tau} d\tau'\,\frac{D(\tau,\tau')}{\tau_R(\tau')}\,T^4(\tau')\,\widetilde{H}_\varepsilon\!\left[\frac{\tau'}{\tau}\,,\,\frac{m}{T(\tau')}\right], \tag{2.75}$$

$$P_L(\tau) = D(\tau,\tau_0)\,\frac{\Lambda_0^4}{4\pi^2\alpha_0}\,\widetilde{H}_L\!\left[\frac{\tau_0}{\tau}\sqrt{1+\Sigma_0}\,,\,\frac{m}{\Lambda_0}\right] + \frac{1}{4\pi^2}\int_{\tau_0}^{\tau} d\tau'\,\frac{D(\tau,\tau')}{\tau_R(\tau')}\,T^4(\tau')\,\widetilde{H}_L\!\left[\frac{\tau'}{\tau}\,,\,\frac{m}{T(\tau')}\right], \tag{2.76}$$

$$P_T(\tau) = D(\tau,\tau_0)\,\frac{\Lambda_0^4}{8\pi^2\alpha_0}\,\widetilde{H}_T\!\left[\frac{\tau_0}{\tau}\sqrt{1+\Sigma_0}\,,\,\frac{m}{\Lambda_0}\right] + \frac{1}{8\pi^2}\int_{\tau_0}^{\tau} d\tau'\,\frac{D(\tau,\tau')}{\tau_R(\tau')}\,T^4(\tau')\,\widetilde{H}_T\!\left[\frac{\tau'}{\tau}\,,\,\frac{m}{T(\tau')}\right]. \tag{2.77}$$

These expressions encode the full microscopic dynamics of a boost-invariant system undergoing longitudinal expansion within the relaxation-time approximation. The evolution is governed primarily by two functions: the damping factor $D(\tau,\tau')$ and the $\widetilde{H}$ functions (defined in Sec. 2.4.2), each reflecting distinct aspects of the underlying physics. The relaxation time $\tau_R(\tau')$ controls the rate of approach toward local equilibrium and may depend on microscopic properties such as temperature or coupling strength. The damping factor $D(\tau,\tau')$ quantifies the relative weight of free-streaming and collisional processes—its exponential decay encodes how quickly the system loses memory of its initial conditions. For constant τ_R, when $\tau \gg \tau_R$, $D(\tau,\tau')$ becomes negligible, signalling the dominance of collisions and the onset of local equilibrium.

In Eqs. (2.75)–(2.77), each quantity naturally separates into two distinct physical contributions. The first term originates from the initial phase-space distribution and is exponentially attenuated by $D(\tau,\tau_0)$, reflecting the gradual loss of information about the system's initial anisotropy, parameterized by Λ_0, α_0, and Σ_0 in the Romatschke–Strickland form. The second term arises from the cumulative effect of collisions, represented by a time integral over the equilibrium source weighted by the same damping factor. Together, these

two components describe the dynamic competition between free streaming and collisional relaxation, providing a unified description of how microscopic interactions drive the macroscopic evolution of energy density and pressure in an expanding relativistic medium.

2.4.2 H-functions in the Free-Streaming Limit

In the free-streaming regime, where collisional effects are absent, the evolution of the system simplifies considerably. The energy density and the longitudinal and transverse pressures can then be expressed in terms of the $\widetilde{H}$ functions,

$$\varepsilon_{\mathrm{fs}}(\tau) = \frac{\Lambda_0^4}{4\pi^2\alpha_0}\,\widetilde{H}_\varepsilon\!\left(\frac{\tau_0}{\tau}\sqrt{1+\Sigma_0},\,\frac{m}{\Lambda_0}\right), \tag{2.78}$$

$$P_T^{\mathrm{fs}}(\tau) = \frac{\Lambda_0^4}{8\pi^2\alpha_0}\,\widetilde{H}_T\!\left(\frac{\tau_0}{\tau}\sqrt{1+\Sigma_0},\,\frac{m}{\Lambda_0}\right), \tag{2.79}$$

$$P_L^{\mathrm{fs}}(\tau) = \frac{\Lambda_0^4}{4\pi^2\alpha_0}\,\widetilde{H}_L\!\left(\frac{\tau_0}{\tau}\sqrt{1+\Sigma_0},\,\frac{m}{\Lambda_0}\right), \tag{2.80}$$

which capture the purely kinematic evolution of the distribution function under longitudinal expansion. The resulting free-streaming energy density and pressures coincide with the damped initial contributions, illustrating that the collision term is entirely responsible for the eventual isotropization of the system.

The functions $\widetilde{H}_\varepsilon$, $\widetilde{H}_L$, and $\widetilde{H}_T$ are dimensionless kinematic kernels obtained from analytic integration over the momentum phase space. They encapsulate the effects of finite particle mass, anisotropy, and any external perturbations through their dependence on the ratios τ'/τ and $m/T(\tau')$. These kernels effectively translate the microscopic dynamics contained in the distribution function into macroscopic observables such as energy density and

pressures. They are defined by the following momentum integrals [80, 79]:

$$\widetilde{H}_{\varepsilon}(\alpha, z) = \alpha \int_0^\infty du\, u^3 \int_{-1}^1 dx\, \sqrt{u^2 + z^2}\, \exp\left[-\sqrt{u^2 + z^2(1 + \alpha^2 x^2)}\right], \tag{2.81}$$

$$\widetilde{H}_{T}(\alpha, z) = \frac{\alpha}{2} \int_0^\infty du\, u^3 \int_{-1}^1 dx\, (1 - x^2)\, \exp\left[-\sqrt{u^2 + z^2(1 + \alpha^2 x^2)}\right], \tag{2.82}$$

$$\widetilde{H}_{L}(\alpha, z) = \alpha \int_0^\infty du\, u^3 \int_{-1}^1 dx\, x^2\, \exp\left[-\sqrt{u^2 + z^2(1 + \alpha^2 x^2)}\right], \tag{2.83}$$

where the parameters are defined as

$$\alpha = \frac{\tau_0}{\tau}\sqrt{1 + \Sigma_0}, \qquad z = \frac{m}{\Lambda_0}.$$

Conformal (massless) limit

In the conformal (massless) limit ($m \to 0$), the dependence of the kernels $\widetilde{H}_X(\alpha, z)$ on the ratio m/T (or m/Λ_0) vanishes. The integral expressions therefore simplify substantially, and the system's dynamics depend only on the scaled time variable τ'/τ and the initial anisotropy parameter Σ_0. In this limit, the equilibrium equation of state takes the conformal form

$$\varepsilon_{\text{eq}} = 3P_{\text{eq}} = \frac{3T^4}{\pi^2}, \tag{2.84}$$

and the evolution equations become scale invariant.

In the conformal limit, the integral equations for the energy density and pressures reduce

to

$$\varepsilon_{\text{conf}}(\tau) = D(\tau,\tau_0)\,\frac{\Lambda_0^4}{4\pi^2\alpha_0}\,\widetilde{H}_\varepsilon\Big(\frac{\tau_0}{\tau}\sqrt{1+\Sigma_0},\,0\Big) + \frac{1}{4\pi^2}\int_{\tau_0}^{\tau} d\tau'\,\frac{D(\tau,\tau')}{\tau_R(\tau')}\,T^4(\tau')\,\widetilde{H}_\varepsilon\Big(\frac{\tau'}{\tau},\,0\Big), \tag{2.85}$$

$$P_{L,\text{conf}}(\tau) = D(\tau,\tau_0)\,\frac{\Lambda_0^4}{4\pi^2\alpha_0}\,\widetilde{H}_L\Big(\frac{\tau_0}{\tau}\sqrt{1+\Sigma_0},\,0\Big) + \frac{1}{4\pi^2}\int_{\tau_0}^{\tau} d\tau'\,\frac{D(\tau,\tau')}{\tau_R(\tau')}\,T^4(\tau')\,\widetilde{H}_L\Big(\frac{\tau'}{\tau},\,0\Big), \tag{2.86}$$

$$P_{T,\text{conf}}(\tau) = D(\tau,\tau_0)\,\frac{\Lambda_0^4}{8\pi^2\alpha_0}\,\widetilde{H}_T\Big(\frac{\tau_0}{\tau}\sqrt{1+\Sigma_0},\,0\Big) + \frac{1}{8\pi^2}\int_{\tau_0}^{\tau} d\tau'\,\frac{D(\tau,\tau')}{\tau_R(\tau')}\,T^4(\tau')\,\widetilde{H}_T\Big(\frac{\tau'}{\tau},\,0\Big). \tag{2.87}$$

In the massless (conformal) limit, $z \to 0$, the integrals can be evaluated analytically, yielding [52]

$$\widetilde{H}_\varepsilon(y,0) = \frac{6}{y}\,\tan^{-1}\!\Big(\frac{1}{y}\Big) + \frac{3y^2-1}{(1+y^2)^2}, \tag{2.88}$$

$$\widetilde{H}_T(y,0) = \frac{3}{2(1+y^2)} + \frac{3y^2}{2(1+y^2)^2}\left[y\,\tan^{-1}\!\Big(\frac{1}{y}\Big) - 1\right], \tag{2.89}$$

$$\widetilde{H}_L(y,0) = \frac{3}{(1+y^2)^2}\left[y\,\tan^{-1}\!\Big(\frac{1}{y}\Big) - \frac{y^2}{3}\right]. \tag{2.90}$$

The conformal kernels $\widetilde{H}_X(y,0)$ depend only on the ratio of proper times and the initial anisotropy. The absence of any mass scale implies that the overall normalization, set by the initial momentum scale Λ_0, can be absorbed into the initial energy density for a fixed Σ_0. Consequently, all physical observables can be expressed in terms of dimensionless combinations such as $\tau T(\tau)$, making the evolution manifestly scale invariant.

This intrinsic scale invariance explains why, in conformal kinetic systems, the solutions exhibit early-time attractor behaviour: different initial conditions collapse onto a single universal curve. Conversely, introducing finite masses or other non-conformal effects breaks

this invariance and delays the onset of hydrodynamization, leading to system-dependent evolution at early times.

2.5 Relaxation-time ansatz for the QGP

A commonly used parametrisation of the microscopic relaxation time [81, 82, 83] in studies of the quark-gluon plasma is

$$\tau_R(\tau) \;=\; \frac{\eta}{s}\,\frac{1}{T(\tau)}, \tag{2.91}$$

where η is the shear viscosity, s the entropy density and T the local temperature. This ansatz captures two physically motivated features: (i) τ_R should scale inversely with temperature because higher temperatures increase particle densities and collision rates, and (ii) the dimensionless ratio η/s controls the overall collisionality of the medium and therefore sets the timescale for relaxation relative to microscopic scales.

A simple kinetic argument leading to the functional form (2.91) starts from the scaling of transport coefficients in a relativistic, approximately conformal gas. For massless degrees of freedom the entropy density scales as $s \sim T^3$ and, up to order-one numerical factors that depend on the microscopic theory, the shear viscosity in a relaxation-time model behaves like

$$\eta \;\sim\; (\text{const.})\; T^4\, \tau_R \;,$$

i.e. η is proportional to the product of the entropy density and the characteristic relaxation time (this relation can be obtained more precisely in AW-RTA kinetic theory, where prefactors such as $4/5$ appear). Rearranging gives $\tau_R \sim \eta/T^4$, and inserting the conformal scaling of s yields the convenient form $\tau_R \propto (\eta/sT)$. The precise numerical prefactor is model dependent and depends on the choice of kinetic approximation and particle content; hence (2.91) is usually quoted up to an $\mathcal{O}(1)$ factor.

Typical values for the dimensionless viscosity η/s used in phenomenological studies

range from the conjectured lower bound $\eta/s \sim 1/(4\pi)$ up to $\eta/s \sim \mathcal{O}(0.1-0.2)$ [84, 14, 85, 13]. Equation (2.91) then implies that the microscopic relaxation time is of order

$$\tau_R \sim \frac{0.05-0.2}{T},$$

modulo order-one prefactors. Thus, at temperatures of several hundred MeV typical of the early quark–gluon plasma, τ_R is a fraction of a fm, consistent with the short microscopic timescales inferred from heavy-ion phenomenology.

It is important to emphasise limitations and variants of this ansatz. The relation (2.91) is motivated by conformal, weakly coupled kinetic theory and assumes that a single timescale controls relaxation. In realistic systems the relaxation time can depend on particle momentum, chemical composition, or coupling strength; one may therefore consider generalized forms such as $\tau_R(p) \propto p^{\Lambda}/T^{1+\Lambda}$ (momentum dependence) or more general temperature power laws $\tau_R \propto T^{-\alpha}$. Moreover, numerical prefactors that relate η, s and τ_R differ between AW-RTA, Chapman–Enskog, or full Boltzmann treatments and must be fixed by microscopic calculation or matching to transport theory.

Finally, the choice (2.91) has direct consequences for macroscopic evolution. Because τ_R increases as temperature decreases, the effective collisionality of the medium weakens at late times, enhancing memory effects encoded by the damping factor $D(\tau,\tau') = \exp\big[-\int_{\tau'}^{\tau} d\bar{\tau}/\tau_R(\bar{\tau})\big]$. This temperature scaling therefore affects isotropization and hydrodynamisation times: for fixed η/s a hotter system relaxes faster, while for larger η/s relaxation is slower and hydrodynamic behaviour sets in later. When more realistic momentum dependence is included, the simple picture implied by (2.91) must be refined.

Chapter 3

Equilibration Under Perturbations: External Forces

Studies of the $0+1$D Boltzmann equation, particularly in the relaxation-time approximation, have shown that hydrodynamic attractors [40, 38, 39, 37, 44, 41, 42, 43] arise naturally in conformal systems. In these systems, which describe massless particles with a scale-invariant equation of state, far-from-equilibrium initial conditions rapidly converge onto a universal evolution curve for observables such as the pressure anisotropy and shear stress. This behaviour indicates that hydrodynamics can effectively describe the system even before local thermal equilibrium is reached. The attractor represents a non-perturbative resummation of the hydrodynamic gradient series, which is divergent and asymptotic, and demonstrates that the system quickly loses memory of its initial conditions. At late times, the attractor seamlessly merges with standard second-order hydrodynamics.

In contrast, non-conformal systems, such as those consisting of massive particles with nonzero bulk viscosity, do not exhibit a universal early-time attractor [79, 86, 87, 88]. Numerical solutions of the integral Boltzmann equation for a range of initial conditions show that the evolution of shear and bulk viscous stresses remains strongly dependent on the initial state. The breaking of conformal symmetry introduces additional scales and couplings—particularly between shear and bulk sectors—that prevent the system from collapsing onto a single universal trajectory at early times. While the system eventually converges to hydrodynamic behaviour at late times, this convergence is not considered an attractor in the same sense, as it requires the system to be nearly isotropic. These observations highlight that early-time attractor formation is closely tied to conformal symmetry, and in

its absence, the early-time dynamics retain significant memory of the initial conditions.

A natural extension of these studies, to confirm the symmetry dependence of early time attractors, is to introduce further perturbations to the simple $0+1$D system. External perturbations can significantly modify both the attractor structure and the hydrodynamisation dynamics. In particular, they can suppress the formation of early-time attractors, leaving only late-time attractors that dominate the asymptotic evolution. The introduction of external fields adds additional energy scales and drives the system away from the simple scaling behaviour observed in unperturbed cases. This has important implications for physical systems subjected to strong fields or gradients, such as the electromagnetic fields present in heavy-ion collisions.

Another important extension concerns the role of momentum-dependent relaxation times. Much of the previous work on hydrodynamisation has assumed a momentum-independent relaxation time, simplifying the moment equations of the Boltzmann equation. However, in realistic systems, the relaxation time is generally momentum-dependent, reflecting the underlying collision cross section. Incorporating this momentum dependence introduces a new physical scale into the otherwise simple $0+1$D system, coupling different energy scales in a nontrivial way. As a result, multiple characteristic decay times emerge, affecting both the rate of thermalisation and the structure of any emergent attractors. Studying these effects is therefore crucial for connecting the microscopic dynamics of far-from-equilibrium quark-gluon plasma with its macroscopic hydrodynamic behaviour.

Taken together, these extensions—considering both external forces and momentum-dependent relaxation times—provide a more realistic framework for exploring attractor phenomena in non-equilibrium systems. They allow for the investigation of how additional physical scales and perturbations influence the onset of universal behaviour, the emergence of multiple decay modes, and the eventual convergence to hydrodynamics. This framework will facilitate a thorough understanding of far-from-equilibrium dynamics in systems like

the quark-gluon plasma generated in heavy-ion collisions

3.1 External forces

In this section, we investigate the influence of proper-time–dependent longitudinal forces on the evolution of a far-from-equilibrium system governed by the relativistic Boltzmann equation under Bjorken symmetry. Employing the AW-RTA for the collision kernel, we derive an exact integral solution to the Boltzmann equation in the presence of such external forces and analyze their effect on the hydrodynamic attractor behaviour of conformal and non-conformal systems.

The motivation for this study arises from the physics of relativistic heavy-ion collisions, where extremely strong, transient magnetic fields—of the order of 10^{18}–10^{19} G—are generated during the early stages of non-central Au+Au collisions at RHIC ($\sqrt{s_{NN}} = 200\,\text{GeV}$) and Pb+Pb collisions at the LHC ($\sqrt{s_{NN}} = 2.76 - 5.02\,\text{TeV}$) [89, 90, 91]. These fields induce external forces on the quark–gluon plasma (QGP), influencing its microscopic evolution toward local equilibrium. Given that early time hydrodynamic attractors are proposed as solution to the hydrodynamisation problem, it becomes essential to explore whether these attractors persist when external fields peturb evolution dynamics.

3.1.1 Boltzmann equation in the presence of an external force

To investigate the effect of external fields on the evolution of a boost-invariant system, we extend the $0+1$D Boltzmann equation in the relaxation-time approximation to include an external longitudinal force term. In the presence of such a force, the kinetic equation in Milne coordinates takes the form

$$\left(\frac{\partial}{\partial\tau} - \frac{p_z}{\tau}\frac{\partial}{\partial p_z} + F_z\frac{\partial}{\partial p_z}\right) f(\tau, p_T, p_z) = -\frac{1}{\tau_R(\tau)}\big(f(\tau, p_T, p_z) - f_{\text{eq}}(\tau, p_T, p_z)\big), \quad (3.1)$$

where F_z denotes the external longitudinal force. The standard Bjorken term $-p_z/\tau\,\partial_{p_z} f$ shift of longitudinal momentum due to expansion, while the new term $F_z\,\partial_{p_z} f$ represents the additional acceleration (or deceleration) of particles along the z direction.

The introduction of an external force inevitably breaks one or more of the spacetime symmetries that underlie Bjorken flow. In particular, a longitudinal force modifies the boost-invariant expansion by introducing an additional scale and directionality along the beam axis. To approximately preserve the Bjorken flow profile, we consider the simplest possible configuration in which the external force depends only on the proper time τ and acts along the longitudinal (z) direction. This choice breaks the reflection symmetry about $z = 0$. Furthermore, we assume that the applied force is weak enough so that the induced perturbation in the flow velocity, δu^μ, remains small compared to the equilibrium Bjorken velocity u_B^μ and therefore the system is approximately boost invariant. Thus, the four-velocity can be expressed as

$$u^\mu = u_B^\mu + \delta u^\mu, \tag{3.2}$$

where $|\delta u^\mu| \ll |u_B^\mu|$. This approximation remains valid as long as the modifications of the macroscopic fields due to the external force are smaller than their equilibrium values.

Under these assumptions, the Boltzmann equation in the relaxation-time approximation for a system experiencing a time-dependent longitudinal force $\mathcal{F}(\tau)$ can be written as (see Appendix A.1.1 for details)

$$\left[\mathcal{F}(\tau)\,\tau\,\frac{\partial}{\partial w} + \frac{\partial}{\partial \tau}\right] f(\tau, w, p_T) = -\,\frac{(f - f_{\text{eq}})}{\tau_R(\tau)}\,, \tag{3.3}$$

where $w \equiv \tau\, p_z$ denotes the longitudinal momentum variable defined in the Bjorken frame. Here we have absorbed the p_z term by the variable redefinition elucidated in section (2.4) to obtain Eq. (3.1). The first term on the left-hand side represents the effect of the external force, while the second term corresponds to the usual expansion-driven dilution. The right-hand side describes relaxation toward local equilibrium over the microscopic timescale τ_R.

To obtain the formal solution of Eq. (3.3), we assume that the force $\mathcal{F}(\tau)$ is nonzero over the interval $\tau_i < \tau < \tau_f$, where τ_i and τ_f denote the initial and final proper times, respectively. For convenience, we introduce a dimensionless function $F(\tau)$ and express the force as

$$\mathcal{F}(\tau) = \frac{\alpha}{\tau_F} F(\tau), \tag{3.4}$$

where α has dimensions of momentum and τ_F is a characteristic time scale such that α/τ_F carries dimensions of force.

Following the method of characteristics, we perform a change of variables from (w, τ) to (r, s):

$$r = w - \alpha s, \tag{3.5}$$

$$s = \int_0^\tau F(\tau') \frac{\tau'}{\tau_F} \, d\tau'. \tag{3.6}$$

Here, the new variable $s(\tau)$ serves as a rescaled proper time that accounts for the cumulative effect of the external force. In these transformed coordinates, the Boltzmann equation (3.3) reduces to

$$\frac{\partial f(r, s, p_T)}{\partial s} = - \frac{\tau_F}{\tau_R(\tau(s))} \frac{f - f_{\text{eq}}}{F(\tau(s))\, \tau(s)}. \tag{3.7}$$

This is a first-order ordinary differential equation in s whose formal solution is analogous to that of the standard AW-RTA equation, with the force dependence entering through the variable transformation. The general solution is given by

$$f(s, r, p_T) = D(s, s_0)\, f_0(r, p_T) + \int_{s_0}^{s} ds' \, \frac{D(s, s')}{\tau_R(s')} \, f_{\text{eq}}(s', r, p_T), \tag{3.8}$$

where f_0 is the initial distribution function and the damping function is defined as

$$D(s_1, s_2) = \exp\left[- \int_{s_1}^{s_2} \frac{ds'}{F(\tau(s'))\, (\tau(s')/\tau_F)\, \tau_R(s')} \right]. \tag{3.9}$$

At first glance, the damping function appears to depend explicitly on the external force through $F(\tau)$. However, when changing the coordinates back to τ the explicit dependence on force disappears (Appendix (A.1.1)). Therefore, the external force influences the microscopic evolution only implicitly through its effect on $\tau_R(\tau)$ or through the modified characteristic variables, while the structure of the damping function itself remains unchanged.

The solution (3.8) represents the formal integral solution of the AW-RTA Boltzmann equation in the presence of a longitudinal force. The first term captures the exponentially damped memory of the initial state, while the second term describes the cumulative approach toward equilibrium. The presence of the external force modifies the phase-space trajectories of the particles, thereby altering the mapping between microscopic and macroscopic variables and influencing the system's approach to hydrodynamic behaviour.

3.1.2 Model parameters and numerical implementation

For the remainder of this study, we employ the conformal parametrisation of the relaxation time,

$$\tau_R(\tau) = \frac{5c}{T(\tau)}\,, \tag{3.10}$$

where c is a dimensionless constant proportional to the ratio η_0/s_0, and therefore controls the initial shear viscosity of the system. This choice of τ_R reflects the conformal scaling expected in a relativistic gas, where the microscopic relaxation time is inversely proportional to temperature. In all simulations, the initial proper time is taken to be $\tau_0 = 0.1$ fm, and the initial temperature is set to $T_0 = 500$ MeV, consistent with conditions in the early stages of a heavy-ion collision. For non-conformal calculations, a finite particle mass $m = 200$ MeV is introduced, thereby breaking conformal symmetry and generating a non-zero bulk viscosity.

3.1.3 Initial conditions

The initial single-particle distribution function is taken to be of the Romatschke–Strickland (RS) form [51], which provides a convenient parametrisation of momentum-space anisotropy in a longitudinally expanding system. The RS distribution is expressed as

$$f_0(p_T, p_z, : N_0, \Lambda_0, \Sigma_0) = \frac{2}{(2\pi)^3 N_0} \exp\left[-\frac{\sqrt{p_T^2 + (1+\Sigma_0)p_z^2 + m^2}}{\Lambda_0}\right], \tag{3.11}$$

where Λ_0 is an energy scale analogous to an effective temperature, Σ_0 is the initial anisotropy parameter, and N_0 is a normalisation constant.

The three parameters N_0, Σ_0, and Λ_0 together determine the initial thermodynamic properties of the system—namely the temperature T_0, longitudinal pressure P_L, and transverse pressure P_T. In the isotropic limit ($\Sigma_0 \to 0$), the distribution (3.11) reduces to the local equilibrium Maxwell–Jüttner form with temperature Λ_0. A positive anisotropy parameter ($\Sigma_0 > 0$) corresponds to an oblate momentum-space distribution ($P_L < P_T$), while $\Sigma_0 < 0$ describes a prolate deformation ($P_L > P_T$).

The parameters Λ_0 and N_0 are fixed by imposing Landau matching, ensuring that the energy density obtained from the anisotropic distribution equals that of an equilibrium system at the same initial temperature T_0. This guarantees that the macroscopic energy density remains same at the initial time τ_0 for systems with different initial anisotropy. To explore different physical regimes, the ratio m/Λ_0 can be varied by adjusting N_0, while keeping the initial energy density and anisotropy parameter Σ_0 fixed.

Non-conformal initial conditions

For the non-conformal case ($m/\Lambda_0 \neq 0$), a finite particle mass is introduced to break conformal symmetry and generate a non-zero bulk viscous pressure. The initial distribution function parameters are chosen to match those used in Ref. [92], allowing for direct comparison with previously studied non-conformal attractor dynamics. The corresponding pa-

rameters m/Λ_0, N_0, and Σ_0 for different initial viscous conditions are listed in Table 3.1. These parameter sets span a broad range of initial anisotropies and mass-to-temperature ratios, providing a consistent foundation for studying the effects of conformal symmetry breaking.

SNo.	0	1	2	3	4	5	6
m/Λ_0	0.016	4.808	10.89	0.294	1.818	2.023	20
N_0	0.655	4×10^{-5}	2.5×10^{-8}	0.078	0.0632	1.06×10^{-3}	1.48×10^{-13}
Σ_0	-0.832	-0.908	-0.949	1208.05	-0.987	0	0

Table 3.1: Values of m/Λ_0, N_0, and Σ_0 corresponding to different initial values of $(\Pi/P)_0$ and $(\pi/P)_0$ given in Table 3.3, used for the non-conformal Romatschke–Strickland initialization.

Conformal initial conditions

For the conformal case ($m = 0$), we fix the anisotropy parameter Σ_0 and the normalisation constant N_0 to be the same as in the corresponding non-conformal cases, but vary the value of Λ_0 to ensure that the initial energy density matches between the two setups. This procedure maintains consistency across conformal and non-conformal systems while isolating the effects of mass and conformal symmetry breaking. The conformal initial conditions for different values of $(\Pi/P)_0$ and $(\pi/P)_0$ are listed in Table 3.2. These values are reproduced from Ref. [92] for ease of comparison and validation.

SNo.	0	1	2	3	4	5	6
Λ_0 [MeV]	321.74	314	275	1089	198	500	500
Σ_0	-0.832	-0.908	-0.949	1208.05	-0.987	0	0

Table 3.2: Values of Λ_0 and Σ_0 corresponding to different initial shear stress ratios $(\pi/P)_0$ for the conformal case ($m = 0$), chosen to match the initial energy density of the non-conformal setup.

The corresponding initial viscous pressure ratios $(\Pi/P)_0$ and $(\pi/P)_0$, which quantify the degree of bulk and shear viscous corrections to the equilibrium pressure, are shown

in Table 3.3. Each entry is assigned a numerical label for convenience and for consistent reference across conformal and non-conformal configurations.

No.	0	1	2	3	4	5	6
$(\Pi/P)_0$	0	-0.25	-0.37	0	0	0.25	-0.85
$(\pi/P)_0$	-1	-1	-1	0.99	-1.8	0	0

Table 3.3: Initial values of the bulk pressure and shear stress ratios $(\Pi/P)_0$ and $(\pi/P)_0$, respectively, along with their reference numbers used for different initial conditions.

3.1.4 Parametrisation of the External Force

To model the influence of external fields in heavy-ion collisions, we consider an exponentially decaying longitudinal force. This choice is motivated by the rapid decay of chromoelectric and electromagnetic fields generated immediately after the collision. The force is parametrised as

$$F(\tau) = \frac{\tau}{\tau_F} \exp\left(1 - \frac{\tau}{\tau_F}\right), \tag{3.12}$$

where τ_F denotes the characteristic decay timescale of the force. The force reaches its maximum value at $\tau = \tau_F$, with the corresponding magnitude of the physical force given by $\mathcal{F}_{\text{max}} = \alpha/\tau_F$. Here, α has dimensions of momentum, such that α/τ_F carries the dimensions of a squared momentum (i.e., a force). By varying the parameters α and τ_F, one can independently control the strength and duration of the external force, allowing for systematic exploration of its impact on the system's evolution.

A plot of the normalised force profile for different decay timescales is shown in Fig. 3.1. The parameter τ_F determines the width of the force pulse: smaller values correspond to a sharper, more rapidly decaying field, while larger τ_F values result in a broader, slowly decaying profile. This parametrisation provides a physically motivated yet analytically tractable way to study the response of an expanding medium to transient external fields.

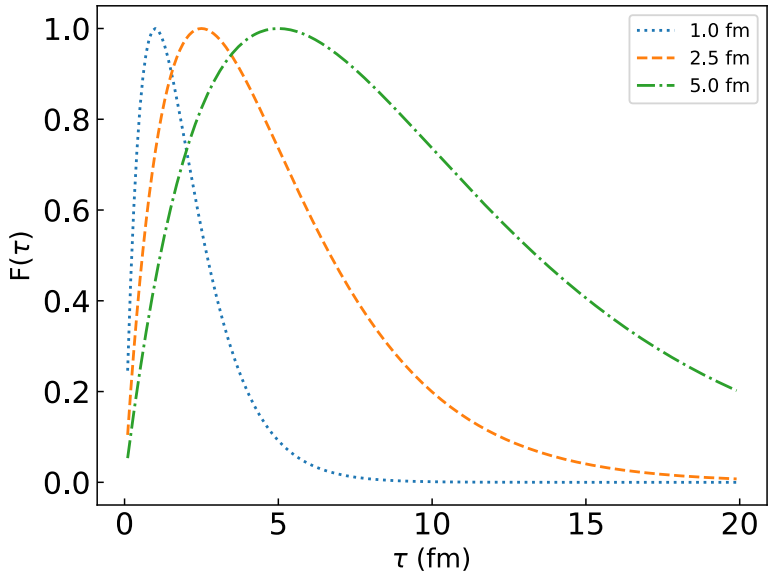

Figure 3.1: Normalised external force profile (with $\max(F) = 1$) for different decay timescales: $\tau_F = 1$ fm (dotted), $\tau_F = 2.5$ fm (dashed), and $\tau_F = 5$ fm (dot-dashed).

Macroscopic observables

Using the Romashke-Strickland distribution as the initial condition and taking momentum moments of the distribution function in Eq.(3.8), we get the energy density and pressure components in the presence of the external force,

$$\varepsilon(s) = D(s,s_0)\,\frac{\Lambda_0^4}{4\pi N_0}\,H_F^{\varepsilon}\big[s_0,s,\Sigma_0,\alpha/\Lambda_0,m/\Lambda_0\big] + \int_{s_0}^{s} ds'\,\frac{D(s,s')}{\tau_R(s')}\,T^4(s')\,H_F^{\varepsilon}\big[s',s,\alpha/T(s'),m/T(s')\big], \tag{3.13}$$

$$P_L(s) = D(s,s_0)\,\frac{\Lambda_0^4}{4\pi N_0}\,H_F^{L}\big[s_0,s,\Sigma_0,\alpha/\Lambda_0,m/\Lambda_0\big] + \int_{s_0}^{s} ds'\,\frac{D(s,s')}{\tau_R(s')}\,T^4(s')\,H_F^{L}\big[s',s,\alpha/T(s'),m/T(s')\big], \tag{3.14}$$

$$P_T(s) = D(s,s_0)\,\frac{\Lambda_0^4}{4\pi N_0}\,H_F^{T}\big[s_0,s,\Sigma_0,\alpha/\Lambda_0,m/\Lambda_0\big] + \int_{s_0}^{s} ds'\,\frac{D(s,s')}{\tau_R(s')}\,T^4(s')\,H_F^{T}\big[s',s,\alpha/T(s'),m/T(s')\big]. \tag{3.15}$$

where the functions H_F^{ε}, H_F^L, and H_F^T are modified kernel functions that encode the effects of the external force α (See Appendix (A.2) for explicit expressions). These kernels reduce to the standard force-free forms when $\alpha = 0$. The parameter α introduces an additional scale that affects the isotropization process and modifies the evolution of the macroscopic observables.

The off-diagonal component appearing when reflection symmetry is broken is

$$T^{03}(s) = \int_{s_0}^{s} ds' \, \frac{D(s,s')}{\tau_R(s')} \, T^4(s') \, H_F^{03}\big[s', s, m/T(s')\big]. \tag{3.16}$$

The coupled evolution equations for the energy density and temperature, given in Eq. (3.13), are solved numerically using an iterative method. An enhanced and computationally more efficient version of the algorithm described in the literature is presented in Appendix A.3. Once the temperature profile $T(\tau)$ is determined, the pressure components can be evaluated directly using Eqs. (3.14) and (3.15). The relationship between energy density and temperature for a system of massive particles is given by

$$\mathcal{E}(T) = \frac{3T^4}{\pi^2} \left[\frac{z^2}{2} K_2(z) + \frac{z^3}{6} K_1(z) \right], \tag{3.17}$$

where $z = m/T$ and K_1, K_2 are modified Bessel functions of the second kind. In the conformal limit ($m \to 0$), this expression reduces to the familiar relation $\mathcal{E} = 3T^4/\pi^2$. The use of Eq. (3.17) allows for a consistent treatment of both conformal and non-conformal dynamics within the same numerical framework.

3.2 Emergence of attractors

Previous studies have shown that for non-conformal systems, a universal attractor is not obtained for all hydrodynamic variables. In particular, Jaiswal *et al.* [92] demonstrated that only the scaled longitudinal pressure, $\bar{P}_L = \frac{P_L}{P}$ where P is the equilibrium isotropic pressure, exhibits attractor-like behaviour, whereas other scaled quantities such as the bulk

pressure (Π/P) and the shear pressure (π/P) do not collapse onto a universal curve. Here, we examine how the presence of an external longitudinal force influences the attractor structure of hydrodynamic observables.

Figure 3.2 shows the evolution of the scaled longitudinal pressure $\bar{P}_L$ for three different force strengths: $\alpha = 0$ (top panel), $\alpha = 50$ (middle panel), and $\alpha = 100$ (bottom panel), each corresponding to a fixed decay timescale $\tau_F = 1$ fm/c. In each subplot, the coloured curves represent different initial anisotropies as specified in Table 3.1. For the zero-force case ($\alpha = 0$), our results reproduce the attractor behaviour observed in the previous study [92]. However, when the external force is non-zero, the early-time convergence is lost, and only a late-time attractor persists. This indicates that the presence of a longitudinal force disrupts the universality of the early-time attractor, delaying the onset of hydrodynamic scaling.

3.2.1 Attractor behaviour in the massless limit

Conformal systems, by contrast, are known to exhibit robust early-time attractor behaviour across a wide range of initial conditions and flow configurations [37, 93, 76, 94, 95, 96]. To test the persistence of such behaviour under the influence of an external force, we examine the massless limit ($m = 0$) of our model.

In Figure 3.3, the scaled longitudinal and transverse pressures,

$$\bar{P}_L = \frac{P_L}{P}, \qquad \bar{P}_T = \frac{P_T}{P},$$

are plotted for different initial conditions (given in Table 3.2) in the presence of an external force of strength $\alpha = 100$. Even when the system is subjected to an external perturbation, we find that an early-time attractor persists in both $\bar{P}_L$ and $\bar{P}_T$. The convergence occurs much earlier than in the massive case (see Fig. 3.2), indicating that conformal symmetry enhances the robustness of attractor dynamics.

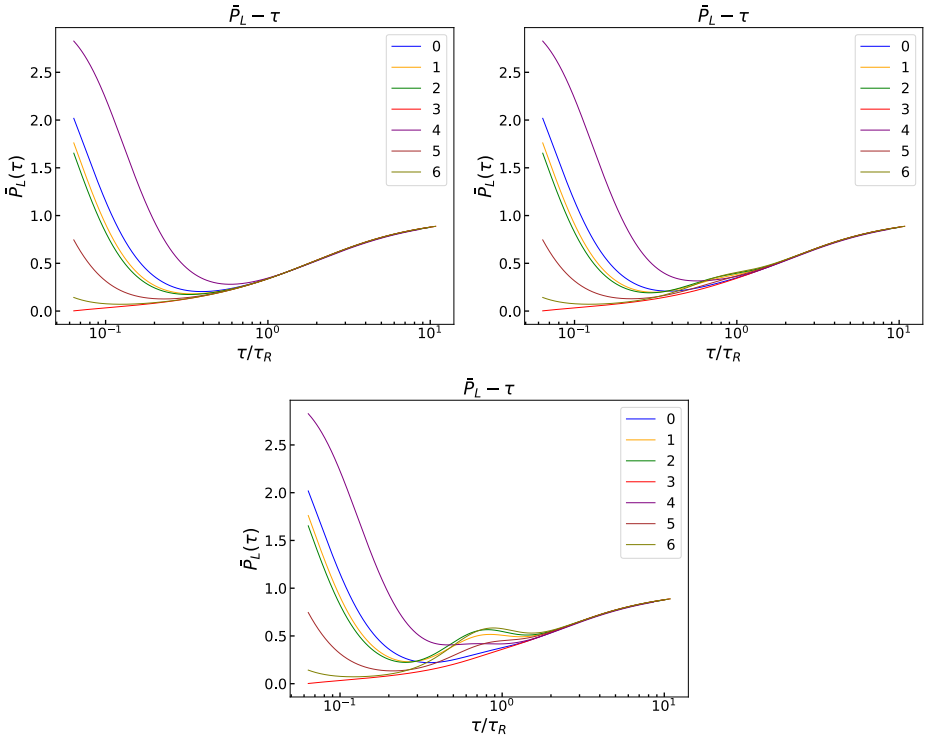

Figure 3.2: Evolution of the scaled longitudinal pressure $\bar{P}_L = P_L/P$ for $\alpha = [0,\ 50,\ 100]$, $\tau_F = 1$ fm/c, and various initial conditions. The system reproduces the results of Ref. [92] for $\alpha = 0$, while finite forces suppress early-time universality and preserve only the late-time attractor.

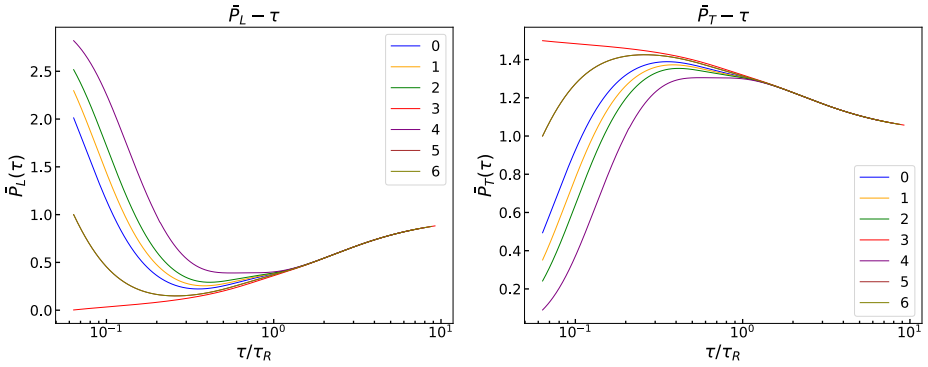

Figure 3.3: Scaled transverse ($\bar{P}_T$) and longitudinal ($\bar{P}_L$) pressures plotted for varying initial conditions (given in Table 3.2) in the presence of an external force of strength $\alpha = 100$ for the massless case.

However, this result holds only when the external force decays sufficiently before the system equilibrates. If the forcing persists for longer times, it can distort or delay the onset of

hydrodynamic scaling. The equilibration rate is primarily controlled by the exponentially decaying damping function $D(\tau, \tau')$, defined in Eq. (3.9). From Eqs. (3.13)–(3.15), it is evident that the system's relaxation dynamics arise from the interplay between this damping function and the kinematic functions $H_{\mathcal{E}}$, H_{P_L}, and H_{P_T}.

The primary modifications, therefore, originate from the H_{P_L/P_T} functions, which are more sensitive to the presence of mass and external force. In the massless limit, conformal symmetry effectively removes these sensitivities, restoring the early-time attractor. This combination of factors—reduced sensitivity to force and conformal scaling symmetry—explains the re-emergence of early-time universality in the conformal regime.

3.3 Summary

In this section, we investigated the impact of external longitudinal forces on the evolution and attractor behaviour of systems described by the $0+1$D Boltzmann equation within the relaxation-time approximation. By extending the formal integral solution to include a time-dependent external force, we demonstrated that such perturbations significantly modify the system's hydrodynamic response. For non-conformal systems, which already lack a universal early-time attractor, the presence of an external force further suppresses convergence among different initial conditions, leaving only a late-time attractor that emerges as the system approaches equilibrium. This behaviour arises from the explicit breaking of boost and reflection symmetries induced by the force, which disrupts the simple scaling structure that underlies attractor formation.

In contrast, in the conformal (massless) limit, where scale invariance is restored, the system retains an early-time attractor even in the presence of moderate external forces. The robustness of the conformal attractor stems from the reduced sensitivity of the damping dynamics to the force and the dominance of conformal scaling in governing relaxation.

These findings indicate that while conformal symmetry enables early-time universality, its breaking—either through finite mass or external perturbations—destroys this universality, delaying hydrodynamisation. Thus, the study of forced kinetic evolution reveals that early-time attractors are not a generic feature of the quark–gluon plasma but rather a manifestation of underlying conformal symmetry and the absence of external driving.

Chapter 4

Equilibration Under Perturbations: Momentum Dependent Relaxation Time

In kinetic theory, the assumption of a single, momentum–independent relaxation time τ_R is a strong simplification. In general, microscopic scattering processes do not drive all momentum modes back to equilibrium at the same rate. A more realistic description accounts for a momentum–dependent relaxation time $\tau_R(p)$. By introducing momentum dependence in the relaxation time, one can capture the multi–scale nature of microscopic dynamics. However, introducing $\tau_R(p)$ requires modifying the simple Anderson–Witting collision kernel and employing a more general Novel Relaxation Time Approximation (NRTA) [74, 73] to ensure that conservation laws hold for arbitrary hydrodynamic frame choices (i.e., definitions of the non-equilibrium temperature and chemical potential), which in this thesis is the Landau frame.

When the relaxation time depends on particle momentum, different moments of the distribution function approach equilibrium at distinct rates. For example, in a quark–gluon plasma, low-momentum particles undergo more frequent collisions, resulting in shorter relaxation times and faster equilibration. High-momentum particles, on the other hand, scatter less efficiently, leading to larger values of $\tau_R(p)$ and slower relaxation [97]. Unlike the momentum-independent relaxation-time model, which features a single exponential decay governed by $1/\tau_R$, the momentum-dependent case exhibits multiple relaxation modes corresponding to different moments of the distribution. Consequently, hydrodynamic quantities such as shear stress, bulk pressure, and diffusion currents become sensitive to the microscopic energy dependence of scattering processes. This leads to a slower relaxation

of transport coefficients than in constant-τ_R models and yields equilibration patterns that more accurately reflect QCD dynamics, where the collision rates are intrinsically momentum dependent [97].

To incorporate momentum dependence, we employ a simple power–law ansatz,

$$\tau_R(p) = \tau_R^0(T)\, p^\Lambda \,. \tag{4.1}$$

The relaxation time $\tau_R(p)$ is factorised into a temperature–dependent prefactor $\tau_R^0(T)$, independent of momentum, and a momentum–dependent factor that scales with the single–particle energy p, raised to a positive exponent $\Lambda > 0$ [97, 98].

The temperature–dependent prefactor $\tau_R^0(T)$can be related to the shear viscosity to entropy density ratio of the medium, and is given by [98]

$$\tau_R^0(T) = \left(\frac{\eta}{s}\right) \frac{5!}{\Gamma(5+\Lambda)} \frac{1}{T^{1+\Lambda}} \,. \tag{4.2}$$

In what follows, the notation τ_R, whether appearing in the main text or in the figures, will always refer to this thermal prefactor $\tau_R^0(T)$, and should not be confused with the full relaxation time $\tau_R(p)$.

4.1 The moment equations

Moment equations are a systematic set of evolution equations derived from kinetic theory that describe the dynamics of a many-particle system in terms of moments of the distribution function. The moments are obtained by integrating the single partice distribution function against powers of momentum or other weight functions. The hierarchy of moment equations provides a bridge between microscopic kinetic theory and macroscopic hydrodynamics. By taking successive momentum moments of the Boltzmann equation, one obtains evolution equations for conserved quantities such as particle number, energy, and momentum, as well as for higher–order fluxes like shear stress, bulk pressure, and heat flow. In principle, this

procedure generates an infinite set of coupled equations, often each moment depends on higher order ones. For numerical applications, however, this hierarchy needs to be truncated to a finite set of equations. This makes the moment method a practical tool for simulating non-equilibrium dynamics, since it captures both the conservation laws and the dissipative corrections needed for realistic hydrodynamic modeling.

The moment hierarchy can be used to study the hydrodynamization process, i.e. how a far-from-equilibrium system evolves toward a state where hydrodynamics becomes applicable. Since the lowest moments correspond to conserved densities and currents while the higher moments encode increasingly fine details of the non-equilibrium distribution, tracking their evolution provides a direct way to monitor how quickly different moments of the system relax. In practice, one can solve the truncated set of moment equations numerically and compare the time scales over which higher moments (e.g. anisotropies in momentum space) decay relative to the conserved ones. This makes it possible to identify when the system's dynamics can be reliably described by hydrodynamics, even if full local thermal equilibrium has not yet been reached. The moment approach therefore can provide quantitative insight into the onset of hydrodynamic behavior.

In this section, we consider a system of massless particles undergoing Bjorken expansion [77], which is invariant under longitudinal Lorentz boosts. The moments $\rho_{n,l}$ are defined as

$$\rho_{n,l}(\tau) = \int dP p^n P_{2l}(\cos\theta) f(\tau, p^0, p_z) \,, \tag{4.3}$$

where $f(\tau, p^0, p_z)$ is the single–particle distribution function depending on the proper time τ, the energy p^0 and longitudinal momentum p_z. Here P_{2l} denotes the Legendre polynomial of order $2l$, phase-space measure is $dP = \frac{d^3p}{(2\pi)^3 p^0}$, the single-particle energy is $E = p^0 = p$, and $\cos\theta = p_z/p = p_\eta/(\tau p)$. In this definition, the index n characterizes the energy scaling of the moment, while l encodes the degree of momentum anisotropy in the system.

In particular, the moments $\rho_{1,0}$ and $\rho_{2,0}$ correspond to the particle number density (n) and the equilibrium energy density (ϵ), respectively. For the equilibrium distribution function, the moment expressions can be computed explicitly,

$$\rho^{eq}_{n,l}(T,\mu) = e^{\mu/T}\frac{T^{n+2}}{2\pi^2}\Gamma(n+2)\delta_{l0}\,. \tag{4.4}$$

The isotropy of the Maxwell-Juttner distribution function implies that l moments higher than 0 vanish.

The hierarchy of moment evolution equations can be derived from the kinetic equation (2.29), which under Bjorken flow in $0+1$ dimensions takes the form [78]

$$\left[\frac{\partial}{\partial\tau} - \frac{p_z}{\tau}\frac{\partial}{\partial p_z}\right] f_p = -\frac{1}{p}\,\mathbf{L}[\phi_p]\,, \tag{4.5}$$

where $\mathbf{L}$ denotes the linearized collision operator acting on the deviation ϕ_p from equilibrium (See Appendix B.1). From this kinetic equation, one obtains the corresponding hierarchy of moment equations:

$$\frac{\partial}{\partial\tau}\rho_{n,l} + \frac{1}{\tau}\Big[\mathcal{P}(n,l)\,\rho_{n,l-1} + \mathcal{Q}(n,l)\,\rho_{n,l} + \mathcal{R}(n,l)\,\rho_{n,l+1}\Big] = \int dP\, p^{n-1} P_{2l}(\cos\theta)\,\mathbf{L}[\phi_p]\,, \tag{4.6}$$

where the coefficients $\mathcal{P}(n,l)$, $\mathcal{Q}(n,l)$, and $\mathcal{R}(n,l)$ couple neighboring moments in the hierarchy and are given by

$$\begin{aligned}
\mathcal{P}(n,l) &= 2l\,\frac{(2l-1)}{(4l-1)}\,\frac{(n+2l)}{(4l+1)}\,,\\
\mathcal{Q}(n,l) &= \frac{2}{3} + \frac{n(8l^2+4l-1)}{(4l-1)(4l+3)} + \frac{2l(2l+1)}{3(4l-1)(4l+3)}\,,\\
\mathcal{R}(n,l) &= (n-2l-1)\,\frac{(2l+1)}{(4l+1)}\,\frac{(2l+2)}{(4l+3)}\,.
\end{aligned} \tag{4.7}$$

This set of coupled equations describes the evolution of the energy–momentum moments $\rho_{n,l}$ in a boost-invariant expanding system, with the coefficients encoding the kinematic couplings between different angular moments.

On the left-hand side of the moment equation, the streaming term of the Boltzmann equation generates couplings between different l-moments. For the AW-RTA with a momentum-independent relaxation time, the collision term on the right-hand side of Eq. (4.6) reduces to

$$C_{n,l} = \int dP\,(p)^{n-1}\, P_{2l}(\cos\theta)\mathbf{L}[\phi_p] = -\frac{1}{\tau_R}\left[\rho_{n,l} - \rho^{eq}_{n,l}\right] . \tag{4.8}$$

For in-cooperating the momentum-dependent relaxation time, we employ the generalized RTA defined in Eq. (2.37). For the system under study, the collision kernel reduces to (see Appendix B.1)

$$\begin{aligned} C_{n,l,\Lambda} = -\frac{1}{\tau^0_R}\Bigg[&\left\{\rho_{n-\Lambda,l} - \delta_{l0}\,\rho^{eq}_{n-\Lambda,l}\right\} - A\,\delta_{l0}\,\rho^{eq}_{n-\Lambda,0} \\ &- B\,\delta_{l0}\left\{\rho^{eq}_{n-\Lambda,0} - \frac{\rho^{eq}_{1-\Lambda,0}}{\rho^{eq}_{2-\Lambda,0}}\rho^{eq}_{n-\Lambda+1,0}\right\}\Bigg] , \end{aligned} \tag{4.9}$$

where the coefficients A and B take the form,

$$A = \frac{\rho_{1-\Lambda,0} - \rho^{eq}_{1-\Lambda,0}}{\rho^{eq}_{1-\Lambda,0}} , \tag{4.10}$$

$$B = \frac{\rho_{1-\Lambda,0} - \frac{\rho^{eq}_{1-\Lambda,0}}{\rho^{eq}_{2-\Lambda,0}}\rho_{2-\Lambda,0}}{\rho^{eq}_{3-\Lambda,0}\left(\frac{\rho^{eq}_{1-\Lambda,0}}{\rho^{eq}_{2-\Lambda,0}}\right)^2 - \rho^{eq}_{1-\Lambda,0}} . \tag{4.11}$$

Further simplification can be achieved if we use the equilibrium moment expression from (4.4) and use it to replace the equilibrium moment terms in (4.9). We then get the simplified expression (see Appendix B.1),

$$\begin{aligned} C_{n,l,\Lambda} = -\frac{1}{\tau_R}\Big[\rho_{n-\Lambda,l} - \delta_{l0}\Big\{ &T^{n-1}K(n,1,\Lambda)[1 - C(n,\Lambda)]\rho_{1-\Lambda,l} \\ &+ T^{n-2}K(n,2,\Lambda)C(n,\Lambda)\rho_{2-\Lambda,l}\Big\}\Big] . \end{aligned} \tag{4.12}$$

where we have defined the two functions,

$$K(n,m,\Lambda) = \frac{\Gamma(n-\Lambda+2)}{\Gamma(m-\Lambda+2)} , \tag{4.13}$$

$$C(n,\Lambda) = \frac{1 - K(1,n,\Lambda)K(n+1,2,\Lambda)}{1 - K(1,2,\Lambda)K(3,2,\Lambda)} . \tag{4.14}$$

Note that

$$K(n,n,\Lambda) = \frac{\Gamma(n-\Lambda+2)}{\Gamma(n-\Lambda+2)} = 1\,, \tag{4.15}$$

$$C(1,\Lambda) = \frac{1-K(1,1,\Lambda)K(2,2,\Lambda)}{1-K(1,2,\Lambda)K(3,2,\Lambda)} = 0 \tag{4.16}$$

$$C(2,\Lambda) = \frac{1-K(1,2,\Lambda)K(3,2,\Lambda)}{1-K(1,2,\Lambda)K(3,2,\Lambda)} = 1\,, \tag{4.17}$$

and enforce the conservation laws for energy density $\epsilon = \rho_{2,0}$ and number density $n = \rho_{1,0}$,

$$C_{1,0,\Lambda} = 0\,,$$

$$C_{2,0,\Lambda} = 0\,,$$

independent of the value of Λ.

For a momentum–dependent relaxation time, i.e. $\Lambda \neq 0$, the collision kernel induces couplings between different n-moments. In particular, for fractional values of Λ, an n-moment becomes coupled to a fractional moment of order $n - \Lambda$. Truncation of this hierarchy at finite n gives rise to pathologies in the numerical solutions, which necessitate the introduction of a suitable closure procedure, as will be demonstrated in the subsequent analysis.

4.1.1 Collision kernel regularization

To understand the structural features of the hierarchy of moment equations, one can write it in vector form,

$$\frac{\mathrm{d}\vec{\rho}}{\mathrm{d}\tau} = -\frac{1}{\tau}\mathbf{F}\vec{\rho} - \frac{1}{\tau_R^0}\mathbf{C}(\Lambda)\vec{\rho} \tag{4.18}$$

where $\vec{\rho}$ denotes a vector containing either the infinite set of (n,l) moments or a truncated subset thereof. The entries of $\vec{\rho}$ are ordered as $\vec{\rho} = (\rho_{0,0}, \rho_{0,1}, \ldots, \rho_{1,0}, \rho_{1,1}, \ldots)$, with $n_{\text{min}} < n < n_{\text{max}}$ and $0 < l < l_{\text{max}}$. The matrices $\mathbf{F}$ and $\mathbf{C}(\Lambda)$ encode the couplings among

the moments (see Appendix B.1.1). The operator **F** couples different l-modes at fixed n, while $\mathbf{C}(\Lambda)$ generates couplings between moments with different values of n.

The matrix **F** encodes the free–streaming dynamics and dominates in the regime $\tau/\tau_R \ll 1$. In contrast, the matrix $\mathbf{C}(\Lambda)$governs the collisional dynamics. Since $1/\tau_R \sim T^{1+\Lambda}$, the resulting differential equation is nonlinear. Nevertheless, the local (in time) dynamical properties can be inferred from the eigenvalue spectrum of $\mathbf{C}(\Lambda)$. At late times, when $\tau/\tau_R \gg 1$, the evolution is effectively controlled by $\mathbf{C}(\Lambda)$. In this regime, the free–streaming contribution $\mathbf{F}/\tau$ can be neglected, and the formal solution of Eq. (4.18) reduces to

$$\vec{\rho}_n(\tau) \sim \exp\left[-\int d\tau, \frac{1}{\tau_R^0}\mathbf{C}(\Lambda)\right]\vec{\rho}_n(\tau_0), \qquad \tau/\tau_R \gg 1. \tag{4.19}$$

For $\Lambda = 0$, the collision matrix is diagonal, $\mathbf{C}(\Lambda) \sim \mathbf{I}$, with positive eigenvalues that generate a purely decaying behavior. By contrast, when $\Lambda \neq 0$, $\mathbf{C}(\Lambda)$ acquires off–diagonal structure and resembles a left–shift operator, e.g. for a truncation at $n = 4$,

$$\mathbf{C}(\Lambda) \sim \begin{bmatrix} 0 & 0 & 0 & 0 \\ c_{n-4\Lambda} & 0 & 0 & 0 \\ 0 & c_{n-3\Lambda} & 0 & 0 \\ 0 & 0 & c_{n-2\Lambda} & 0 \end{bmatrix}. \tag{4.20}$$

For such finite truncations, the spectrum of $\mathbf{C}(\Lambda)$is no longer guaranteed to be positive definite, meaning that late–time decay can break down. This feature is illustrated in Fig. (4.1), where the temperature evolution for $\Lambda = 0$ follows the expected decay, while for $\Lambda = 0.125$ it deviates and exhibits divergent behavior at late times.

Since the late–time dynamics are controlled by the spectrum of $\mathbf{C}(\Lambda)$, the divergent behavior can be traced to its structural properties. Because $\mathbf{C}(\Lambda)$ is lower–triangular, all of its eigenvalues vanish, making it a nilpotent operator: $\mathbf{C}^N(\Lambda) = 0$ for a truncated matrix of size N. If $\mathbf{C}(\Lambda)$ were time–independent, the formal solution of Eq.(4.19) becomes

$$\vec{\rho}(\tau) = \left(\sum_{k=0}^{N-1} \tau^k \, \mathbf{C}(\Lambda)^k\right)\vec{\rho}(\tau_0)\, v. \tag{4.21}$$

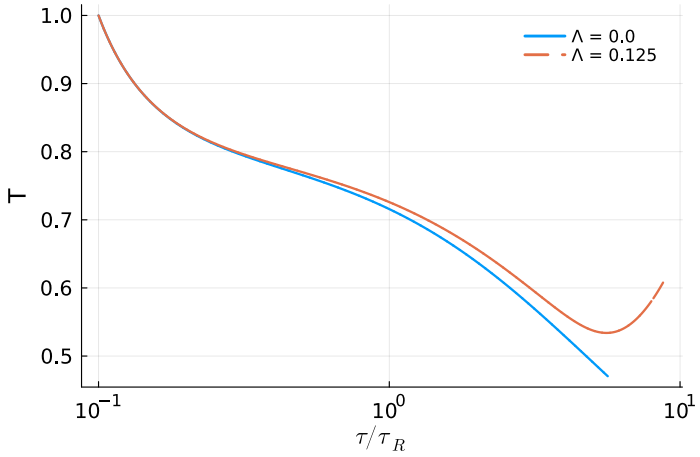

Figure 4.1: The evolution of temperature for $\Lambda = 0$ and $\Lambda = 0.125$. We see a growth in temperature when $\tau/\tau_R > 1$.

Such a solution grows polynomially in τ, rather than decaying exponentially as one would expect from a physically consistent collision operator with positive–definite spectrum. This mismatch originates from the truncation of the moment hierarchy: once the infinite tower is cut off, the nilpotent structure of $\mathbf{C}(\Lambda)$ prevents proper late–time damping. Numerically, this manifests as instabilities and unphysical growth of macroscopic quantities such as the temperature, as illustrated in Fig.(4.1).

For the Boltzmann equation, the linearized collision operator $\mathbf{L}$

$$p^\mu \partial_\mu f = -\mathbf{L}(f - f_{\text{eq}})\,, \tag{4.22}$$

is known to be positive semi-definite [72]. The vanishing eigenvalues of $\mathbf{L}$ correspond to the collision invariants, i.e., the conserved quantities. This structure ensures both the system's relaxation toward equilibrium and the generation of entropy. We therefore expect any moment-based representation of the Boltzmann equation to retain this property.

To recover the correct late–time behavior, one must go beyond naive truncation and introduce a closure procedure for the moment hierarchy. The role of the closure is to approximate the effect of the neglected higher–order moments on the truncated system, thereby

modifying the effective structure of $\mathbf{C}(\Lambda)$. Instead of a nilpotent operator with vanishing eigenvalues, the closure generates an effective collision matrix with a nontrivial spectrum whose eigenvalues are negative definite, ensuring exponential damping at late times.

To restore the positive definiteness of the collision kernel, we adopt the Grad moment closure scheme. In this approach, the single–particle distribution function is approximated by a truncated series expansion in momentum,

$$f(\tau, p, \cos\theta) = f_{\text{eq}} \left[\sum_{m=0}^{N} \sum_{l=0}^{L} A_{m,l}(\tau) p^n P_{2l}(\cos\theta) \right], \tag{4.23}$$

where the coefficients $A_{m,l}(\tau)$ encode the dynamical information, and the expansion is truncated at finite orders N and L. While the Grad expansion (4.23) is not generally convergent [99], it is asymptotic and provides reliable approximations for lower–order momentum moments, particularly when the system remains close to equilibrium.

Once the coefficients $A_{m,l}$ are determined, any moment can be computed by integrating over the approximate distribution function. Using the definition of the moments in (4.3), we obtain a set of linear relations between the integer moments $\rho_{n,l}$ and the coefficients $A_{n,l}$:

$$\vec{\rho}_l = \mathbf{H}(T, 0)\vec{A}_l \,, \tag{4.24}$$

where $\mathbf{H}(T, \Lambda)$ is an $N \times N$ matrix,

$$[\mathbf{H}(T, \Lambda)]_{n,m} = T^{n+m+2+\Lambda}\, \Gamma(n + m + 2 + \Lambda) \,, \tag{4.25}$$

while $\vec{A}_l$ and $\vec{\rho}_l$ are column vectors of the expansion coefficients and moments, respectively, constructed by fixing l and varying n (explicit definitions are provided in Appendix B.1.1). Since this system of equations is linear, it can be inverted to yield

$$\vec{A}_l = \mathbf{H}^{-1}(T, 0)\vec{\rho}_l \,. \tag{4.26}$$

Thus, knowledge of a finite set of $N \times L$ integer moments completely specifies the expansion coefficients $A_{n,l}$.

This allows us to express fractional moments $\rho_{n-\Lambda,l}$, which appear in the collision term, in terms of integer ones:

$$\vec{\rho}_{n-\Lambda,l} = T^{\Lambda}\mathbf{H}(T,-\Lambda)\mathbf{H}^{-1}(T,0)\vec{\rho}_{n,l}, \tag{4.27}$$

In this way, the problematic fractional moments are replaced by linear combinations of integer moments. The vector form of the moment equations then takes the form

$$\frac{d}{d\tau}\vec{\rho}_l = -\frac{1}{\tau}\mathbf{F}\vec{\rho}_l - \frac{1}{\tau_R^0}\mathbf{M}(T,\Lambda)\vec{\rho}_l \,, \tag{4.28}$$

with the modified collision matrix defined as

$$\mathbf{M}(T,\Lambda) = T^{\Lambda}\mathbf{H}(T,-\Lambda)\mathbf{H}^{-1}(T,0)\,. \tag{4.29}$$

An analytic proof of the positive definiteness of $\mathbf{M}(T,\Lambda)$ is given in Appendix B.1.1. Numerical analysis confirms that, for suitable choices of the truncation order N, the eigenvalues of $\mathbf{M}$ remain positive definite. In Fig. (4.2), we show the minimum eigenvalue of $\mathbf{M}(1,\Lambda)$ for N=5 as a function of Λ. The plot demonstrates that the eigenvalue remains positive but exponentially decreases towards zero with increasing Λ.

4.2 Approach to equilibrium

Once the collision kernel is appropriately regularized the set of coupled differential equations can be solved using standard algorithms. We plot the temperature evolution of the system for various values of Λ in Fig.(4.3) and two different values of initial viscosity $(\eta/s)_0 = 0.2, 0.02$. The temperature evolution no longer shows pathological behavior at late time and shows a clear ordering with respect to Λ. We see that stronger momentum dependence, i.e., larger values of Λ, implies slower cooling as expected.

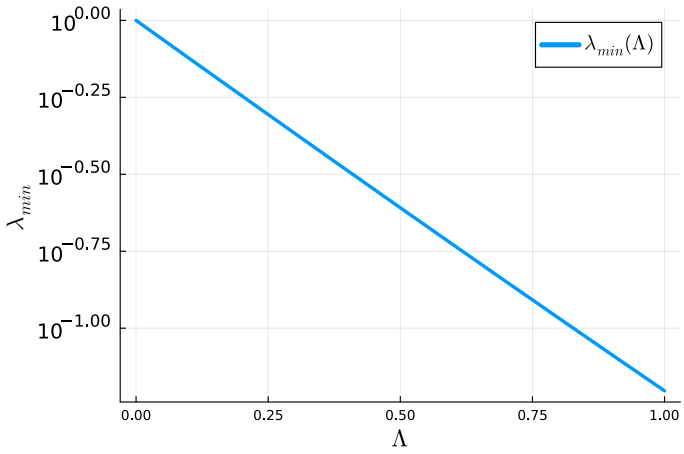

Figure 4.2: log plot of the minimum eigenvalue of $M(1, \Lambda)$ for $N = 5$ as a function of Λ.

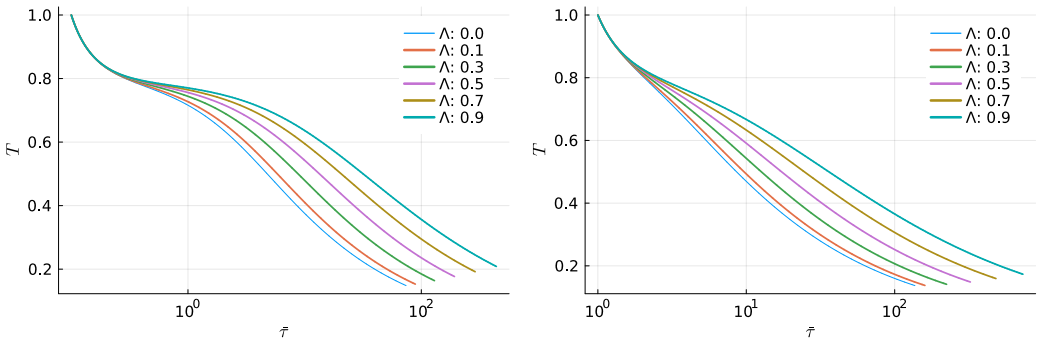

Figure 4.3: Evolution of temperature for various Λ values and initial $\eta/s = 0.2$ (left) and $\eta/s = 0.02$ (right).

To understand the approach to equilibrium, the primary quantity of interest is the scaled moment $\rho_{2,1}/\rho_{2,0}$ which corresponds to the scaled momentum anisotropy $(P_L - P_T)/\epsilon$. In Fig (4.4) we plot the momentum anisotropy as a function of scaled time $\bar{\tau} = T^{-\Lambda}(\tau/\tau_R^0)$.

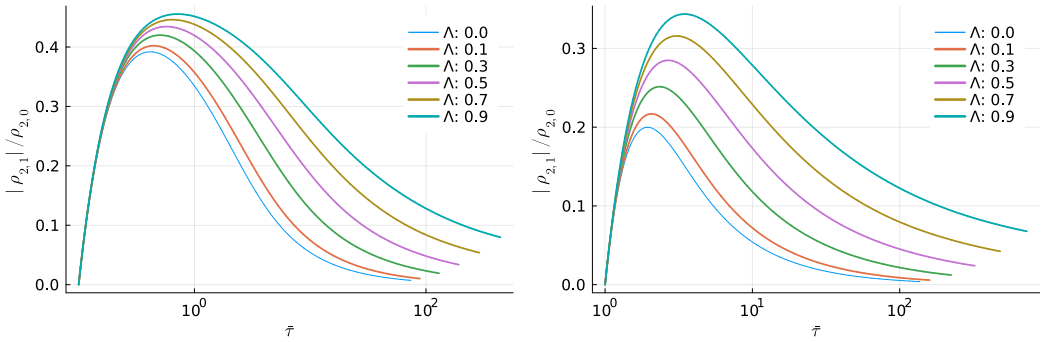

Figure 4.4: Evolution of $\rho_{2,1}/\rho_{2,0}$ for various Λ values and $\eta/s = 0.2$ (left) and $\eta/s = 0.02$ (right).

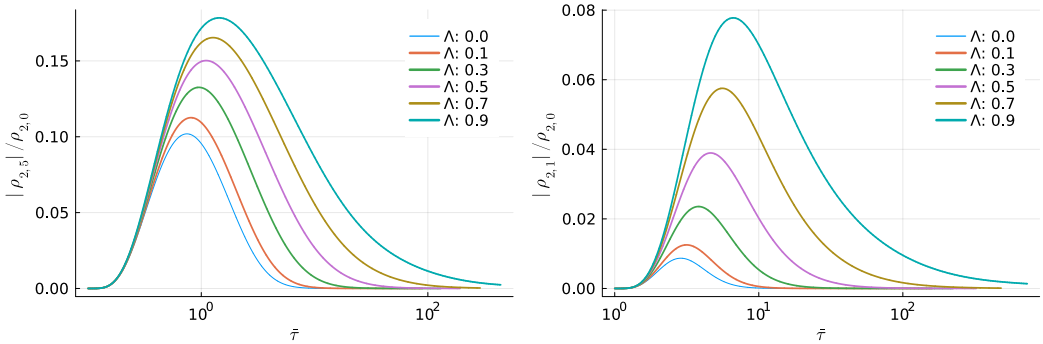

Figure 4.5: Evolution of $\rho_{2,5}/\rho_{2,0}$ for various Λ values and $\eta/s = 0.2$ (left) and $\eta/s = 0.02$ (right).

The results lead to several noteworthy observations. First, the temperature evolution as a function of scaled time τ/τ_R becomes noticeably flatter around $\tau/\tau_R \sim 1$ as the value of Λ increases, indicating a slower cooling rate once collisions begin to dominate over free streaming. Second, from figures (4.4) and (4.5) we see that for fixed values of n and l, the magnitude of the ρ moments grows with larger Λ, reflecting an enhancement of momentum anisotropy in the system. This sensitivity to Λ is particularly pronounced for higher-order

moments at smaller values of η/s and for earlier initialization times. Finally, the enhanced anisotropy observed at intermediate times for larger Λ points to a delayed isotropization, and consequently, a slower approach to local equilibrium.

4.2.1 Summary

We developed a kinetic-theoretical framework to investigate the approach toward equilibrium in a relativistic, boost-invariant system by incorporating a momentum-dependent relaxation time approximation (MDRTA) into the Boltzmann equation. Using the method of moments, we systematically analyzed how the inclusion of a momentum-dependent relaxation time modifies the evolution of the moments of the distribution function and, consequently, the macroscopic hydrodynamic variables that describe the system's far-from-equilibrium dynamics.

The introduction of a power-law momentum dependence, $\tau_R(p) = \tau_0\, p^{\Lambda}$ in the relaxation time leads to a significant conceptual and mathematical extension of the standard Anderson-Witting relaxation time approximation. While the conventional AW-RTA couples only moments with different angular indices, the MDRTA introduces coupling between both energy and angular moments, resulting in a richer and more intricate hierarchy of coupled equations. This coupling brings in additional physical scales that alter the relaxation dynamics and highlight the nontrivial interplay between microscopic scattering and macroscopic expansion.

To ensure a physically consistent truncation of the infinite moment hierarchy, we developed a systematic closure scheme based on a generalised Grad-type expansion of the distribution function. This closure yields a collision matrix that preserves energy–momentum conservation and remains positive definite, guaranteeing the stability of numerical evolution and preventing unphysical divergences at late times. The analytical proof of positive definiteness, supported by numerical verification, constitutes a key methodological contri-

bution of this work.

Through detailed numerical studies for a range of viscosities and momentum-dependence parameters Λ, we found that increasing Λ enhances the system's momentum anisotropy and delays isotropization. The scaled pressure anisotropy and higher-order angular moments display a clear dependence on the degree of momentum dependence, reflecting the slower relaxation of high-momentum modes. The temperature evolution shows a flattening behavior at intermediate times for larger Λ, consistent with reduced collisional efficiency, while the chemical potential-to-temperature ratio (μ/T) exhibits larger deviations from equilibrium. These findings collectively demonstrate that incorporating momentum dependence in the relaxation time results in a slower approach to equilibrium and modifies the onset of hydrodynamic behaviour.

4.3 Conclusion on hydrodynamization and attractor behaviour

In the last two chapters, we examined the mechanisms that govern hydrodynamization and the emergence of attractor behavior in far-from-equilibrium relativistic systems using the kinetic theory framework based on the Boltzmann equation under Bjorken symmetry. Our investigations focused on two key extensions of the conventional AW-RTA: the inclusion of external longitudinal forces and the implementation of a momentum-dependent relaxation time (MDRTA). Together, these studies provide deeper insight into how microscopic physics and external perturbations influence the system's evolution toward hydrodynamic behaviour.

In the first part of this work, we analyzed the role of proper-time-dependent longitudinal forces on the hydrodynamic evolution of conformal and non-conformal systems. By solving the Boltzmann equation exactly in the presence of such forces, we found that they substantially modify both the hydrodynamization dynamics and the attractor structure. In

the absence of forcing, conformal systems exhibit a universal early-time attractor, wherein macroscopic observables such as pressure anisotropy rapidly converge toward a common evolution path, largely independent of initial conditions. However, the inclusion of longitudinal forces breaks this universality, causing the system to retain memory of its initial conditions until much later times. Only a late-time attractor remains, corresponding to the hydrodynamic regime. In the conformal, massless limit, an early-time attractor can reappear if the external force decays sufficiently rapidly compared to the microscopic relaxation time, underscoring the sensitivity of attractor formation to both conformal symmetry and the time dependence of external fields.

In the second part, we extended the kinetic description by incorporating a momentum-dependent relaxation time, $\tau_R(p) = \tau_0\, p^{\Lambda}$, which captures the natural dependence of microscopic relaxation processes on particle momentum. The resulting MDRTA framework couples different energy and angular moments of the distribution function, producing a richer hierarchy of evolution equations. Our numerical analysis revealed that stronger momentum dependence (larger Λ) enhances momentum anisotropies and delays isotropization, thereby postponing hydrodynamization. The emergence of multiple decay times, associated with different momentum scales, leads to a gradual rather than universal transition to hydrodynamic behaviour.

Taken together, these studies demonstrate that while conformal symmetry and simple relaxation dynamics promote the appearance of early-time attractors, the introduction of additional physical scales—through particle masses, external forces, or momentum-dependent relaxation times-breaks this universality and shifts the onset of hydrodynamics to later stages of the evolution. Despite these differences, the system consistently approaches a late-time attractor described by viscous hydrodynamics, confirming the emergent nature of hydrodynamization as a general feature of relativistic kinetic theory.

The analysis in this chapter thus points toward a broader conclusion: hydrodynamiza-

tion in relativistic kinetic theory cannot be fully described by universal attractor dynamics alone. While attractor solutions encapsulate aspects of far-from-equilibrium evolution, their existence depends on restrictive assumptions that rarely hold in realistic scenarios. The absence of early-time universality in non-conformal and forced systems suggests that hydrodynamization should instead be viewed as a structural property of the Boltzmann equation itself. This motivates a shift in perspective—from searching for universal scaling solutions to examining the intrinsic features of kinetic theory: its fixed points, asymptotic expansions, and non-perturbative corrections. The following chapters pursue this direction by constructing an exact, convergent gradient expansion of the Boltzmann equation, demonstrating that hydrodynamics emerges naturally as an interpolation between the collisionless and locally equilibrated regimes. In this formulation, hydrodynamization appears not as the consequence of a universal attractor, but as a manifestation of the analytic and causal structures inherent to the kinetic theory itself. This conceptual shift forms the foundation for the analysis developed in Chapter 5, where we move beyond attractor models and develop an exact, convergent gradient expansion of the Boltzmann equation to provide a unified and analytic description of hydrodynamization.

Chapter 5

Divergence Of Chapmann-Enskog Expansion

The Chapman–Enskog expansion, although widely used to derive hydrodynamic equations from kinetic theory, is an *asymptotic* and generally divergent series solution of the Boltzmann equation [100, 101, 102, 103, 37]. This behaviour can be understood within the framework of singular perturbation theory. To illustrate the essential idea, consider a simple toy model differential equation that captures the structure of the Boltzmann equation in the hydrodynamic limit:

$$\delta \frac{df(t)}{dt} = -\left(f(t) - g(t)\right), \tag{5.1}$$

where δ is a small parameter that plays the role of a scaled mean free path or relaxation time. Despite its simplicity, Eq. (5.1) exhibits the key features underlying the divergence of the Chapman–Enskog series.

In Eq. (5.1), the highest derivative term is multiplied by the small perturbative factor δ, rendering the equation *singularly perturbed*. Expanding $f(t)$ in powers of δ leads to the Chapman–Enskog-like derivative expansion around $g(t)$:

$$f(t) = g(t) - \delta\, g'(t) + \delta^2\, g''(t) + \dots . \tag{5.2}$$

While this formal series correctly reproduces the behaviour of the system in the limit $\delta \to 0$, it fails to accommodate arbitrary initial conditions for $f(t)$ and diverges for $\delta \gtrsim 1$, unless $g(t)$ is an analytic polynomial. Hence, the perturbative solution loses validity when the microscopic relaxation time becomes comparable to macroscopic timescales.

By contrast, the exact solution of Eq. (5.1) can be written as

$$f(t) = e^{-t/\delta} f(0) + \int_0^t \frac{dt'}{\delta} e^{-(t-t')/\delta} g(t'). \tag{5.3}$$

This expression is manifestly finite for all δ and incorporates the initial condition through the exponentially decaying term $e^{-t/\delta} f(0)$, which rapidly dies out for $t \gg \delta$. Performing integration by parts on the second term yields

$$f(t) = e^{-t/\delta} f(0) + \left[g(t) - e^{-t/\delta} g(0)\right] - \delta \left[g'(t) - e^{-t/\delta} g'(0)\right] + \dots . \tag{5.4}$$

In the long-time limit $t \gg \delta$, the exponential terms vanish, and the perturbative expansion in Eq. (5.2) is recovered. However, for early times $t \lesssim \delta$, the perturbative expansion breaks down, as it neglects the exponentially suppressed non-perturbative contributions that encode memory of the initial conditions.

If $g(t)$ is analytic, one may expand it in a Taylor series and perform the time integration in Eq. (5.3) explicitly, obtaining

$$f(t) = e^{-t/\delta} f(0) + \sum_{n=0}^{\infty} \left[1 - e^{-w} \sum_{k=0}^{n} \frac{w^k}{k!}\right] \frac{d^n g(t)}{dt^n}, \tag{5.5}$$

where $w = (t - t_0)/\delta$ and the bracketed expression can be written in terms of the lower incomplete gamma function $\gamma(n+1, w)$ as

$$\frac{\gamma(n+1, w)}{n!} = 1 - e^{-w} \sum_{k=0}^{n} \frac{w^k}{k!}. \tag{5.6}$$

This form is particularly useful because it expresses the exact solution as a local derivative series, with each term weighted by time-dependent coefficients that ensure convergence for all t. In the late-time regime $e^{-t/\delta} \ll 1$, the exponentially suppressed term becomes negligible, and the gradient expansion approximates the exact solution well.

Fixed point interpretation

The structure of Eq. (5.1) admits a clear physical interpretation in terms of fixed points. For $\delta \to 0$, the system approaches the *hydrodynamic fixed point*, where $f = g$, corresponding

to instantaneous local relaxation to equilibrium. Conversely, in the opposite limit $\delta \to \infty$, the equation admits a *free-streaming fixed point* where $\dot{f} = 0$. The full solution (5.3) interpolates smoothly between these two fixed points, with the exponentially suppressed term describing the transient relaxation between them. A perturbative expansion around the hydrodynamic fixed point yields the derivative series (5.2), while an expansion around the free-streaming fixed point captures the non-perturbative transient corrections. This simple example illustrates how the applicability of hydrodynamics emerges from the interplay between these two asymptotic regimes.

5.1 Exact gradient Expansion: relaxation time approximation

Building on the discussion of the divergence of the Chapman–Enskog series, we now present an exact and convergent gradient expansion for the relativistic Boltzmann equation within the relaxation time approximation, following the formalism of [104]. This treatment provides a mathematically rigorous understanding of how hydrodynamic ($\lambda/L \ll 1$) and non-hydrodynamic ($\lambda/L \sim 1$) contributions emerge naturally from the kinetic equation, and under what conditions the gradient expansion remains convergent.

Formal Integral Solution

For simplicity, we restrict to Minkowski space without external forces (for generalization see Appendix C.4):

$$p^\mu \partial_\mu f = -\frac{u \cdot p}{\tau_R}(f - f_{\text{eq}}). \tag{5.7}$$

The solution of this first-order PDE can be obtained via the method of characteristics. Given some initial condition on $x^\mu(t') = c^\mu$, any function $h(t)$ on the characteristic curve has the

parametric dependence:

$$h(t,t') \Rightarrow h\left(x^\mu - \frac{p^\mu}{p^0}(t-t')\right) . \tag{5.8}$$

From here on we will assume this dependence is implied unless otherwise specified.

Along a characteristic trajectory $x^\mu(t) = x_0^\mu + (p^\mu/p^0)(t-t_0)$ for some initial time t_0, Eq. (5.7) reduces to

$$\frac{\mathrm{d}f(t,t')}{\mathrm{d}t} = -\left(\frac{u(t,t')\cdot p}{p^0\tau_R(t,t')}\right)(f(t,t') - f_{eq}(t,t')) . \tag{5.9}$$

Integrating from t_0 to t yields the exact integral solution (Appendix C.1):

$$\begin{aligned} f(x^i,t) &= e^{-\xi(t,t_0)} f_0(t,t_0) \\ &\quad + \int_{t_0}^{t} \frac{dt'}{p^0} e^{-\xi(t,t')} \left(\frac{u(t,t')\cdot p}{\tau_R(t,t')}\right) f_{eq}(t,t') , \end{aligned} \tag{5.10}$$

where

$$\xi(t,t') = \int_{t'}^{t} \left(\frac{u(t,t'')\cdot p}{\tau_R(t,t'')}\right) \frac{dt''}{p^0} . \tag{5.11}$$

The first term represents the free-streaming evolution of the initial distribution, exponentially damped by interactions. The second term, called the *hydrodynamic generator* f_G, contains the accumulated contributions of local equilibrium states along the particle's trajectory:

$$f_G(x^i,t) = \int_{t_0}^{t} \frac{dt'}{p^0} e^{-\xi(t,t')} \left(\frac{u(t,t')\cdot p}{\tau_R(t,t')}\right) f_{eq}(t,t') , \tag{5.12}$$

Expansion in terms of the damping factor

To construct the exact gradient expansion, it is convenient to express the integral solution of the Boltzmann equation in terms of the damping factor $\xi(t,t')$ (Appendix C.1.1), defined by

$$\xi(t,t') = \int_{t'}^{t} dt'' \frac{u\cdot p}{p^0\tau_R}, \tag{5.13}$$

which measures the accumulated relaxation of the distribution function between times t' and t. The damping factor satisfies the properties $\xi(t,t) = 0$ and $\frac{d\xi(t,t')}{dt'} = -\frac{u\cdot p}{p^0\tau_R} < 0$, ensuring that $\xi(t,t')$ is positive and monotonically decreasing with t'. Consequently, it admits a well-defined inverse map $t'(\xi)$, which can be expressed as a Taylor (or Lie) series expansion around $\xi = 0$:

$$t'(\xi,t) - t = \sum_{n=1}^{\infty} \frac{\xi^n}{n!} \left(\frac{d}{d\xi'}\right)^{n-1} \left[-\frac{p^0\tau_R}{u\cdot p}\right]_{\xi'=0} . \tag{5.14}$$

For analytic functions, this expansion can be compactly written using the Lie-series operator as

$$t'(\xi,t) - t = e^{\xi \frac{d}{d\xi'}} (t'(\xi',t) - t)\Big|_{\xi'=0} . \tag{5.15}$$

A similar representation holds for the particle trajectory,

$$x^\mu - \frac{p^\mu}{p^0}(t-t') = e^{\xi \frac{d}{d\xi'}} \left(x^\mu - \frac{p^\mu}{p^0}(t-t')\right)\Big|_{\xi'=0} , \tag{5.16}$$

which demonstrates that the evolution of the distribution function along characteristic curves can be written as an exponential flow in the damping variable ξ. This reformulation is central to deriving the exact gradient expansion, as it systematically organizes the time evolution of $f(x,p)$ in terms of local derivatives weighted by powers of the damping factor.

Expanding the integrand using the Lie series formalism gives

$$f_G = \int_0^{\xi_0} d\xi\, e^{-\xi} \exp\left(\xi \frac{d}{d\xi'}\right) f_{\text{eq}}\left(x^\mu - \frac{p^\mu}{p^0}(t-t')\right)\Big|_{\xi'=0} , \tag{5.17}$$

which, upon expanding the exponential and converting back to spacetime derivatives, yields the expression (see Appendix C.1.2):

$$f_G = \int_0^{\xi_0} d\xi\, e^{-\xi} \sum_{n=0}^{\infty} \frac{\xi^n}{n!} \left[-\frac{\tau_R}{u\cdot p} p^\mu \partial_\mu\right]^n f_{\text{eq}}(x,t) . \tag{5.18}$$

Carrying out the ξ-integration gives exact gradient expansion,

$$f_G = \sum_{n=0}^{\infty} \left(1 - e^{-\xi_0} \sum_{k=0}^{n} \frac{\xi_0^k}{k!}\right) \left[-\frac{\tau_R}{u\cdot p} p^\mu \partial_\mu\right]^n f_{\text{eq}}(x,t) . \tag{5.19}$$

Equation (5.19) is the central result: it represents the *exact gradient expansion* of the AW-RTA Boltzmann equation. The first term corresponds to the usual Chapman–Enskog expansion, while the second term provides exponentially suppressed, non-perturbative corrections. In the late-time limit $\xi_0 \to \infty$, the exponential terms vanish, and Eq. (5.19) reduces to the Borel resummation of the Chapman–Enskog series:

$$\lim_{\xi_0\to\infty} f_G = \int_0^\infty d\xi\, e^{-\xi} \sum_{n=0}^{\infty} \frac{\xi^n}{n!} \left[-\frac{\tau_R}{u\cdot p}\, p^\mu \partial_\mu\right]^n f_{\text{eq}}. \tag{5.20}$$

Non-hydrodynamic corrections

To gain deeper insight into the physical meaning of the non-hydrodynamic terms, we perform integration by parts on Eq. (5.12) to obtain

$$\begin{aligned} f_G = \sum_{n=0}^{\infty} \Bigg\{ & \left(-\frac{\tau_R}{u\cdot p}\mathcal{D}\right)^n f_{\text{eq}}(x^i,t) \\ & - e^{-\xi'(t,t')} \left(-\frac{\tau_R(t,t')}{u(t,t')\cdot p}\mathcal{D}\right)^n f_{\text{eq}}(t,t') \Big|_{t'=t_0} \Bigg\}. \end{aligned} \tag{5.21}$$

The form of f_G given in Eqs. (5.21) and (5.19) are equivalent (when the series converges Appendix (C.2.1)); however, the non-hydrodynamic terms differ order by order. These two representations correspond to distinct re-summations of the same underlying series (see Appendix (C.2)).

From Eq. (5.21), it is evident that the non-hydrodynamic terms represent free-streaming contributions that carry not only the initial data but also information about the full dynamical history of the system. The factor ξ_0 is a time integral over functions of U^μ and τ_R, both of which evolve in time, thereby encoding memory of the system's evolution. The approach to hydrodynamics corresponds to the decay of these non-hydrodynamic terms, indicating that the system's behavior becomes independent of its history (local in time).

The coefficients of the gradient terms in Eq. (5.19), have the form of the lower incom-

plete gamma function,

$$\gamma(n+1,\xi_0) = n!\left(1 - e^{-\xi_0}\sum_{k=0}^{n}\frac{\xi_0^k}{k!}\right). \tag{5.22}$$

These coefficients have the asymptotic limits,

$$\lim_{\xi_0\to\infty}\left(1 - e^{-\xi_0}\sum_{k=0}^{n}\frac{\xi_0^k}{k!}\right) = 1\,, \tag{5.23}$$

$$\lim_{n\to\infty}\left(1 - e^{-\xi_0}\sum_{k=0}^{n}\frac{\xi_0^k}{k!}\right) = 0\,. \tag{5.24}$$

Equation (5.23) shows that at late times or for large decay factors ξ_0, the influence of the initial conditions—and therefore the non-hydrodynamic contributions—becomes negligible. Equation (5.24), on the other hand, implies that higher-order gradients are initially suppressed, with lower-order terms decaying more rapidly. Consequently, large initial higher-order gradients lead to a slower approach to hydrodynamics. Understanding the behavior of these non-hydrodynamic terms is thus essential for determining how early-time dynamics influence the onset of hydrodynamic behavior.

Although the exponential damping appears identical at every order, the effective decay rate depends on the polynomial (exponential-sum) function

$$e_n(\xi) \equiv \sum_{k=0}^{n}\frac{\xi^k}{k!}, \tag{5.25}$$

which multiplies the gradient terms in Eq. (5.19). The k-th derivative of the prefactor to the non-hydrodynamic term satisfies

$$\frac{d^k}{d\xi^k}\left(e^{-\xi}e_n(\xi)\right)\Big|_{\xi=0} = 0\,, \qquad k < n\,. \tag{5.26}$$

Hence, increasing n corresponds to a slower decay rate at $\xi_0 = 0$ ($t = t_0$). From the asymptotic limit of the gamma function,

$$\gamma(n,\xi) \sim \frac{e^{-\xi}\xi^n}{n}\left[1 + O\left(\frac{\xi}{n}\right)\right], \tag{5.27}$$

it follows that for large n, the decay time scales as $\xi_0 \sim n$. The coefficients of the gradient terms can thus be interpreted as defining characteristic length (or time) scales associated with each gradient order. Specifically, we can write

$$e^{-\xi_0} \propto \exp\left[-\frac{(t-t_0)}{\sigma_0(p,t,t_0)}\right], \tag{5.28}$$

where $\sigma_0(p,t,t_0)$ defines the local time or length scale over which free-streaming contributions remain significant for the zeroth-order gradient. For constant τ_R, one has $\sigma_0 \propto \tau_R$. For higher-order gradients, this scale is modified by the polynomial prefactor $e_n(\xi_0)$, leading to $\sigma_n \sim \sigma_0(p,t,t_0)\, n$.

Convergence of the gradient expansion

The convergence properties of the exact gradient expansion can be analyzed by examining the ξ_0-dependent coefficients appearing in Eq. (5.19). As $n \to \infty$, these coefficients exhibit the asymptotic behavior

$$\gamma(n,\xi) \sim \frac{e^{-\xi}\xi^n}{n}\left[1 + \mathcal{O}\left(\frac{\xi}{n}\right)\right], \tag{5.29}$$

which implies that, for large n, the factorial divergence of the conventional Chapman–Enskog series is replaced by a much milder geometric growth. If the nth derivative of the equilibrium distribution grows as

$$\left[-\frac{\tau_R}{u\cdot p}\mathcal{D}\right]^n f_{\text{eq}} \sim n!\, K^n, \tag{5.30}$$

with $|K| < \infty$, then the nth term of the expansion scales as $(\xi K)^n$. Therefore, the series converges whenever $\xi K < 1$. Physically, this condition corresponds to the late-time regime where the damping factor ξ is large and the gradients K are small, i.e., when the system has sufficiently relaxed toward local equilibrium. At early times, when ξ is small and gradients are large, convergence is not guaranteed, reflecting the dominance of non-hydrodynamic, transient modes.

A more rigorous statement about convergence can be made by appealing to the uniform convergence of the Taylor expansion of f_{eq} in the damping variable ξ. If f_{eq} is analytic in ξ and its Taylor series converges uniformly over the finite range $\xi \in [0, \xi_0]$, then the order of summation and integration in Eq. (5.18) can be interchanged, ensuring that the resulting gradient expansion is finite and absolutely convergent. Moreover, since the damping function $\xi(t, t')$ is a monotonic, analytic function of t', the Lagrange–Burmann inversion theorem [105] guarantees that its inverse $t'(\xi, t)$ also possesses a convergent series expansion with a finite radius of convergence.

However, because the Boltzmann equation is nonlinear, the analyticity of $\xi(t, t')$ and the uniform convergence of the expansion depend on the distribution function $f(x, p)$ itself, unless U^μ and τ_R are prescribed externally. If the initial conditions are analytic and the time evolution preserves analyticity (i.e., no discontinuities such as shocks develop), then the gradient series retains a finite radius of convergence around t. Thus, the convergence of the exact gradient expansion follows from the analyticity of the microscopic evolution and the smoothness of the hydrodynamic fields, ensuring that the Chapman–Enskog procedure remains well-defined in the AW-RTA framework under physically realistic conditions.

Domain of validity

The full solution,

$$f = e^{-\xi_0}\left[f_0 - f_G^H\right] + f_G^H, \tag{5.31}$$

shows that the Chapman–Enskog approximation $f \approx f_G^H$ is valid whenever the first term is small, i.e.

$$\left| e^{-\xi_0} \frac{f_0 - f_G^H}{f_G^H} \right| \ll 1. \tag{5.32}$$

This condition implies that hydrodynamics remains accurate even when gradients are large, provided that ξ_0 is sufficiently large—i.e., that the system is far from the free-streaming

regime. Hence, in the AW-RTA model, the range of validity of hydrodynamics extends beyond near-equilibrium conditions.

5.1.1 The Boltzmann kernel and gradient expansion

A similar structure arises in the Boltzmann equation when one explicitly separates the streaming and collision terms. If the characteristic interaction range is much smaller than the mean free path, the Boltzmann equation can be cast in the schematic form

$$v^\mu \partial_\mu f + \frac{v}{\delta} f = \frac{1}{\delta} L[f], \tag{5.33}$$

where $v^\mu = p^\mu/p^0$ is the particle four-velocity, and $v(p) \sim 1/\tau_R$ represents the effective collision frequency and δ is some parameter say for example the Knudsen number. The collision operator $L[f]$ and the collision rate $\nu(p)$ are given by

$$\nu(p) = \int dP_1\, dP'\, dP_1'\, W(p, p_1 \mid p', p_1')\, f(p_1), \tag{5.34}$$

$$L[f] = \int dP'\, dP_1'\, dP_1\, W(p', p_1' \mid p, p_1)\, f' f_1', \tag{5.35}$$

where $W(p, p_1 \mid p', p_1')$ is the transition probability per unit time.

Integrating Eq. (5.33) using the method of characteristics yields the exact solution [106],

$$f(p^\mu, x^\mu) = e^{-\frac{1}{\delta}\int_{t_0}^{t} v(t,t')\,dt'} f(t, t_0) + \int_{t_0}^{t} \frac{v(t,t')}{\delta} e^{-\frac{1}{\delta}\int_{t'}^{t} v(t,t'')\,dt''} g(t, t')\, dt', \tag{5.36}$$

where $g = L/v$. This structure is directly analogous to the exact solution of the toy model (5.3), with $v(p)$ playing the role of $1/\tau_R$. Defining $\chi' = \frac{1}{\delta}\int_{t'}^{t} v\, dt'$, one obtains the formal gradient series expansion

$$f = e^{-\chi_0} f(t, t_0) + \sum_{n=0}^{\infty} \delta^n \frac{\gamma(n+1, \chi_0)}{n!} \left(-\frac{p^\mu \partial_\mu}{v}\right)^n g, \tag{5.37}$$

where $\chi_0 = \chi(t, t_0)$. This series mirrors the structure of the corresponding expansion in the relaxation-time approximation [104],

$$f = e^{-\xi_0} f^0(t, t_0) + \sum_{n=0}^{\infty} \frac{\gamma(n+1, \xi_0)}{n!} \left(-\frac{\tau_R}{p \cdot u} p^\mu \partial_\mu\right)^n f_{\text{eq}}, \tag{5.38}$$

where $\xi_0 = \int_{t_0}^{t} (u\cdot p)/\tau_R \, dt'$ is the damping factor. Under the identifications $v(p) \sim u\cdot p/\tau_R$, $\chi_0 \sim \xi_0$, and $g \sim f_{\text{eq}}$, Eqs. (5.37) and (5.38) become structurally equivalent. This structural similarity suggests that the results derived in this section may extend beyond the simple AW-RTA setting and could hold more broadly across kinetic models with analogous operator structure.

5.1.2 Validity of the gradient expansion

It is essential to distinguish between the *gradient expansion* itself and *relativistic hydrodynamics*. The gradient expansion refers specifically to the perturbative Chapman–Enskog series in powers of the Knudsen number (Kn), while relativistic hydrodynamics encompasses both this perturbative structure and the non-perturbative (exponentially suppressed) contributions that arise naturally in the exact kinetic solution.

The exponentially decaying non-perturbative component of the AW-RTA solution (5.38) can be written as [104]

$$f_{\text{NP}} = -e^{-\xi'(t,t')} \left(-\frac{\tau_R(t,t_0)}{p\cdot u(t,t_0)} \, p^\mu \partial_\mu \right)^n f_{\text{eq}}(t,t_0), \tag{5.39}$$

which explicitly encodes the memory of the initial conditions through the damping factor $e^{-\xi'}$. These terms become relevant when the Knudsen number approaches unity (Kn ~ 1), corresponding to early times $t < \tau_R$, when the system is far from equilibrium and the free-streaming dynamics dominate. In this regime, the gradient expansion breaks down, as it cannot capture the non-local structure of the exact kinetic evolution.

Physically, this corresponds to the pre-collisional phase of the system, where the microscopic relaxation processes have not yet established local equilibrium. The Chapman–Enskog expansion, by construction, assumes that one can expand around the equilibrium fixed point at finite times. However, in a realistic dynamical system, fixed points are approached only asymptotically and cannot be reached at finite time. This inconsistency un-

derlies both the divergence of the gradient series and the acausal behavior of first-order relativistic hydrodynamics.

The validity of the Chapman–Enskog expansion, therefore, does not solely depend on the smallness of the gradients, but rather on the dominance of collisional processes over free-streaming effects. This condition can be expressed as χ_0 or $\xi_0 \gg 1$, which ensures that non-perturbative terms are exponentially suppressed. Thus, hydrodynamic behavior persists even for relatively large gradients, provided the system remains sufficiently far from the free-streaming regime.

Finally, it is important to emphasize that the *applicability of relativistic hydrodynamics* is not equivalent to the *convergence of the Chapman–Enskog expansion*. While the gradient expansion diverges, the underlying hydrodynamic attractor solution provides a resummed, non-perturbative description that remains valid far beyond the formal radius of convergence of the perturbative series.

5.2 Summary

In this chapter, we established a rigorous understanding of the divergence of the Chapman–Enskog (CE) expansion and demonstrated how a convergent formulation of the hydrodynamic gradient series can be obtained directly from the Boltzmann equation. Starting from a singularly perturbed toy model, we showed that the divergence of the CE series originates from its neglect of exponentially suppressed, non-perturbative contributions that encode the system's initial conditions and transient relaxation dynamics. The exact solution of the toy model revealed that the Chapman–Enskog expansion represents only the asymptotic limit of a broader structure in which non-perturbative terms play a central role in reproducing the full kinetic evolution.

Extending this insight to the relativistic Boltzmann equation within the relaxation time

approximation, we derived an exact integral solution and reformulated it in terms of the damping factor $\xi(t, t')$. This led to the construction of the *exact gradient expansion*, in which the evolution of the distribution function is expressed as a power series in space–time gradients weighted by the damping factor. Unlike the conventional Chapman–Enskog series, this expansion contains both perturbative and exponentially suppressed terms, ensuring that it remains finite and well-defined for all finite times. We demonstrated that the factorial divergence characteristic of the CE expansion is replaced by a geometric growth pattern, and that convergence is guaranteed whenever the product of the damping factor ξ and the maximum gradient scale K satisfies $\xi K < 1$. Physically, this condition corresponds to the hydrodynamic regime, where microscopic relaxation dominates over free streaming and the system evolves smoothly toward local equilibrium.

A deeper examination of the convergence properties revealed that the existence of a finite, convergent gradient expansion is intimately linked to the analyticity of the microscopic dynamics. If the damping function $\xi(t, t')$ is analytic and its inverse map $t'(\xi, t)$ admits a convergent series expansion, then the gradient expansion remains uniformly convergent for all finite ξ. This result follows from the Lagrange–Burmann inversion theorem and assumes that the equilibrium distribution f_{eq} admits a uniformly convergent Taylor expansion in ξ. Under analytic and smooth initial conditions—i.e., in the absence of discontinuities such as shock formations—the Chapman–Enskog procedure is therefore mathematically consistent and physically meaningful, even far from strict equilibrium.

Finally, we extended these arguments to the full Boltzmann collision kernel and demonstrated that the structural form of the exact gradient expansion is universal. When the collision operator $L[f]$ and the collision frequency $\nu(p)$ are analytic, the resulting series retains the same form as in the AW-RTA, with the damping factor $\chi_0 = \int_{t_0}^{t} \nu(p)\, dt'$ replacing ξ_0. This universality implies that the geometric convergence of the gradient expansion and the presence of well-behaved non-perturbative corrections are not artifacts of the relaxation

time approximation, but intrinsic features of kinetic theory itself. Hence, the divergence of the traditional Chapman–Enskog expansion reflects the intrinsic breakdown of the hydrodynamic gradient series at finite orders, indicating that a purely perturbative expansion around equilibrium is insufficient. This breakdown, however, does not imply the failure of hydrodynamics itself, but rather underscores the necessity of resumming the asymptotic series into a convergent formulation that consistently incorporates non-perturbative contributions.

In conclusion, this chapter establishes that the hydrodynamic gradient expansion derived from kinetic theory is asymptotic but resummable, and that hydrodynamic behavior emerges naturally from the analytic and causal structure of the Boltzmann equation. The exact gradient expansion provides a unified and convergent description of both hydrodynamic and non-hydrodynamic modes, forming a rigorous bridge between microscopic kinetic dynamics and macroscopic fluid evolution. This framework clarifies the nature of the divergence of the Chapman–Enskog expansion and contributes to a unified theoretical understanding of hydrodynamization and attractor formation in far-from-equilibrium systems such as the quark–gluon plasma.

Chapter 6

Relativistic Hydrodynamics Beyond Local Equilibrium

In this chapter, we investigate the validity and applicability of relativistic hydrodynamics within the $(0+1)$ D boost-invariant system. The system evolves under Bjorken symmetry, making it an ideal testing ground for understanding how hydrodynamics emerges from the Boltzmann equation and how far it remains valid beyond local equilibrium.

We begin by formulating the moment equations of the Boltzmann equation in the relaxation-time approximation. Using the linearity of the AW-RTA kernel, we construct formal operator solutions for the dynamical moments, which are then used to derive exact evolution equations for hydrodynamic quantities such as the energy density, bulk and shear pressures. By comparing these exact solutions to those obtained from second-order hydrodynamics, we delineate the limits of hydrodynamic validity in kinetic theory. By using a general operator approach, we extend these results to $3+1$D systems.

6.0.1 Setup and symmetries

We consider a system invariant under boosts along the longitudinal (z) direction and rotations and translations in the transverse (x–y) plane. This symmetry restricts the spacetime dependence to the proper time τ, leading to an effectively $(0+1)$-dimensional description.

We work in Milne coordinates (2.69) and under the symmetries constrain the energy-

momentum tensor to the diagonal form

$$T^{\mu\nu} = \begin{pmatrix} \varepsilon & 0 & 0 & 0 \\ 0 & P + \Pi + \frac{\pi}{2} & 0 & 0 \\ 0 & 0 & P + \Pi + \frac{\pi}{2} & 0 \\ 0 & 0 & 0 & P + \Pi - \pi \end{pmatrix}, \tag{6.1}$$

where ε is the energy density, P the equilibrium pressure, Π the bulk viscous pressure and π the shear pressure. The transverse and longitudinal pressures are therefore

$$P_T = P + \Pi + \frac{\pi}{2}, \qquad P_L = P + \Pi - \pi. \tag{6.2}$$

6.0.2 RTA Boltzmann equation in $0 + 1$D

Under the above symmetries, the Boltzmann equation in the AW-RTA simplifies to

$$\frac{\partial f}{\partial \tau} - \frac{p^z}{\tau}\frac{\partial f}{\partial p^z} = -\frac{1}{\tau_R}\left(f - f_{\text{eq}}\right). \tag{6.3}$$

Transverse momentum space remains isotropic, and the on-shell relation reads

$$(p^0)^2 - (p^z)^2 - p_T^2 = m^2, \qquad p_T = \sqrt{(p^x)^2 + (p^y)^2}. \tag{6.4}$$

6.1 Moment equations

To extract macroscopic dynamics we introduce the moments of the distribution function [103]:

$$\rho_{n,l}(\tau) = \int \frac{d^3p}{(2\pi)^3 p^0} \left(p^0\right)^{n+1} \left(\frac{p^z}{p^0}\right)^{2l} f(p^0, p^z, \tau). \tag{6.5}$$

Here, the integer n labels the energy-weighting and l captures the degree of anisotropy. Particularly we have, the number density n $= \rho_{0,0}$ and the energy desnity $\varepsilon = \rho_{1,0}$. For a Maxwell-Juttner equilibrium distribution, the equilibrium moments read

$$\rho_{n,l}^{\text{eq}}(T, z) = \frac{T^{n+3}}{2\pi^2} \frac{G_{n+3,l}(z)}{2l+1} e^{\mu/T}, \tag{6.6}$$

where $z \equiv m/T$ and $G_{n,l}(z)$ is defined in Appendix D.1; in the massless limit $\lim_{z\to 0} G_{n,l}(z) = \Gamma(n)$.

Integrating Eq. (6.3) with the weight of Eq. (6.5) yields the coupled moment equations

$$\frac{\partial \rho_{n,l}}{\partial \tau} + \frac{2l+1}{\tau}\rho_{n,l} - \frac{2l-n}{\tau}\rho_{n,l+1} = -\frac{1}{\tau_R}\left(\rho_{n,l} - \rho^{\mathrm{eq}}_{n,l}\right). \tag{6.7}$$

This defines an infinite hierarchy: each $\rho_{n,l}$ couples to $\rho_{n,l+1}$ and so on. Practical computations require a truncation or closure scheme for the moment hierarchy [107, 103, 47, 108].

6.2 Operator formulation and formal solutions

To exploit the linear-algebraic structure of (6.7) we adopt an operator notation. Writing the identity operator as $\hat{\mathbf{I}}$ and the shift operator $\hat{\mathbf{S}}$ acting on functions of l by $\hat{\mathbf{S}}[h(l)] = h(l+1)$, Eq. (6.7) can be compactly expressed as

$$\left(\frac{d}{d\tau} + \frac{2l+1}{\tau}\hat{\mathbf{I}} - \frac{2l-n}{\tau}\hat{\mathbf{S}}\right)\rho_{n,l} = -\frac{1}{\tau_R}\hat{\mathbf{I}}\left(\rho_{n,l} - \rho^{\mathrm{eq}}_{n,l}\right). \tag{6.8}$$

Define the operators

$$\hat{\mathbf{F}}(\tau) = \frac{2l+1}{\tau}\hat{\mathbf{I}} - \frac{2l-n}{\tau}\hat{\mathbf{S}}, \tag{6.9}$$

$$\hat{\mathbf{D}}(\tau) = \partial_\tau + \hat{\mathbf{F}}(\tau). \tag{6.10}$$

From the collision-free evolution equation,

$$\left(\partial_\tau + \hat{\mathbf{F}}(\tau)\right) g_{n,l}(\tau) = 0, \tag{6.11}$$

we infer that $\hat{\mathbf{F}}(\tau)$ plays the role of a Liouville-like free-streaming generator in moment space. This equation can be solved using an integrating factor (propagator)

$$g_{n,l}(\tau) = e^{-\hat{\mathbf{K}}(\tau,\tau_0)} g_{n,l}(\tau_0), \qquad \hat{\mathbf{K}}(\tau,\tau_0) = \int_{\tau_0}^{\tau} \hat{\mathbf{F}}(\tau')\, d\tau'. \tag{6.12}$$

If $g_{n,l}(\tau_0)$ are moments of some initial distribution function, then $g_{n,l}(\tau)$ are the moments of the corresponding free-streamed distribution. An explicit representation of the free-streaming propagator yields

$$g_{n,l}(\tau) = \sum_{k=0}^{\infty} K_{n,l,k}(\tau, \tau_0)\, g_{n,l+k}(\tau_0), \tag{6.13}$$

with the kernel (see Appendix. D.2.1)

$$K_{n,l,k}(\tau, \tau') = \frac{\left(l - \frac{n}{2}\right)^{(k)}}{k!} \left(\frac{\tau'}{\tau}\right)^{2l+1} \left[1 - \left(\frac{\tau'}{\tau}\right)^2\right]^k, \tag{6.14}$$

where $(x)^{(k)}$ denotes the rising Pochhammer symbol. The late-time scaling follows immediately:

$$g_{n,l}(\tau \gg \tau_0) \sim \left(\frac{\tau_0}{\tau}\right)^{2l+1},$$

independent of n.

Using the free-streaming propagator, the exact solution of the full AW-RTA moment equation (6.8) can be written as (see Appendix (D.2.1))

$$\rho_{n,l}(\tau) = e^{-\xi_0}\, e^{-\hat{\mathbf{K}}(\tau,\tau_0)}\, \rho_{n,l}(\tau_0) + \int_{\tau_0}^{\tau} \frac{d\tau'}{\tau_R(\tau')}\, e^{-\xi(\tau,\tau')}\, e^{-\hat{\mathbf{K}}(\tau,\tau')}\, \rho_{n,l}^{\mathrm{eq}}(\tau'), \tag{6.15}$$

where

$$\xi(\tau, \tau') \equiv \int_{\tau'}^{\tau} \frac{d\bar{\tau}}{\tau_R(\bar{\tau})}, \qquad \xi_0 \equiv \xi(\tau, \tau_0).$$

The integral term is the *hydrodynamic generator* $\rho_{n,l}^{G}(\tau)$, which encodes the cumulative collisional approach toward equilibrium. Expanding this generator leads to the gradient-type series described in the next section.

6.3 Gradient expansion of the moments

A systematic gradient expansion of the moment equations can be derived from the formal solution (6.15). Using the definition of the propagator and the properties of the incomplete

gamma function, one obtains (see Appendix D.2.2)

$$\rho_{n,l}(\tau) = e^{-\xi_0}\, e^{-\hat{\mathbf{K}}(\tau,\tau_0)}\, \rho_{n,l}(\tau_0) + \sum_{k=0}^{\infty} \frac{\gamma(k+1,\xi_0)}{k!} \left[-\tau_R \hat{\mathbf{D}}\right]^k \rho_{n,l}^{\mathrm{eq}}(\tau). \tag{6.16}$$

The first term represents the exponentially damped free-streaming contribution, while the second encodes both the gradient expansion and the non-perturbative corrections through the incomplete gamma function $\gamma(k+1,\xi_0)$. The structure closely parallels the singulant formalism introduced in [109].

To make the physical content more transparent, we explicitly separate the perturbative and non-perturbative contributions:

$$\begin{aligned}\rho_{n,l}(\tau) = &\sum_{k=0}^{\infty} \left(-\tau_R \hat{\mathbf{D}}\right)^k \rho_{n,l}^{\mathrm{eq}}(\tau) \\ &- e^{-\xi_0}\, e^{-\hat{\mathbf{K}}(\tau,\tau_0)} \left[\sum_{k=0}^{\infty} \left(-\tau_R \hat{\mathbf{D}}\right)^k \rho_{n,l}^{\mathrm{eq}}(\tau_0) - \rho_{n,l}(\tau_0)\right].\end{aligned} \tag{6.17}$$

The first line represents the Chapman-Enskog-type gradient series, while the second carries exponentially suppressed memory of the initial conditions. Neither series is convergent by itself; only their combination yields the exact, well-behaved solution. This decomposition is directly analogous to the trans-series structure of the full Boltzmann solution discussed in C.1.2.

6.4 Decomposition into gradient and non-perturbative parts

The formal solution motivates a natural separation of the non-equilibrium contributions into a perturbative (gradient) part and a transient (non-perturbative) part. Decomposing each moment as

$$\rho_{n,l} = \rho_{n,l}^{\mathrm{eq}} + \pi_{n,l}, \tag{6.18}$$

the deviation $\pi_{n,l}$ satisfies, from Eq. (6.8),

$$\hat{\mathbf{D}}\pi_{n,l} = -\frac{\pi_{n,l}}{\tau_R} - \hat{\mathbf{D}}\rho_{n,l}^{\mathrm{eq}}. \tag{6.19}$$

Iterating Eq. (6.19) gives a Chapman–Enskog-type expansion,

$$\pi^G_{n,l} = \sum_{k=1}^{\infty} \left[-\tau_R \hat{\mathbf{D}}\right]^k \rho^{\text{eq}}_{n,l}, \tag{6.20}$$

while the full, exact solution obtained from Eq. (6.15) reads

$$\begin{aligned}\pi_{n,l}(\tau) = &\sum_{k=1}^{\infty} (-\tau_R \hat{\mathbf{D}})^k \rho^{\text{eq}}_{n,l}(\tau) \\ &+ e^{-\xi_0}\, e^{-\hat{\mathbf{K}}(\tau,\tau_0)} \left[\rho_{n,l}(\tau_0) - \sum_{k=0}^{\infty} (-\tau_R \hat{\mathbf{D}})^k \rho^{\text{eq}}_{n,l}(\tau_0)\right].\end{aligned} \tag{6.21}$$

This expression naturally splits the solution into

$$\pi_{n,l} = \pi^G_{n,l} + \pi^T_{n,l}, \tag{6.22}$$

where the non-perturbative (transient) term is

$$\pi^T_{n,l}(\tau) = e^{-\xi_0}\, e^{-\hat{\mathbf{K}}(\tau,\tau_0)} \left[\rho_{n,l}(\tau_0) - \sum_{k=0}^{\infty} (-\tau_R \hat{\mathbf{D}})^k \rho^{\text{eq}}_{n,l}(\tau_0)\right]. \tag{6.23}$$

The term in brackets corresponds to the initial discrepancy between the exact and gradient-expanded initial data, $\pi^T_{n,l}(\tau_0) = \pi_{n,l}(\tau_0) - \pi^G_{n,l}(\tau_0)$.

The corresponding evolution equations for these two components follow directly from Eq. (6.19):

$$\hat{\mathbf{D}}\pi^G_{n,l} = -\frac{\pi^G_{n,l}}{\tau_R} - \hat{\mathbf{D}}\rho^{\text{eq}}_{n,l}, \tag{6.24}$$

$$\hat{\mathbf{D}}\pi^T_{n,l} = -\frac{\pi^T_{n,l}}{\tau_R}. \tag{6.25}$$

A key observation is that Eq. (6.24) for the gradient component has *the same structure* as the full evolution equation (6.19). Hence, hydrodynamic evolution can be constructed from the gradient expansion provided the transport coefficients are appropriately renormalized by non-perturbative terms. We show this by explicitly constructing the hydrodynamic evolution equations in the next section. This explains the surprising accuracy of viscous hydrodynamics even far from local equilibrium.

6.5 Hydrodynamic limit and validity condition

We now derive the hydrodynamic evolution equations explicitly for the $(0+1)$D system and identify the condition under which the hydrodynamic description remains valid. The moments can be grouped into equilibrium and anisotropic parts,

$$\rho_{n,l} = \rho_{n,l}^{\mathrm{eq}}(T,\mu) + \pi_{n,l}, \tag{6.26}$$

with temperature and chemical potential determined by the Landau matching conditions

$$\rho_{0,0} = \rho_{0,0}^{\mathrm{eq}}(T,\mu), \qquad \rho_{1,0} = \rho_{1,0}^{\mathrm{eq}}(T,\mu). \tag{6.27}$$

These yield the conservation laws

$$\begin{aligned} &\hat{\mathbf{D}}\rho_{0,0} = 0, && \text{(particle number conservation)}, \\ &\hat{\mathbf{D}}\rho_{1,0} = 0, && \text{(energy conservation)}. \end{aligned} \tag{6.28}$$

The evolution of the anisotropic components $\pi_{n,l}$ is governed by Eq. (6.19). For the physically relevant hydrodynamic variables—the bulk pressure Π and shear pressure π—we obtain

$$\partial_\tau \Pi + \frac{\Pi}{\tau_R} = \frac{\Pi}{\tau} - \hat{\mathbf{D}}P - \frac{m^2}{3}\frac{\pi_{-1,1}}{\tau}, \tag{6.29}$$

$$\partial_\tau \pi + \frac{\pi}{\tau_R} = -(4-c_s^2)\frac{\pi}{\tau} + 2(2-c_s^2)\frac{\Pi}{\tau} - \frac{\pi_{1,2}}{\tau} - \frac{m^2}{3}\frac{\pi_{-1,1}}{\tau}, \tag{6.30}$$

where $c_s^2 = \partial P/\partial\varepsilon$ is the squared speed of sound, and the operator $\hat{\mathbf{D}}P$ denotes the thermodynamic derivative,

$$\hat{\mathbf{D}}P = -c_s^2\frac{(\varepsilon + P + \Pi - \pi)}{\tau} - \frac{\kappa}{\tau} + \frac{3P}{\tau} - \frac{\rho_{1,2}^{\mathrm{eq}}}{\tau}, \tag{6.31}$$

with $\kappa = n\,\partial P/\partial n$ the bulk modulus. The relation $T^\mu_{\ \mu} = \varepsilon - 3(P+\Pi) = m^2\rho_{-1,1}$ acts as an effective equation of state linking bulk pressure and mass.

Equations (6.29) and (6.30) resemble those of second-order hydrodynamics [110, 62, 111, 66, 112], but here they are derived directly from the exact kinetic solution. Closure of the system requires expressing the higher-order moments $\pi_{-1,1}$ and $\pi_{1,2}$ in terms of the hydrodynamic variables $(\varepsilon, n, \Pi, \pi)$. From Eq. (6.16) these moments can be expressed as

$$\pi_{-1,1} = e^{-\xi_0}\, e^{-\hat{\mathbf{K}}(\tau,\tau_0)}\rho_{-1,1}(\tau_0) - e^{-\xi_0}\rho^{\mathrm{eq}}_{-1,1}(\tau) + \sum_{k=1}^{\infty} \frac{(-1)^k\,\gamma(k+1,\xi_0)}{k!}\left[-\tau_R\hat{\mathbf{D}}\right]^k \rho^{\mathrm{eq}}_{-1,1}(\tau), \tag{6.32}$$

$$\pi_{1,2} = e^{-\xi_0}\, e^{-\hat{\mathbf{K}}(\tau,\tau_0)}\rho_{1,2}(\tau_0) - e^{-\xi_0}\rho^{\mathrm{eq}}_{1,2}(\tau) + \sum_{k=1}^{\infty} \frac{(-1)^k\,\gamma(k+1,\xi_0)}{k!}\left[-\tau_R\hat{\mathbf{D}}\right]^k \rho^{\mathrm{eq}}_{1,2}(\tau). \tag{6.33}$$

A complete closure is not possible because the initial-condition term $e^{-\xi_0}e^{-\hat{\mathbf{K}}}\rho_{n,l}(\tau_0)$ cannot be expressed through local gradients alone. However, if the ratio

$$\frac{e^{-\xi_0}\left[e^{-\hat{\mathbf{K}}(\tau,\tau_0)}\rho_{n,l}(\tau_0) - \rho^{\mathrm{eq}}_{n,l}(\tau)\right]}{\pi_{n,l}} \ll 1, \tag{6.34}$$

for $(n,l) = (-1,1)$ and $(1,2)$, then the system can be approximately closed, leading to

$$\partial_\tau\Pi + \frac{\Pi}{\tau_R} = \frac{\Pi}{\tau} - \hat{\mathbf{D}}P + \frac{m^2}{3\tau}\sum_{k=1}^{\infty}\frac{\gamma(k+1,\xi_0)}{k!}\left[-\tau_R\hat{\mathbf{D}}\right]^k \rho^{\mathrm{eq}}_{-1,1}(\tau), \tag{6.35}$$

$$\begin{aligned}\partial_\tau\pi + \frac{\pi}{\tau_R} = &-(4-c_s^2)\frac{\pi}{\tau} + 2(2-c_s^2)\frac{\Pi}{\tau} - \frac{1}{\tau}\sum_{k=1}^{\infty}\frac{\gamma(k+1,\xi_0)}{k!}\left[-\tau_R\hat{\mathbf{D}}\right]^k \rho^{\mathrm{eq}}_{1,2}(\tau) \\ &- \frac{m^2}{3\tau}\sum_{k=1}^{\infty}\frac{\gamma(k+1,\xi_0)}{k!}\left[-\tau_R\hat{\mathbf{D}}\right]^k \rho^{\mathrm{eq}}_{-1,1}(\tau).\end{aligned} \tag{6.36}$$

The resulting equations coincide structurally with those from the standard gradient expansion, but with *transport coefficients renormalised* by non-perturbative corrections involving $\gamma(k+1,\xi_0)$. The operators $[\tau_R\hat{\mathbf{D}}]^k\rho^{\mathrm{eq}}_{n,l}$ can always be expressed in terms of the hydrodynamic variables (T,μ,Π,π), providing a rigorous foundation for the renormalized transport coefficients proposed in earlier analyses [45, 49].

The central result may be summarised schematically as

Hydrodynamic evolution $\sim$ *Gradient expansion* $+$ *Modified (renormalized) transport coefficients*,

and the accuracy of this hydrodynamic approximation is quantitatively measured by the smallness of the ratio in Eq. (6.34). This provides a precise criterion for the validity of relativistic hydrodynamics beyond local equilibrium.

6.6 Generalisation to 3 + 1D

The conclusions obtained in the $(0+1)$D setting extend to full $3+1$D dynamics. Two structural observations lie at the heart of this generalisation. First, the exact evolution equations for the non-equilibrium moments retain the same operator structure as the equations obeyed by the terms of the gradient expansion. Second, the non-perturbative, exponentially decaying pieces that carry initial-condition information can be written in terms of appropriately scaled local gradients. In this section, we show how these properties persist in the $3+1$D moment formalism and discuss the consequences for constructing hydrodynamic equations.

6.6.1 Linearised moment equations

Motivated by the moment hierarchy for the Boltzmann equation [62, 113], we consider a general linearised relaxation-type model for the moment vector $\vec{\rho}(x)$,

$$\left(\partial_\tau + \hat{\mathbf{F}}\right)\vec{\rho} = -\hat{\mathbf{C}}\,\vec{\rho}, \tag{6.37}$$

where $\hat{\mathbf{F}}$ is a Liouville–type operator encoding streaming and gradient couplings, and $\hat{\mathbf{C}}$ is the linearised collision operator in moment space. This schematic form preserves the essential algebraic and spectral properties of the full Boltzmann collision kernel while allowing for a transparent operator treatment. In particular, the operator $\hat{\mathbf{C}}$ is positive semi-definite (as for the linearised Boltzmann kernel). Its kernel contains the conserved moments associated with particle number, energy and momentum; these zero-modes correspond to hydrodynamic variables. The operator $\hat{\mathbf{F}}$ is the moment-space streaming (Liouville) operator; it couples spatial gradients to moment indices and, in general, has a matrix structure [114, 115, 99]

$$\hat{\mathbf{F}} = \mathbf{F}_\mu\,\nabla^\mu + \mathbf{A}, \tag{6.38}$$

where ∇^μ are comoving derivatives and $\mathbf{F}_\mu, \mathbf{A}$ are (matrix) operators acting on the moment vector.

A convenient and physically transparent subclass of models is given by relaxation-type kernels, for which one may write

$$\hat{\mathbf{C}} = \hat{\boldsymbol{\nu}} - \hat{\mathbf{G}}, \tag{6.39}$$

with $\hat{\boldsymbol{\nu}}$ a positive-definite "collision-frequency" operator and $\hat{\mathbf{G}}$ its equilibrium projection. In the AW-RTA, $\hat{\boldsymbol{\nu}} = \hat{\mathbf{I}}/\tau_R$ and $\hat{\mathbf{G}}\vec{\rho} = \hat{\boldsymbol{\nu}}\vec{\rho}^{\,\mathrm{eq}}$, recovering the familiar single-timescale relaxation.

6.6.2 Moment equations in a general relaxation-time model

Under a general relaxation-time model the moment equations take the compact form

$$\hat{\mathbf{D}}\,\vec{\rho}(\tau) = -\hat{\boldsymbol{\nu}}_R\big(\vec{\rho} - \vec{\rho}^{\,\mathrm{eq}}\big), \qquad \hat{\mathbf{D}} \equiv \partial_\tau + \hat{\mathbf{F}}. \tag{6.40}$$

Decomposing $\vec{\rho} = \vec{\rho}^{\,\mathrm{eq}} + \boldsymbol{\pi}$ yields the exact evolution of the non-equilibrium piece

$$\hat{\mathbf{D}}\,\boldsymbol{\pi}(\tau) = -\hat{\boldsymbol{\nu}}_R\,\boldsymbol{\pi} - \hat{\mathbf{D}}\,\vec{\rho}^{\,\mathrm{eq}}(\tau). \tag{6.41}$$

Iterating (6.41) produces the formal gradient expansion

$$\boldsymbol{\pi}^{G}(\tau) = \sum_{k=1}^{\infty}\big(-\hat{\boldsymbol{\nu}}_R^{-1}\hat{\mathbf{D}}\big)^k\,\vec{\rho}^{\,\mathrm{eq}}(\tau), \tag{6.42}$$

while the transients must satisfy

$$\hat{\mathbf{D}}\,\boldsymbol{\pi}^{T} = -\hat{\boldsymbol{\nu}}_R\,\boldsymbol{\pi}^{T}. \tag{6.43}$$

Equations (6.42) and (6.43) display the same operator structure as in the $(0+1)$D analysis: the gradient component obeys the same type of relaxation–driving equation as the full non-equilibrium moment, and the hidden transient part decays exponentially with rates set by $\hat{\boldsymbol{\nu}}_R$.

Because $\hat{\boldsymbol{\nu}}_R$ acts in an infinite-dimensional moment space, its spectrum typically contains a continuous component and many timescales. The null space of $\hat{\mathbf{C}}$ contains the con-

served hydrodynamic modes; for truncated moment systems, the operators become finite-dimensional and the spectrum discrete. These spectral features are responsible for the appearance of multiple decay times and the possible delay of hydrodynamization when higher-moment or momentum-dependent relaxation effects are important.

6.6.3 Formal solution via the interaction (collision) picture

To obtain a compact formal solution, it is convenient to move to the collision (interaction) picture with respect to the free-streaming operator $\hat{\mathbf{F}}$. Define the free-streaming propagator $\hat{\mathcal{F}}_{\tau,\tau_0}$ by

$$\partial_\tau \hat{\mathcal{F}}_{\tau,\tau_0} = -\hat{\mathbf{F}}\,\hat{\mathcal{F}}_{\tau,\tau_0}, \qquad \hat{\mathcal{F}}_{\tau_0,\tau_0} = \hat{\mathbf{I}}. \tag{6.44}$$

The collision-picture moments and collision-frequency operator are

$$\vec{\rho}_c(\tau) = \hat{\mathcal{F}}^{-1}_{\tau,\tau_0}\vec{\rho}(\tau), \qquad \hat{\boldsymbol{\nu}}_c(\tau) = \hat{\mathcal{F}}^{-1}_{\tau,\tau_0}\,\hat{\boldsymbol{\nu}}_R(\tau)\,\hat{\mathcal{F}}_{\tau,\tau_0}. \tag{6.45}$$

The evolution equation (6.40) becomes

$$\big(\partial_\tau + \hat{\boldsymbol{\nu}}_c(\tau)\big)\vec{\rho}_c(\tau) = \hat{\boldsymbol{\nu}}_c(\tau)\,\vec{\rho}_c^{\,\mathrm{eq}}(\tau). \tag{6.46}$$

Its solution is

$$\vec{\rho}_c(\tau) = \hat{\mathcal{W}}_{\tau,\tau_0}\,\vec{\rho}_c(\tau_0) + \int_{\tau_0}^{\tau} d\tau'\,\hat{\mathcal{W}}_{\tau,\tau'}\,\hat{\boldsymbol{\nu}}_c(\tau')\,\vec{\rho}_c^{\,\mathrm{eq}}(\tau'), \tag{6.47}$$

where $\hat{\mathcal{W}}_{\tau,\tau'} = \mathcal{T}\exp\big[-\int_{\tau'}^{\tau} d\bar{\tau}\,\hat{\boldsymbol{\nu}}_c(\bar{\tau})\big]$ is the time-ordered exponential satisfying $\partial_\tau\hat{\mathcal{W}}_{\tau,\tau'} = -\hat{\boldsymbol{\nu}}_c(\tau)\,\hat{\mathcal{W}}_{\tau,\tau'}$.

Commuting case: $[\hat{\mathbf{F}}, \hat{\boldsymbol{\nu}}_R] = 0$

If the operators commute at all times, $[\hat{\mathbf{F}}, \hat{\boldsymbol{\nu}}_R] = 0$, then $\hat{\boldsymbol{\nu}}_c = \hat{\boldsymbol{\nu}}_R$ and the collision-picture propagator reduces to a scalar damping factor analogous to the $(0+1)$D damping,

$$\hat{\mathcal{W}}_{\tau,\tau'} = \exp\big(-\xi(\tau,\tau')\big), \qquad \xi(\tau,\tau') = \int_{\tau'}^{\tau} d\bar{\tau}\,\hat{\boldsymbol{\nu}}_R(\bar{\tau}). \tag{6.48}$$

Transforming back to the Schrodinger picture gives the familiar form

$$\vec{\rho}(\tau) = e^{-\xi_0}\,\hat{\mathcal{F}}_{\tau,\tau_0}\,\vec{\rho}(\tau_0) + \int_{\tau_0}^{\tau} d\tau'\,\frac{e^{-\xi(\tau,\tau')}}{\tau_R(\tau')}\,\hat{\mathcal{F}}_{\tau,\tau'}\,\vec{\rho}^{\,\mathrm{eq}}(\tau'). \tag{6.49}$$

Proceeding as in the $(0+1)$D case by changing variables to ξ and Taylor-expanding the integrand yields an exact gradient-type expansion with incomplete-gamma coefficients; this expansion is the direct $3+1$D analogue of the $0+1$D series and admits the same separation into a gradient series plus exponentially suppressed transients.

Non-commuting case

When $[\hat{\mathbf{F}}, \hat{\boldsymbol{\nu}}_R] \neq 0$ the analysis is algebraically more involved because $\hat{\boldsymbol{\nu}}_c(\tau)$ and the time-ordered exponential $\hat{\mathcal{W}}_{\tau,\tau'}$ are nontrivial operator-valued functions of time. Nevertheless, an analogous decomposition persists. Using integration by parts together with the propagator equation (6.47) one may show (see Appendix D.3.1) that

$$\begin{aligned}\vec{\rho}(\tau) = &\sum_{k=0}^{\infty}\left(-\hat{\boldsymbol{\nu}}_R^{-1}\hat{\mathbf{D}}\right)^k \vec{\rho}^{\,\mathrm{eq}}(\tau) \\ &+ \hat{\mathcal{F}}_{\tau,\tau_0}\,\hat{\mathcal{W}}_{\tau,\tau_0}\left[\vec{\rho}(\tau_0) - \sum_{k=0}^{\infty}\left(-\hat{\boldsymbol{\nu}}_R^{-1}\hat{\mathbf{D}}\right)^k \vec{\rho}^{\,\mathrm{eq}}(\tau_0)\right].\end{aligned} \tag{6.50}$$

The first line is the gradient expansion; the second line is an operator-valued transient that encodes the initial data and decays under the combined action of free streaming and collisions. Thus the decomposition $\vec{\rho} = \vec{\rho}^{\,\mathrm{eq}} + \boldsymbol{\pi}^G + \boldsymbol{\pi}^T$ remains valid even in the non-commuting, fully $3+1$D case. The explicit form of the renormalised transport coefficients in the general non-commuting case is more complicated than in the commuting case, but conceptually they arise from the same mechanism.

6.6.4 Hydrodynamic generator and transients in $3+1$D

The hydrodynamic generator in (6.47) generalises the $0+1$D generator: it is the time integral of the equilibrium source acted on by the damping propagator $\hat{\mathcal{W}}$ and the free-streaming

operator $\hat{\mathcal{F}}$. By integration by parts one rewrites the generator as a series of local differential operators acting on $\vec{\rho}^{\,\mathrm{eq}}(\tau)$ with operator-valued coefficients (generalised incomplete gamma functions). The transient piece is likewise expressed as

$$\boldsymbol{\pi}^{T}(\tau) = \hat{\mathcal{F}}_{\tau,\tau_0}\,\hat{\mathcal{W}}_{\tau,\tau_0}\left[\boldsymbol{\pi}(\tau_0) - \boldsymbol{\pi}^{G}(\tau_0)\right], \tag{6.51}$$

which is the straightforward $3+1$D analogue of the $0+1$D transient (compare Eq. (6.23)). For analytic initial data and smooth evolution, each gradient operator $[-\hat{\boldsymbol{\nu}}_R^{-1}\hat{\mathbf{D}}]^k\vec{\rho}^{\,\mathrm{eq}}(\tau_0)$ may be Taylor-expanded about τ, and the Taylor coefficients identify the modifications required to the transport coefficients in the gradient expansion.

The $3+1$D analysis shows that the conclusions drawn from the $0+1$D model are generic: the exact kinetic solution decomposes into a gradient (Chapman–Enskog) contribution plus exponentially decaying transients carrying initial data. The hydrodynamic approximation is therefore obtained by (i) truncating the gradient series and (ii) renormalising transport coefficients to account for operator-valued non-perturbative weights. In the commuting case this renormalisation admits a compact closed form; in the general non-commuting case it must be expressed through more complicated series expansions (see Appendix D.3.2 for the AW–RTA example).

In practice, this means that hydrodynamic theories that allow for time- and gradient-dependent transport coefficients (or equivalently include the leading non-perturbative weights) can faithfully reproduce the exact kinetic evolution over a much wider regime than the naive Chapman–Enskog truncation. This observation underpins the success of modern second-order and resumed hydrodynamic frameworks in describing far-from-equilibrium systems.

6.7 Summary

In this chapter, we developed a framework for understanding the validity and emergence of relativistic hydrodynamics directly from kinetic theory. Starting from the $(0+1)$D

system, we demonstrated that the exact solutions of the Boltzmann equation within the relaxation-time approximation can be decomposed into two distinct components: a gradient (Chapman–Enskog) contribution and an exponentially decaying non-perturbative contribution that encodes the system's initial conditions. The gradient component captures the near-equilibrium dynamics through a systematic expansion in spacetime derivatives, while the non-perturbative term describes transient effects that fade exponentially as the system evolves toward local equilibrium.

We showed that this decomposition is not unique to simplified geometries but persists in the full $(3+1)$D framework. In both cases, the evolution equations for the non-equilibrium components retain the same operator structure as those governing the gradient expansion. This structural equivalence implies that hydrodynamic equations can be constructed directly from the gradient hierarchy, provided that the transport coefficients are appropriately modified to incorporate the effects of non-perturbative damping. In the special case where the free-streaming and collision operators commute, this modification can be expressed in closed form through incomplete gamma functions. For the general, non-commuting case, the same physical picture holds, albeit with a more complicated structural form.

In summary, this chapter demonstrates that the validity of relativistic hydrodynamics does not depend on proximity to local equilibrium. The exact-moment formulation presented here reveals that hydrodynamic behaviour emerges as an interpolation between the collisionless and equilibrated limits, with transport coefficients renormalised by microscopic relaxation dynamics. These results establish that relativistic hydrodynamics emerges as a resummed and renormalised form of the kinetic evolution, rather than a simple truncation of the Chapman–Enskog expansion. This perspective provides a consistent theoretical foundation for understanding hydrodynamization and paves the way for the final chapters, where we explore how these principles generalise to more realistic systems and connect to effective hydrodynamic theories used in quark–gluon plasma phenomenology.

Chapter 7

Conclusion and Outlook

The central objective of this thesis was to investigate the microscopic foundations and regime of validity of relativistic hydrodynamics beyond local thermal equilibrium. Hydrodynamics, though formulated as an effective long-wavelength theory, has been remarkably successful in describing systems that are far from equilibrium, most notably the quark–gluon plasma (QGP) produced in relativistic heavy-ion collisions. This apparent paradox-the success of a near-equilibrium theory in a far-from-equilibrium regime motivated the present work. Using relativistic kinetic theory as a microscopic framework, this thesis developed a systematic understanding of how hydrodynamics emerges from the Boltzmann equation, the role of asymptotic expansions, and the manner in which non-perturbative contributions determine the true dynamical behavior of many-particle systems.

The thesis began with a general overview of relativistic hydrodynamics and its microscopic underpinnings in kinetic theory. The ideal hydrodynamic equations were obtained from the conservation laws of energy-momentum and charge, assuming local thermal equilibrium. The framework was then extended to include dissipative effects, introducing the viscous corrections that give rise to second-order hydrodynamics. This established the theoretical context in which the later kinetic analysis was carried out.

We investigated the emergence of hydrodynamic attractors and the process of hydrodynamization in expanding relativistic systems using the Boltzmann equation under Bjorken symmetry. For conformal systems with a constant relaxation time, we found that macroscopic observables such as the pressure anisotropy rapidly converge toward a universal early-time attractor, largely independent of initial conditions. This behaviour illustrates

that hydrodynamization can occur well before local thermal equilibrium is achieved. In contrast, when conformal symmetry is broken—either by introducing particle masses, external longitudinal forces, or a momentum-dependent relaxation time—the early-time universality is lost. The system retains memory of its initial conditions for a much longer period, and only a late-time attractor corresponding to the hydrodynamic regime survives. These results demonstrate that early-time attractors, though characteristic of simple conformal dynamics, do not represent a general mechanism for hydrodynamization. Instead, the transition to hydrodynamics depends sensitively on microscopic physics and the breaking of scale invariance.

Building on this understanding, Chapter 5 developed an *exact, convergent gradient expansion* of the Boltzmann equation, providing a new perspective on the relation between kinetic theory and hydrodynamics. This analysis revealed that the traditional Chapman-Enskog series, often viewed as divergent, is in fact only an asymptotic representation of a convergent series. The apparent divergence reflects the presence of exponentially suppressed non-perturbative contributions of the so-called transient or non-hydrodynamic modes that carry memory of initial conditions. Once these contributions are properly accounted for, the full series converges and smoothly interpolates between the collisionless (free-streaming) and hydrodynamic regimes.

The results obtained for the single-particle distribution function were subsequently interpreted within the framework of relativistic hydrodynamics by taking successive moments of the distribution function. A linear-operator formulation was employed, exploiting the inherent linearity of the RTA moment equations to analyse the structure of their exact solutions. In the $(0+1)$-dimensional case, the exact moment equations and their formal operator solutions revealed that the system's evolution naturally decomposes into two distinct components: a perturbative (gradient) part, which satisfies the same evolution equation as the hydrodynamic expansion, and a non-perturbative (transient) part, which decays

exponentially on microscopic timescales. This structural correspondence explains why hydrodynamics remains accurate even far from local equilibrium—the hydrodynamic sector captures the long-lived collective modes of the microscopic dynamics, while the transient contributions rapidly fade away.

The analysis was then extended to the full $(3+1)$-dimensional framework, where the same operator structure and decomposition persist. In this more general setting, the evolution of non-equilibrium moments continues to separate into gradient and transient contributions. In the commuting limit of the streaming and collision operators, we derived closed-form expressions for the hydrodynamic generator, providing a direct generalisation of the $(0+1)$D results. When the operators do not commute, a more intricate transient structure emerges; nevertheless, the qualitative features remain unchanged.

Outlook and future directions

The operator-based formulation of hydrodynamics developed in this thesis opens several promising avenues for future research. On the theoretical side, it can be extended to more realistic collision kernels beyond the RTA—such as the full Boltzmann or quantum kinetic equations—to investigate how multi-scale relaxation processes influence the analytic structure of the hydrodynamic expansion. Incorporating momentum-dependent relaxation times and quantum statistical effects would further refine the microscopic foundations of transport coefficients.

A second direction concerns phenomenological applications to the quark–gluon plasma. The exact gradient resummation and renormalized transport coefficients obtained here can be implemented in numerical hydrodynamic simulations to assess their impact on experimental observables, including flow harmonics and particle spectra. Because the resummed formulation provides a controlled interpolation between free streaming and hydrodynamics,

it offers a natural framework for setting initial conditions in heavy-ion collision modelling.

The influence of the renormalized coefficients is expected to be most pronounced at early times, when the system transitions from free streaming to collective hydrodynamic behavior. Experimental constraints on transport coefficients during these initial stages—together with dedicated simulations tracking the evolution from pre-equilibrium dynamics to hydrodynamics—would provide meaningful tests of the framework developed in this thesis. Such combined theoretical and phenomenological studies would deepen our understanding of the microscopic origins, limitations, and applicability of hydrodynamic behavior in strongly interacting matter.

Concluding remarks

The Chapman-Enskog expansion offers a systematic gradient-based route to hydrodynamics, but in the relativistic regime, it remains intrinsically acausal because it captures only the slow, near-equilibrium sector of the dynamics. Modern causal formulations—beginning with Israel-Stewart theory and later generalisations—address this limitation by promoting dissipative currents to independent dynamical fields with finite relaxation times. This restructuring ensures stability and causality while incorporating the fast transient modes that are absent in the traditional gradient expansion.

This promotion has a clear physical interpretation. The Chapman-Enskog expansion captures only the asymptotic, long-wavelength sector of the dynamics, whereas the full Boltzmann equation contains additional fast transient modes that decay on microscopic time scales. By elevating dissipative quantities to dynamical variables, Israel-Stewart-type theories effectively incorporate these fast modes into the macroscopic description. Although these modes are traditionally referred to as ”non-hydrodynamic”, this terminology is somewhat misleading: they are essential for ensuring causality and stability, and they appear

naturally in the exact solution of the kinetic theory. In this broader sense, they should be regarded as part of the correct relativistic hydrodynamic description.

In this thesis the conventional terminology is retained, with the slow, gradient-controlled sector referred to as ”hydrodynamic” and the fast, exponentially decaying sector as ”non-hydrodynamic”. Nevertheless, the analysis presented here shows that the more meaningful distinction is between perturbative gradient contributions and non-perturbative transient contributions. Both are required for a consistent macroscopic description of relativistic fluids, and both emerge naturally from the exact structure of the Boltzmann equation.

In summary, this thesis shows that relativistic hydrodynamics is an emergent, analytic limit of the microscopic Boltzmann dynamics. The apparent breakdown of the traditional Chapman–Enskog expansion does not signal a failure of hydrodynamics, but rather the need to resum it so that both the long-lived collective modes and the decaying transient modes are incorporated consistently. This resummation is carried out implicitly by the promoting of dissipative terms into independent dynamical fields. Hydrodynamics thus emerges as the effective theory capturing both the long-lived and transient modes of the underlying microscopic dynamics, providing an effective framework for describing the collective behavior of matter even far from equilibrium.

Bibliography

[1] ALICE Collaboration. "Centrality dependence of charged-particle pseudorapidity density at mid-rapidity in Pb–Pb collisions at $\sqrt{s_{\mathrm{NN}}} = 5.36$ TeV". In: *Physics Letters B* (2025). DOI: 10.1016/j.physletb.2025.???.

[2] K Aamodt et al. "Elliptic flow of charged particles in Pb-Pb collisions at 2.76 TeV". In: *Phys. Rev. Lett.* 105 (2010), p. 252302. DOI: 10.1103/PhysRevLett.105.252302. arXiv: 1011.3914 [nucl-ex].

[3] Serguei Chatrchyan et al. "Measurement of the Elliptic Anisotropy of Charged Particles Produced in PbPb Collisions at $\sqrt{s_{NN}}$=2.76 TeV". In: *Phys. Rev. C* 87.1 (2013), p. 014902. DOI: 10.1103/PhysRevC.87.014902. arXiv: 1204.1409 [nucl-ex].

[4] S. S. Adler et al. "Elliptic flow of identified hadrons in Au+Au collisions at s(NN)**(1/2) = 200-GeV". In: *Phys. Rev. Lett.* 91 (2003), p. 182301. DOI: 10.1103/PhysRevLett.91.182301. arXiv: nucl-ex/0305013.

[5] John Adams et al. "Particle type dependence of azimuthal anisotropy and nuclear modification of particle production in Au + Au collisions at s(NN)**(1/2) = 200-GeV". In: *Phys. Rev. Lett.* 92 (2004), p. 052302. DOI: 10.1103/PhysRevLett.92.052302. arXiv: nucl-ex/0306007.

[6] Tetsufumi Hirano and Miklos Gyulassy. "Perfect fluidity of the quark gluon plasma core as seen through its dissipative hadronic corona". In: *Nucl. Phys. A* 769 (2006), pp. 71–94. DOI: 10.1016/j.nuclphysa.2006.02.005. arXiv: nucl-th/0506049.

[7] Jean-Yves Ollitrault. "Anisotropy as a signature of transverse collective flow". In: *Phys. Rev. D* 46 (1992), pp. 229–245. DOI: 10.1103/PhysRevD.46.229.

[8] Edward Shuryak. "Strongly coupled quark-gluon plasma in heavy ion collisions". In: *Rev. Mod. Phys.* 89 (2017), p. 035001. DOI: 10.1103/RevModPhys.89.035001. arXiv: 1412.8393 [hep-ph].

[9] Ulrich W. Heinz. "The Strongly coupled quark-gluon plasma created at RHIC". In: *J. Phys. A* 42 (2009). Ed. by David Neilson and Gaetano Senatore, p. 214003. DOI: 10.1088/1751-8113/42/21/214003. arXiv: 0810.5529 [nucl-th].

[10] R. Nouicer. "New State of Nuclear Matter: Nearly Perfect Fluid of Quarks and Gluons in Heavy Ion Collisions at RHIC Energies". In: *Eur. Phys. J. Plus* 131.3 (2016), p. 70. DOI: 10.1140/epjp/i2016-16070-2. arXiv: 1512.08993 [nucl-ex].

[11] Jacquelyn Noronha-Hostler, Jorge Noronha, and Miklos Gyulassy. "The unreasonable effectiveness of hydrodynamics in heavy ion collisions". In: *Nucl. Phys. A* 956 (2016). Ed. by Y. Akiba et al., pp. 890–893. DOI: 10.1016/j.nuclphysa.2016.01.050. arXiv: 1512.07135 [nucl-th].

[12] Jacquelyn Noronha-Hostler et al. “Bulk Viscosity Effects in Event-by-Event Relativistic Hydrodynamics”. In: *Phys. Rev. C* 88.4 (2013), p. 044916. DOI: 10.1103/PhysRevC.88.044916. arXiv: 1305.1981 [nucl-th].

[13] U. Heinz and R. Snellings. “Collective flow and viscosity in relativistic heavy-ion collisions”. In: *Annu. Rev. Nucl. Part. Sci.* 63 (2013), pp. 123–151. DOI: 10.1146/annurev-nucl-102212-170540. arXiv: arXiv:1301.2826 [nucl-th].

[14] Paul Romatschke and Ulrike Romatschke. “Viscosity Information from Relativistic Nuclear Collisions: How Perfect is the Fluid Observed at RHIC?” In: *Phys. Rev. Lett.* 99.17 (2007), p. 172301. DOI: 10.1103/PhysRevLett.99.172301. eprint: arXiv:0706.1522[nucl-th].

[15] J. Noronha-Hostler, J. Noronha, and F. Grassi. “Bulk viscosity-driven suppression of shear viscosity effects on the flow harmonics at energies available at the BNL Relativistic Heavy Ion Collider”. In: *Phys. Rev. C* 90.3 (2014), p. 034907. DOI: 10.1103/PhysRevC.90.034907. arXiv: 1406.3333 [nucl-th].

[16] Matthew Luzum and Jean-Yves Ollitrault. “Extracting the shear viscosity of the quark-gluon plasma from flow in ultra-central heavy-ion collisions”. In: *Nucl. Phys. A* 904-905 (2013). Ed. by Thomas Ullrich, Bolek Wyslouch, and John W. Harris, pp. 377c–380c. DOI: 10.1016/j.nuclphysa.2013.02.028. arXiv: 1210.6010 [nucl-th].

[17] M. I. Abdulhamid et al. “Observation of the electromagnetic field effect via charge-dependent directed flow in heavy-ion collisions at the Relativistic Heavy Ion Collider”. In: *Phys. Rev. X* 14.1 (2024), p. 011028. DOI: 10.1103/PhysRevX.14.011028. arXiv: 2304.03430 [nucl-ex].

[18] Md Rihan Haque, Chitrasen Jena, and Bedangadas Mohanty. “A Review of Elliptic Flow of Light Nuclei in Heavy-Ion Collisions at RHIC and LHC Energies”. In: *Adv. High Energy Phys.* 2017 (2017), p. 1248563. DOI: 10.1155/2017/1248563. arXiv: 1707.09192 [nucl-ex].

[19] Md. Nasim et al. “Energy dependence of elliptic flow from heavy-ion collision models”. In: *Phys. Rev. C* 82 (2010), p. 054908. DOI: 10.1103/PhysRevC.82.054908. arXiv: 1010.5196 [nucl-ex].

[20] D. Teaney, J. Lauret, and E. V. Shuryak. “A hydrodynamic description of heavy ion collisions at the SPS and RHIC”. In: *arXiv e-prints* (Oct. 2001). Preprint of Teaney, Lauret & Shuryak (2001), arXiv: nucl-th/0110037. eprint: nucl-th/0110037.

[21] Peter F. Kolb and Ulrich Heinz. “Hydrodynamic description of ultrarelativistic heavy-ion collisions”. In: *Quark Gluon Plasma 3*. Ed. by R. C. Hwa and X. N. Wang. Also available as arXiv preprint nucl-th/0305084. World Scientific, 2003, pp. 634–714.

[22] Derek A. Teaney. “Viscous Hydrodynamics and the Quark Gluon Plasma”. In: *Quark-gluon plasma 4*. Ed. by Rudolph C. Hwa and Xin-Nian Wang. 2010, pp. 207–266. DOI: 10.1142/9789814293297_0004. arXiv: 0905.2433 [nucl-th].

[23] Ulrich Heinz and Björn Schenke. "Hydrodynamic Description of the Quark-Gluon Plasma". In: Dec. 2024. arXiv: 2412.19393 [nucl-th].

[24] Raimond Snellings. "Elliptic Flow: A Brief Review". In: *New J. Phys.* 13 (2011), p. 055008. DOI: 10.1088/1367-2630/13/5/055008. arXiv: 1102.3010 [nucl-ex].

[25] Serguei Chatrchyan et al. "Studies of Azimuthal Dihadron Correlations in Ultra-Central PbPb Collisions at $\sqrt{s_{NN}} = 2.76$ TeV". In: *JHEP* 02 (2014), p. 088. DOI: 10.1007/JHEP02(2014)088. arXiv: 1312.1845 [nucl-ex].

[26] Chun Shen, Zhi Qiu, and Ulrich Heinz. "Shape and flow fluctuations in ultracentral Pb + Pb collisions at the energies available at the CERN Large Hadron Collider". In: *Phys. Rev. C* 92.1 (2015), p. 014901. DOI: 10.1103/PhysRevC.92.014901. arXiv: 1502.04636 [nucl-th].

[27] Tetsufumi Hirano et al. "Mass ordering of differential elliptic flow and its violation for phi mesons". In: *Phys. Rev. C* 77 (2008), p. 044909. DOI: 10.1103/PhysRevC.77.044909. arXiv: 0710.5795 [nucl-th].

[28] Kevin Dusling, Wei Li, and Björn Schenke. "Novel collective phenomena in high-energy proton–proton and proton–nucleus collisions". In: *Int. J. Mod. Phys. E* 25.01 (2016), p. 1630002. DOI: 10.1142/S0218301316300022. arXiv: 1509.07939 [nucl-ex].

[29] Wei Li. "Collective flow from AA, pA to pp collisions – Toward a unified paradigm". In: *Nucl. Phys. A* 967 (2017). Ed. by Ulrich Heinz, Olga Evdokimov, and Peter Jacobs, pp. 59–66. DOI: 10.1016/j.nuclphysa.2017.05.011. arXiv: 1704.03576 [nucl-ex].

[30] Soren Schlichting and Prithwish Tribedy. "Collectivity in Small Collision Systems". In: *Adv. High Energy Phys.* 2016 (2016), p. 8460349. DOI: 10.1155/2016/8460349. arXiv: 1611.00329 [hep-ph].

[31] James L. Nagle and William A. Zajc. "Small System Collectivity in Relativistic Hadronic and Nuclear Collisions". In: *Ann. Rev. Nucl. Part. Sci.* 68 (2018), pp. 211–235. DOI: 10.1146/annurev-nucl-101917-020902. arXiv: 1801.03477 [nucl-ex].

[32] Piotr Bożek and Wojciech Broniowski. "Collective Flow in Small Systems". In: *Nucl. Phys. A* 1005 (2021), p. 121843. DOI: 10.1016/j.nuclphysa.2020.121843. arXiv: 2012.01931 [nucl-th].

[33] Björn Schenke, Sangyong Jeon, and Charles Gale. "Elliptic and triangular flow in event-by-event (3+1)D viscous hydrodynamics". In: *Phys. Rev. Lett.* 106 (2011), p. 042301. DOI: 10.1103/PhysRevLett.106.042301. arXiv: 1009.3244 [hep-ph].

[34] Björn Schenke, Prithwish Tribedy, and Raju Venugopalan. "Event-by-event gluon multiplicity, energy density, and eccentricities in ultrarelativistic heavy-ion collisions". In: *Phys. Rev. C* 86 (2012), p. 034908. DOI: 10.1103/PhysRevC.86.034908. arXiv: 1206.6805 [hep-ph].

[35] Björn Schenke, Prithwish Tribedy, and Raju Venugopalan. "Fluctuating Glasma initial conditions and flow in heavy-ion collisions". In: *Phys. Rev. Lett.* 108 (2012), p. 252301. DOI: 10.1103/PhysRevLett.108.252301. arXiv: 1202.6646 [hep-ph].

[36] Charles Gale, Sangyong Jeon, and Björn Schenke. "Hydrodynamic modeling of heavy-ion collisions". In: *Int. J. Mod. Phys. A* 28 (2013), p. 1340011. DOI: 10.1142/S0217751X13400113. arXiv: 1301.5893 [nucl-th].

[37] Michal P. Heller and Michal Spalinski. "Hydrodynamics Beyond the Gradient Expansion: Resurgence and Resummation". In: *Phys. Rev. Lett.* 115.7 (2015), p. 072501. DOI: 10.1103/PhysRevLett.115.072501. arXiv: 1503.07514 [hep-th].

[38] Michal P. Heller, Romuald A. Janik, and Przemyslaw Witaszczyk. "The characteristics of thermalization of boost-invariant plasma from holography". In: *Phys. Rev. Lett.* 108 (2012), p. 201602. DOI: 10.1103/PhysRevLett.108.201602. arXiv: 1103.3452 [hep-th].

[39] Michal P. Heller, Romuald A. Janik, and Przemyslaw Witaszczyk. "Hydrodynamic Gradient Expansion in Gauge Theory Plasmas". In: *Phys. Rev. Lett.* 110.21 (2013), p. 211602. DOI: 10.1103/PhysRevLett.110.211602. arXiv: 1302.0697 [hep-th].

[40] Paul Romatschke. "Relativistic Fluid Dynamics Far From Local Equilibrium". In: *Phys. Rev. Lett.* 120.1 (2018), p. 012301. DOI: 10.1103/PhysRevLett.120.012301. arXiv: 1704.08699 [hep-th].

[41] Michał Spaliński. "On the hydrodynamic attractor of Yang–Mills plasma". In: *Phys. Lett. B* 776 (2018), pp. 468–472. DOI: 10.1016/j.physletb.2017.11.059. arXiv: 1708.01921 [hep-th].

[42] Michael Strickland, Jorge Noronha, and Gabriel Denicol. "Anisotropic nonequilibrium hydrodynamic attractor". In: *Phys. Rev. D* 97.3 (2018), p. 036020. DOI: 10.1103/PhysRevD.97.036020. arXiv: 1709.06644 [nucl-th].

[43] "Hydrodynamic attractors for Gubser flow". In: *Physics Letters B* 806 (2020), p. 135481. ISSN: 0370-2693. DOI: https://doi.org/10.1016/j.physletb.2020.135481. URL: https://www.sciencedirect.com/science/article/pii/S0370269320302859.

[44] Alexander Soloviev. "Hydrodynamic attractors in heavy ion collisions: a review". In: *Eur. Phys. J. C* 82.4 (2022), p. 319. DOI: 10.1140/epjc/s10052-022-10282-4. arXiv: 2109.15081 [hep-ph].

[45] Jean-Paul Blaizot and Li Yan. "Fluid dynamics of out of equilibrium boost invariant plasmas". In: *Phys. Lett. B* 780 (2018), pp. 283–286. DOI: 10.1016/j.physletb.2018.02.058. arXiv: 1712.03856 [nucl-th].

[46] Jean-Paul Blaizot and Li Yan. "Analytical attractor for Bjorken flows". In: *Phys. Lett. B* 820 (2021), p. 136478. DOI: 10.1016/j.physletb.2021.136478. arXiv: 2006.08815 [nucl-th].

[47] Sunil Jaiswal et al. "From moments of the distribution function to hydrodynamics: The nonconformal case". In: *Phys. Rev. C* 106.4 (2022), p. 044912. DOI: 10.1103/PhysRevC.106.044912. arXiv: 2208.02750 [nucl-th].

[48] Jean-Paul Blaizot and Li Yan. "Emergence of hydrodynamical behavior in expanding ultra-relativistic plasmas". In: *Annals Phys.* 412 (2020), p. 167993. DOI: 10.1016/j.aop.2019.167993. arXiv: 1904.08677 [nucl-th].

[49] Jean-Paul Blaizot and Li Yan. "Attractor and fixed points in Bjorken flows". In: *Phys. Rev. C* 104.5 (2021), p. 055201. DOI: 10.1103/PhysRevC.104.055201. arXiv: 2106.10508 [nucl-th].

[50] Carlo Cercignani. *The Boltzmann Equation and Its Applications*. Vol. 67. Applied Mathematical Sciences. New York: Springer, 1988.

[51] Paul Romatschke and Michael Strickland. "Collective modes of an anisotropic quark gluon plasma". In: *Phys. Rev. D* 68 (2003), p. 036004. DOI: 10.1103/PhysRevD.68.036004. arXiv: hep-ph/0304092.

[52] Mauricio Martinez and Michael Strickland. "Dissipative Dynamics of Highly Anisotropic Systems". In: *Nucl. Phys. A* 848 (2010), pp. 183–197. DOI: 10.1016/j.nuclphysa.2010.08.011. arXiv: 1007.0889 [nucl-th].

[53] Mauricio Martinez and Michael Strickland. "Non-boost-invariant anisotropic dynamics". In: *Nucl. Phys. A* 856 (2011), pp. 68–87. DOI: 10.1016/j.nuclphysa.2011.02.003. arXiv: 1011.3056 [nucl-th].

[54] Wojciech Florkowski and Radoslaw Ryblewski. "Highly-anisotropic and strongly-dissipative hydrodynamics for early stages of relativistic heavy-ion collisions". In: *Phys. Rev. C* 83 (2011), p. 034907. DOI: 10.1103/PhysRevC.83.034907. arXiv: 1007.0130 [nucl-th].

[55] Michael Strickland. "Anisotropic Hydrodynamics: Three lectures". In: *Acta Phys. Polon. B* 45.12 (2014). Ed. by Michal Praszalowicz, pp. 2355–2394. DOI: 10.5506/APhysPolB.45.2355. arXiv: 1410.5786 [nucl-th].

[56] W. A. Hiscock and L. Lindblom. "Generic instabilities in first-order dissipative relativistic fluid theories". In: *Phys. Rev. D* 31 (1985), pp. 725–733. DOI: 10.1103/PhysRevD.31.725.

[57] W. A. Hiscock and L. Lindblom. "Stability and causality in dissipative relativistic fluids". In: *Annals of Physics* 151 (1983), pp. 466–496. DOI: 10.1016/0003-4916(83)90288-9.

[58] Werner Israel. "Nonstationary irreversible thermodynamics: A causal relativistic theory". In: *Annals of Physics* 100.1–2 (Sept. 1976), pp. 310–331. DOI: 10.1016/0003-4916(76)90064-6.

[59] J. M. Stewart. "On transient relativistic thermodynamics and kinetic theory". In: *Proceedings of the Royal Society of London A* (). DOI: 10.1098/rspa.1977.0155.

[60] W. Israel and J. M. Stewart. "Transient relativistic thermodynamics and kinetic theory". In: *Annals Phys.* 118 (1979), pp. 341–372. DOI: 10.1016/0003-4916(79)90130-1.

[61] A. Muronga. "Causal theories of dissipative relativistic fluid dynamics for nuclear collisions". In: *Phys. Rev. C* 69 (2004), p. 034903. DOI: 10.1103/PhysRevC.69.034903. eprint: nucl-th/0309055.

[62] G. S. Denicol et al. "Derivation of transient relativistic fluid dynamics from the Boltzmann equation". In: *Phys. Rev. D* 85 (2012). [Erratum: Phys.Rev.D 91, 039902 (2015)], p. 114047. DOI: 10.1103/PhysRevD.85.114047. arXiv: 1202.4551 [nucl-th].

[63] P. Romatschke. "New developments in relativistic viscous hydrodynamics". In: *Int. J. Mod. Phys. E* 19 (2010), pp. 1–53. DOI: 10.1142/S0218301310014613. arXiv: 0902.3663 [hep-ph].

[64] Gabriel S. Denicol et al. "Consistency of the 14-moment approximation in relativistic kinetic theory". In: *Eur. Phys. J. A* 48 (2012), p. 170. DOI: 10.1140/epja/i2012-12170-x. arXiv: 1206.1554 [nucl-th].

[65] Amaresh Jaiswal. "Relaxation-time approximation and relativistic third-order viscous hydrodynamics from kinetic theory". In: *Nucl. Phys. A* 931 (2014), pp. 1–23. DOI: 10.1016/j.nuclphysa.2014.04.018. arXiv: 1407.0837 [nucl-th].

[66] Ankit Kumar Panda et al. "Relativistic non-resistive viscous magnetohydrodynamics from the kinetic theory: a relaxation time approach". In: *JHEP* 03 (2021), p. 216. DOI: 10.1007/JHEP03(2021)216. arXiv: 2011.01606 [nucl-th].

[67] Ankit Kumar Panda et al. "Relativistic resistive dissipative magnetohydrodynamics from the relaxation time approximation". In: *Phys. Rev. D* 104 (2021), p. 054004. DOI: 10.1103/PhysRevD.104.054004. arXiv: 2104.12179 [nucl-th].

[68] Dipika Dash et al. "Extended relaxation time approximation and relativistic dissipative hydrodynamics". In: *Phys. Lett. B* 823 (2022), p. 136757. DOI: 10.1016/j.physletb.2021.136757. arXiv: 2112.14581 [nucl-th].

[69] Carlo Cercignani and Gilberto M. Kremer. *The Relativistic Boltzmann Equation: Theory and Applications*. Birkhäuser, 2002. ISBN: 978-0-8176-4148-0. DOI: 10.1007/978-0-8176-8200-1. URL: https://doi.org/10.1007/978-0-8176-8200-1.

[70] Sydney Chapman and Thomas G. Cowling. *The Mathematical Theory of Non-uniform Gases: An Account of the Kinetic Theory of Viscosity, Thermal Conduction and Diffusion in Gases*. 3rd. Cambridge: Cambridge University Press, 1990. ISBN: 9780521408448.

[71] J.L. Anderson and H.R. Witting. "A relativistic relaxation-time model for the Boltzmann equation". In: *Physica* 74.3 (1974), pp. 466–488. ISSN: 0031-8914. DOI: https://doi.org/10.1016/0031-8914(74)90355-3. URL: https://www.sciencedirect.com/science/article/pii/0031891474903553.

[72] C. Cercignani. *Mathematical Methods in Kinetic Theory*. Springer US, 2013. ISBN: 9781489954091. URL: https://books.google.co.in/books?id=9zIBCAAAQBAJ.

[73] Gabriel S. Rocha, Gabriel S. Denicol, and Jorge Noronha. "Novel Relaxation Time Approximation to the Relativistic Boltzmann Equation". In: *Phys. Rev. Lett.* 127.4 (2021), p. 042301. DOI: 10.1103/PhysRevLett.127.042301. arXiv: 2103.07489 [nucl-th].

[74] Rajesh Biswas, Sukanya Mitra, and Victor Roy. "Is first-order relativistic hydrodynamics in a general frame stable and causal for arbitrary interactions?" In: *Phys. Rev. D* 106.1 (2022), p. L011501. DOI: 10.1103/PhysRevD.106.L011501. arXiv: 2202.08685 [nucl-th].

[75] Shi Pu, Tomoi Koide, and Dirk H. Rischke. "Does stability of relativistic dissipative fluid dynamics imply causality?" In: *Phys. Rev. D* 81 (2010), p. 114039. DOI: 10.1103/PhysRevD.81.114039. arXiv: 0907.3906 [hep-ph].

[76] Gabriel S. Denicol and Jorge Noronha. "Exact hydrodynamic attractor of an ultrarelativistic gas of hard spheres". In: *Phys. Rev. Lett.* 124.15 (2020), p. 152301. DOI: 10.1103/PhysRevLett.124.152301. arXiv: 1908.09957 [nucl-th].

[77] J. D. Bjorken. "Highly Relativistic Nucleus-Nucleus Collisions: The Central Rapidity Region". In: *Phys. Rev. D* 27 (1983), pp. 140–151. DOI: 10.1103/PhysRevD.27.140.

[78] G. Baym. " Thermal equilibration in ultrarelativistic heavy ion collisions ". In: *Phys. Lett. B* 138 (1984), pp. 18–22. DOI: 10.1016/0370-2693(84)91863-X.

[79] Sunil Jaiswal et al. "Nonconformal kinetic theory and hydrodynamics for Bjorken flow". In: *Phys. Rev. C* 105.2 (2022), p. 024911. DOI: 10.1103/PhysRevC.105.024911. arXiv: 2107.10248 [hep-ph].

[80] Wojciech Florkowski et al. "Anisotropic hydrodynamics – basic concepts". In: *Nucl. Phys. A* 904–905 (2013). Published Jan 31, 2013, pp. 803c–806c. DOI: 10.1016/j.nuclphysa.2013.02.138. eprint: arXiv:1210.1677.

[81] G. S. Denicol et al. "New Exact Solution of the Relativistic Boltzmann Equation and its Hydrodynamic Limit". In: *Phys. Rev. Lett.* 113 (2014), p. 202301. DOI: 10.1103/PhysRevLett.113.202301. arXiv: 1408.7048 [hep-ph].

[82] Wojciech Florkowski et al. “Leading-order anisotropic hydrodynamics for systems with massive particles”. In: *Phys. Rev. C* 89 (2014), p. 054909. DOI: 10.1103/PhysRevC.89.054909. arXiv: 1403.1223 [hep-ph].

[83] Wojciech Florkowski, Radoslaw Ryblewski, and Michael Strickland. “Testing viscous and anisotropic hydrodynamics in an exactly solvable case”. In: *Phys. Rev. C* 88 (2013), p. 024903. DOI: 10.1103/PhysRevC.88.024903. arXiv: 1305.7234 [hep-ph].

[84] P. Kovtun, D. T. Son, and A. O. Starinets. “Viscosity in Strongly Interacting Quantum Field Theories from Black Hole Physics”. In: *Phys. Rev. Lett.* 94 (2005), p. 111601. DOI: 10.1103/PhysRevLett.94.111601. arXiv: hep-th/0405231 [hep-th].

[85] P. Luzum and P. Romatschke. “Conformal relativistic viscous hydrodynamics: Applications to RHIC results at $\sqrt{s_{NN}} = 200$ GeV”. In: *Phys. Rev. C* 78.3 (2008), p. 034915. DOI: 10.1103/PhysRevC.78.034915. arXiv: arXiv:0804.4015 [nucl-th].

[86] Syo Kamata, Jakub Jankowski, and Mauricio Martinez. “Novel features of attractors and transseries in nonconformal Bjorken flows”. In: *Phys. Rev. D* 107.11 (2023), p. 116004. DOI: 10.1103/PhysRevD.107.116004. arXiv: 2206.00653 [physics.flu-dyn].

[87] Zenan Chen and Li Yan. “Hydrodynamic attractor in the nonconformal Bjorken flow”. In: *Phys. Rev. C* 105.2 (2022), p. 024910. DOI: 10.1103/PhysRevC.105.024910. arXiv: 2109.06658 [nucl-th].

[88] Ashutosh Dash and Victor Roy. “Hydrodynamic attractors for Gubser flow”. In: *Phys. Lett. B* 806 (2020), p. 135481. DOI: 10.1016/j.physletb.2020.135481. arXiv: 2001.10756 [nucl-th].

[89] Vladimir Skokov, Andrey Yu. Illarionov, and Vladimir Toneev. “Estimate of the magnetic field strength in heavy-ion collisions”. In: *Int. J. Mod. Phys. A* 24 (2009), pp. 5925–5932. DOI: 10.1142/S0217751X09047570. arXiv: 0907.1396 [nucl-th].

[90] Dmitri E. Kharzeev, Larry D. McLerran, and Harmen J. Warringa. “The Effects of topological charge change in heavy ion collisions: ’Event by event P and CP violation’”. In: *Nucl. Phys. A* 803 (2008), pp. 227–253. DOI: 10.1016/j.nuclphysa.2008.02.298. arXiv: 0711.0950 [hep-ph].

[91] Kirill Tuchin. “Electromagnetic fields in heavy-ion collisions”. In: *Adv. High Energy Phys.* 2013 (2013), p. 490495. DOI: 10.1155/2013/490495. arXiv: 1301.0099 [hep-ph].

[92] Sunil Jaiswal et al. “Far-from-equilibrium Attractor in Non-conformal Plasmas”. In: *Acta Phys. Polon. Supp.* 16.1 (2023), p. 119. DOI: 10.5506/APhysPolBSupp.16.1-A119. arXiv: 2208.00744 [nucl-th].

[93] Wojciech Florkowski, Ewa Maksymiuk, and Radoslaw Ryblewski. "Coupled kinetic equations for fermions and bosons in the relaxation-time approximation". In: *Phys. Rev. C* 97.2 (2018), p. 024915. DOI: 10.1103/PhysRevC.97.024915. arXiv: 1710.07095 [hep-ph].

[94] Paul Romatschke. "Relativistic Hydrodynamic Attractors with Broken Symmetries: Non-Conformal and Non-Homogeneous". In: *JHEP* 12 (2017), p. 079. DOI: 10.1007/JHEP12(2017)079. arXiv: 1710.03234 [hep-th].

[95] Toshali Mitra et al. "Hydrodynamization in hybrid Bjorken flow attractors". In: (Nov. 2022). arXiv: 2211.05480 [hep-ph].

[96] Ashutosh Dash and Victor Roy. "Far-from-Equilibrium Hydrodynamic Attractor for an Azimuthally Symmetric System". In: *Springer Proc. Phys.* 277 (2022), pp. 339–342. DOI: 10.1007/978-981-19-2354-8_61.

[97] Kevin Dusling, Guy D. Moore, and Derek Teaney. "Radiative energy loss and v(2) spectra for viscous hydrodynamics". In: *Phys. Rev. C* 81 (2010), p. 034907. DOI: 10.1103/PhysRevC.81.034907. arXiv: 0909.0754 [nucl-th].

[98] Sukanya Mitra. "Relativistic hydrodynamics with momentum dependent relaxation time". In: *Phys. Rev. C* 103.1 (2021), p. 014905. DOI: 10.1103/PhysRevC.103.014905. arXiv: 2009.06320 [nucl-th].

[99] Caio V. P. de Brito et al. "Divergence and resummation of the moment expansion for an ultrarelativistic gas in Bjorken flow". In: (Nov. 2024). arXiv: 2411.06267 [nucl-th].

[100] Harold Grad. "Asymptotic Theory of the Boltzmann Equation II". In: *Physics of Fluids* 6.2 (1963), pp. 147–181. DOI: 10.1063/1.1706766.

[101] Michal P. Heller, Romuald A. Janik, and Przemysław Witaszczyk. "Hydrodynamic Gradient Expansion in Gauge Theory Plasmas". In: *Phys. Rev. Lett.* 110 (21 May 2013), p. 211602. DOI: 10.1103/PhysRevLett.110.211602. URL: https://link.aps.org/doi/10.1103/PhysRevLett.110.211602.

[102] Alex Buchel, Michal P. Heller, and Jorge Noronha. "Entropy Production, Hydrodynamics, and Resurgence in the Primordial Quark-Gluon Plasma from Holography". In: *Phys. Rev. D* 94.10 (2016), p. 106011. DOI: 10.1103/PhysRevD.94.106011. arXiv: 1603.05344 [hep-th].

[103] Gabriel S. Denicol and Jorge Noronha. "Divergence of the Chapman-Enskog expansion in relativistic kinetic theory". In: (2016). arXiv: 1608.07869 [nucl-th].

[104] Reghukrishnan Gangadharan and Victor Roy. "Convergence problem of gradient expansion in the relaxation-time approximation". In: *Phys. Rev. D* 111.7 (2025), p. L071901. DOI: 10.1103/PhysRevD.111.L071901. arXiv: 2405.10846 [nucl-th].

[105] E. T. Whittaker and G. N. Watson. *A Course of Modern Analysis*. 4th ed. Cambridge Mathematical Library. Cambridge University Press, 1996.

[106] Harold Grad. "Principles of the Kinetic Theory of Gases". In: *Handbuch der Physik / Encyclopedia of Physics, Thermodynamik der Gase / Thermodynamics of Gases*. Ed. by Siegfried Flügge. Vol. 3/12. Springer, Berlin, Heidelberg, 1958, pp. 205–294. ISBN: 978-3-642-45892-7 (online), 978-3-642-45894-1 (print). DOI: 10.1007/978-3-642-45892-7_3.

[107] Caio V. P. de Brito, Gabriel S. Rocha, and Gabriel S. Denicol. "Hydrodynamic theories for a system of weakly self-interacting classical ultrarelativistic scalar particles: Causality and stability". In: *Phys. Rev. D* 110.3 (2024), p. 036011. DOI: 10.1103/PhysRevD.110.036011. arXiv: 2311.07272 [nucl-th].

[108] Reghukrishnan Gangadharan, Sukanya Mitra, and Victor Roy. "On the Approach Towards Equilibrium Through Momentum-Dependent Relaxation:Insights from Evolution of the Moments in Kinetic Theory". In: (June 2025). arXiv: 2504.00126 [nucl-th].

[109] Michal P. Heller et al. "Relativistic Hydrodynamics: A Singulant Perspective". In: *Phys. Rev. X* 12.4 (2022), p. 041010. DOI: 10.1103/PhysRevX.12.041010. arXiv: 2112.12794 [hep-th].

[110] G. S. Denicol, T. Koide, and D. H. Rischke. "Dissipative relativistic fluid dynamics: a new way to derive the equations of motion from kinetic theory". In: *Phys. Rev. Lett.* 105 (2010), p. 162501. DOI: 10.1103/PhysRevLett.105.162501. arXiv: 1004.5013 [nucl-th].

[111] Amaresh Jaiswal. "Relativistic third-order dissipative fluid dynamics from kinetic theory". In: *Phys. Rev. C* 88 (2013), p. 021903. DOI: 10.1103/PhysRevC.88.021903. arXiv: 1305.3480 [nucl-th].

[112] Ankit Kumar Panda et al. "Relativistic resistive dissipative magnetohydrodynamics from the relaxation time approximation". In: *Phys. Rev. D* 104.5 (2021), p. 054004. DOI: 10.1103/PhysRevD.104.054004. arXiv: 2104.12179 [nucl-th].

[113] Victor E. Ambruş, Etele Molnár, and Dirk H. Rischke. "Relativistic second-order dissipative and anisotropic fluid dynamics in the relaxation-time approximation for an ideal gas of massive particles". In: *Phys. Rev. D* 109.7 (2024), p. 076001. DOI: 10.1103/PhysRevD.109.076001. arXiv: 2311.00351 [nucl-th].

[114] Gabriel S. Rocha and Gabriel S. Denicol. "Transient fluid dynamics with general matching conditions: A first study from the method of moments". In: *Phys. Rev. D* 104.9 (2021), p. 096016. DOI: 10.1103/PhysRevD.104.096016. arXiv: 2108.02187 [nucl-th].

[115] Caio V. P. de Brito and Gabriel S. Denicol. "Third-order relativistic dissipative fluid dynamics from the method of moments". In: *Phys. Rev. D* 108.9 (2023), p. 096020. DOI: 10.1103/PhysRevD.108.096020. arXiv: 2302.09097 [nucl-th].

[116] Masuo Suzuki. “Decomposition formulas of exponential operators and Lie exponentials with some applications to quantum mechanics and statistical physics”. In: *J. Math. Phys.* 26.4 (1985), p. 601. DOI: 10.1063/1.526596.

Appendix A

A.1 RTA Boltzmann Equation with Force

Boltzmann equation would then read

$$\mathcal{F}\tau\frac{\partial f}{\partial w}+\frac{\partial f}{\partial \tau}+\frac{\delta u_z p^z}{u_\tau p^\tau}\frac{\partial f}{\partial z} \tag{A.1}$$

$$=-\frac{p^\tau}{u_\tau p^\tau}\frac{(f-f_{\text{eq}})}{\tau_R}-\frac{\delta u\cdot p}{u_\tau p^\tau}\frac{(f-f_{\text{eq}})}{\tau_R}\,. \tag{A.2}$$

If we now assume that $\delta u/u_\tau << 1$, we can ignore the δu terms from the above equation and get

$$\left(\mathcal{F}(\tau)\tau\frac{\partial}{\partial w}+\frac{\partial}{\partial \tau}\right)f=-\frac{(f-f_{\text{eq}})}{\tau_R}\,. \tag{A.3}$$

For the consistency of the above approximation, we need to keep the strength of the force sufficiently small so that the background flow is still close to Bjorken.

A.1.1 Change of Variables

For computational convenience we write the force $\mathcal{F}$ as

$$\mathcal{F}=\frac{\alpha}{\tau_F}F(\tau)\,. \tag{A.4}$$

We then rewrite the Boltzmann equation as

$$\left(\frac{\alpha}{\tau_F}F(\tau)\tau\frac{\partial}{\partial w}+\frac{\partial}{\partial \tau}\right)f=-\frac{(f-f_{\text{eq}})}{\tau_R}\,. \tag{A.5}$$

To convert Eq.(A.3) to a simpler form, we divide both sides by $F(\tau)\tau/\tau_F$ getting

$$\left(\alpha\frac{\partial}{\partial w}+\frac{\tau_F}{F(\tau)\tau}\frac{\partial}{\partial \tau}\right)f=-\frac{\tau_F}{\tau_R}\frac{(f-f_{\text{eq}})}{F(\tau)\tau}\,. \tag{A.6}$$

We define the variable s

$$s(\tau) = \int_0^\tau F(\tau') \frac{\tau'}{\tau_F} d\tau', \tag{A.7}$$

and rewrite the proper time derivative to get Eq.(**??**),

$$\left(\alpha \frac{\partial}{\partial w} + \frac{\partial}{\partial s}\right) f = -\frac{\tau_F}{\tau_R} \frac{(f - f_{\text{eq}})}{F(\tau)\tau}. \tag{A.8}$$

We now use the standard technique of characteristics for solving partial differential equations and define new variables $(w, s) \to (r, s)$

$$r = w - \alpha s, \tag{A.9}$$

$$s = s, \tag{A.10}$$

and obtain the equation

$$\frac{\partial f(r, s, p_T)}{\partial s} = -\frac{\tau_F}{\tau_R} \frac{(f - f_{\text{eq}})}{F(\tau(s))\tau(s)}. \tag{A.11}$$

Damping term dependence on force

The damping function in the s coordinate is given by

$$D(s_1, s_2) = \exp\left[-\int_{s_1}^{s_2} \frac{ds'}{F(\tau(s'))\,(\tau(s')/\tau_F)\,\tau_R(s')}\right].$$

However using,

$$ds(\tau) = F(\tau) \frac{\tau}{\tau_F} d\tau, \tag{A.12}$$

$$\begin{aligned} D(\tau_1, \tau_2) &= \exp\left[-\int_{\tau_1}^{\tau_2} F(\tau) \frac{\tau(s')}{\tau_F} \frac{d\tau}{F(\tau(s'))\,\frac{\tau(s')}{\tau_F}\,\tau_R(s')}\right]. \\ &= \exp\left[-\int_{\tau_1}^{\tau_2} d\tau \frac{d\tau}{\tau_R(\tau')}\right] \end{aligned}$$

A.2 Integrals

In this section we give the explicit form of the H functions appearing in the equation for $\mathcal{E}$, P etc given in Eq.(**??**) We define the integrals,

$$\tilde{H}^F_\epsilon\,[s',s,m,\alpha] = \frac{1}{4\pi^2}\int du\,u^3\,e^{-\sqrt{u^2+z^2}}\,H^F_\epsilon(u,z,s,s',\alpha), \tag{A.13}$$

$$\tilde{H}^F_L\,[s',s,m,\alpha] = \frac{1}{4\pi^2}\int du\,u^3\,e^{-\sqrt{u^2+z^2}}\,H^F_L(u,z,s,s',\alpha), \tag{A.14}$$

$$\tilde{H}^F_T\,[s',s,m,\alpha] = \frac{1}{4\pi^2}\int du\,u^3\,e^{-\sqrt{u^2+z^2}}\,H^F_T(u,z,s,s',\alpha), \tag{A.15}$$

$$\tilde{H}^F_{03}\,[s',s,m,\alpha] = \frac{1}{4\pi^2}\int du\,u^2\,e^{-\sqrt{u^2+z^2}} \tag{A.16}$$

where $u = p/T$ and $z = m/T$.

The functions inside the integrals can be obtained using analytical techniques. Define

$$h(s) \equiv \tau(s)\,. \tag{A.17}$$

For notational simplicity, we define the following variables

$$\frac{h(s')}{h(s)} \equiv \overline{\hbar}(s,s') \equiv \overline{\hbar}\,, \tag{A.18}$$

$$\frac{\alpha\times(s-s')}{h(s')} \equiv g(s,s') \equiv g, \tag{A.19}$$

and

$$N^2 \equiv \frac{1}{(1-\overline{\hbar}^2)}\left(\frac{u^2+\overline{\hbar}^2g^2+z^2}{u^2} + \frac{g^2\overline{\hbar}^4}{u^2(1-\overline{\hbar}^2)}\right), \tag{A.20}$$

$$G \equiv \frac{g\overline{\hbar}^2}{u(1-\overline{\hbar}^2)}\,. \tag{A.21}$$

Using the above definitions we can write

$$\begin{aligned} H^F(u,z,s,s',\alpha) = -\overline{\hbar}\sqrt{(1-\overline{\hbar}^2)}N^2\Bigg\{&\frac{1}{2}\left[\sin^{-1}\frac{G-1}{N} - \sin^{-1}\frac{(G+1)}{N}\right] \\ &+\frac{1}{2}\left[-\frac{1+G}{N}\sqrt{1-\left(\frac{1+G}{N}\right)^2} + \frac{G-1}{N}\sqrt{1-\left(\frac{G-1}{N}\right)^2}\right]\Bigg\}, \end{aligned} \tag{A.22}$$

$$H_L(u,z,s,s',\alpha) = -\frac{\bar{\hbar}^3}{\sqrt{1-\bar{\hbar}^2}}\left\{\left(\frac{N^2}{2}+(g+G)^2\right)\left[\sin^{-1}\frac{G-1}{N}-\sin^{-1}\frac{1+G}{N}\right]\right.$$
$$+\frac{N^2}{2}\left[\frac{1+G}{N}\sqrt{1-\left(\frac{1+G}{N}\right)^2}-\frac{G-1}{N}\sqrt{1-\left(\frac{G-1}{N}\right)^2}\right]$$
$$\left.-2N(g+G)\left[\sqrt{1-\left(\frac{1+G}{N}\right)^2}-\sqrt{1-\left(\frac{1-G}{N}\right)^2}\right]\right\}, \quad \text{(A.23)}$$

$$H_T(u,z,s,s',\alpha) = -\frac{\bar{\hbar}}{\sqrt{(1-\bar{\hbar}^2)}}\left\{\left(1-G^2-\frac{N^2}{2}\right)\left[\sin^{-1}\frac{G-1}{N}-\sin^{-1}\frac{1+G}{N}\right]\right.$$
$$-\frac{N^2}{2}\left[\frac{1+G}{N}\sqrt{1-\left(\frac{1+G}{N}\right)^2}-\frac{G-1}{N}\sqrt{1-\left(\frac{G-1}{N}\right)^2}\right]$$
$$\left.+2NG\left[\sqrt{1-\left(\frac{1+G}{N}\right)^2}-\sqrt{1-\left(\frac{1-G}{N}\right)^2}\right]\right\}. \quad \text{(A.24)}$$

$$H_{03}^F(u,z,s,s',\alpha) = g\bar{h} \quad \text{(A.25)}$$

A.3 Iterative Solution Algorithm

Consider the integral equation

$$y(t) = K(t,t_0,y)v(t,t_0) \quad \text{(A.26)}$$
$$+\int_{t_0}^{t} dt' K(t,t',y)\frac{H(t,t',y(t'))}{\tau_R(y(t'))}f(y(t')) \quad \text{(A.27)}$$

where,

$$K(t,t',y) = \exp\left\{\int_{t'}^{t} g(y(t''))dt''\right\} \quad \text{(A.28)}$$

and we are given the initial condition

$$y(t_0) = y_0. \quad \text{(A.29)}$$

This implies

$$y(t_0) = v(t_0, t_0) \tag{A.30}$$

as

$$K(t, t, y) = 1 \tag{A.31}$$

The usual method for solving this equation is to consider an arbitrary functional form for the solution $y(t)$ and substitute it in the RHS and get a new solution. This process is continued until the iteration converges to some desired level of accuracy. The drawback of this method is that the speed of convergence depends on the initial guess $y(t)$. Here we take an alternate approach. If the function $y(t)$ is continuous then we approximate at each step $t_n = t_{n-1} + \Delta t_n$,

$$y(t_{n-1} + \Delta t_n) = y(t_{n-1}) + \mathcal{O}(\Delta t_n)\,. \tag{A.32}$$

Therefore with the initial condition $y(t_0) = v(t_0, t_0)$, we start with

$$y(t_0 + \Delta t) \sim y(t_0) \tag{A.33}$$

and continue this procedure in order for each n successively. We show elsewhere that after one iteration this produces an approximation for $y(t)$ accurate up to $\mathcal{O}(\Delta t^2)$. This process gets rid of the need for a good initial guess. It not only converges faster but also allows us to estimate order or error for our computation.

Appendix B

B.1 Collision Kernal

The RTA collision kernel introduced in [73] is

$$\hat{L}_{RTA}\phi(p) = -\frac{p}{\tau_R} f^{\text{eq}} \left(\phi - \frac{\langle p/\tau_R \phi \rangle_{\text{eq}}}{\langle p/\tau_R \rangle_{\text{eq}}} - P_1 \frac{\langle p/\tau_R \phi P_1^0 \rangle_{\text{eq}}}{\langle p/\tau_R P_1^0 P_1^0 \rangle_{\text{eq}}} - 3p^{\langle \mu \rangle} \frac{\langle p/\tau_R p_{\langle \mu \rangle} \phi \rangle_{\text{eq}}}{\langle p/\tau_R p_{\langle \nu \rangle} p^{\langle \nu \rangle} \rangle_{\text{eq}}} \right) , \tag{B.1}$$

where we have used the massless condition $p^0 = |\vec{p}| \equiv p$. Here

$$P_1 = 1 - \frac{\langle p/\tau_R \rangle_{\text{eq}}}{\langle p^2/\tau_R \rangle_{\text{eq}}} p \, , \tag{B.2}$$

$$\phi = \frac{f - f^{\text{eq}}}{f^{\text{eq}}} \, , \tag{B.3}$$

and the angular bracket is defined as

$$\langle ... \rangle = \int dP(...) f \, . \tag{B.4}$$

$$\langle ... \rangle_{\text{eq}} = \int dP(...) \, . \tag{B.5}$$

For notational convenience, we rewrite the Eq.(B.1) as

$$\hat{L}_{RTA}\phi(k) = -\frac{p}{\tau_R} f^{\text{eq}} \left(\phi - A - BP_1 - C_{\langle \mu \rangle} k^{\langle \mu \rangle} \right) \, , \tag{B.6}$$

$$= -L_1 - L_2 - L_3 - L_4 \, , \tag{B.7}$$

where L_i denote the 4 terms in the collision kernel. We use a momentum-dependent relaxation time of the form,

$$\frac{1}{\tau_R} = \frac{1}{\tau_R^0 p^\Lambda} \, , \tag{B.8}$$

where τ_R^0 is independent of momentum. The moments of the distribution function is defined as,

$$\rho_{n,l} = \int dP p^n P_{2l}(\cos\theta) f(\tau, p_T, p_\eta) \ . \tag{B.9}$$

We would like to compute here the quantity,

$$C_{n,l} = \int dP p^n P_{2l}(\cos\theta) \hat{L}_{RTA}\phi(k) \ . \tag{B.10}$$

The first term L_1

$$\begin{aligned}
\langle L_1 \rangle &= \int \frac{d^3p}{(2\pi)^3 p} p^n P_{2l}(\cos\theta) \left[\frac{p}{\tau_R^0} f^{\rm eq} \phi \right] \ , \\
&= \frac{1}{\tau_R^0} \int \frac{d^3p}{(2\pi)^3} p^{n-\Lambda} P_{2l}(\cos\theta) \left(f - f^{\rm eq} \right) \ , \\
&= \frac{1}{\tau_R^0} \left(\rho_{n-\Lambda\, l} - \rho^{\rm eq}_{n-\Lambda\, l} \right) \ .
\end{aligned} \tag{B.11}$$

The second term L_2

$$L_2 = A \frac{p^{1-\Lambda}}{\tau_R} f^{\rm eq} \ ,$$

$$\langle L_2 \rangle = \int \frac{d^3p}{(2\pi)^3} p^n P_{2l}(\cos\theta) \left[\frac{p^{-\Lambda}}{\tau_R} f^{\rm eq} \right] \ , \tag{B.12}$$

$$= \frac{1}{\tau_R^0} \rho^{\rm eq}_{n-\Lambda\, l} \delta_{l,0} \ . \tag{B.13}$$

The coefficient A

$$A = \frac{\langle p/\tau_R \phi \rangle_0}{\langle p/\tau_R \rangle_0} \ , \tag{B.14}$$

$$= \frac{\rho_{1-\Lambda,0} - \rho^{\rm eq}_{1-\Lambda,0}}{\rho^{\rm eq}_{1-\Lambda,0}} \ . \tag{B.15}$$

The third term L_3

$$\begin{aligned}\frac{L_3}{p} &= -BP_1^0\,,\\ &= -B\left(1-\frac{\langle p/\tau_R\rangle_{\text{eq}}}{\langle p^2/\tau_R\rangle_{\text{eq}}}p\right)\,.\end{aligned} \tag{B.16}$$

Using ,

$$\begin{aligned}P_1^0 &= 1-\frac{\langle p/\tau_R\rangle_0}{\langle p^2/\tau_R\rangle_{\text{eq}}}p\,,\\ &= \left[1-\frac{\rho^{\text{eq}}_{1-\Lambda,0}}{\rho^{\text{eq}}_{2-\Lambda,0}}p\right]\,.\end{aligned} \tag{B.17}$$

We get,

$$\begin{aligned}\int dPp^n P_{2l}(\cos\theta)\left[\frac{p^{-\Lambda}}{\tau_R^0}P_1^0\right] &= \frac{1}{\tau_R^0}\int dPp^{n-\Lambda}P_{2l}(\cos\theta)\left[1-\frac{\rho^{\text{eq}}_{1-\Lambda,0}}{\rho^{\text{eq}}_{2-\Lambda,0}}p\right]\,,\\ &= \frac{1}{\tau_R^0}\left(\rho^{\text{eq}}_{n+1-\Lambda,l}-\frac{\rho^{\text{eq}}_{1-\Lambda,0}}{\rho^{\text{eq}}_{2-\Lambda,0}}\rho^{\text{eq}}_{n+2-\Lambda,l}\right)\delta_{l,0}\,.\end{aligned} \tag{B.18}$$

The delta function is due to all equilibrium integrals for $l>0$ being zero. The numerator of **the coefficient** B is

$$\begin{aligned}\text{Nm}(B) &= \langle\frac{p}{\tau_R}\phi P_1^0\rangle_{\text{eq}}\,,\\ &= \left(\left(\rho_{1-\Lambda,0}-\rho^{\text{eq}}_{1-\Lambda,0}\right)-\frac{\rho^{\text{eq}}_{1-\Lambda,0}}{\rho^{\text{eq}}_{2-\Lambda,0}}\left(\rho_{2-\Lambda,0}-\rho^{\text{eq}}_{2-\Lambda,0}\right)\right)/\tau_R^0\,,\\ &= \left(\rho_{1-\Lambda,0}-\frac{\rho^{\text{eq}}_{1-\Lambda,0}}{\rho^{\text{eq}}_{2-\Lambda,0}}\rho_{2-\Lambda,0}\right)/\tau_R^0\,.\end{aligned} \tag{B.19}$$

We have,

$$\left(P_1^0\right)^2 = \left(1-2\frac{\rho^{\text{eq}}_{1-\Lambda,0}}{\rho^{\text{eq}}_{2-\Lambda,0}}p+\left(\frac{\rho^{\text{eq}}_{1-\Lambda,0}}{\rho^{\text{eq}}_{2-\Lambda,0}}\right)^2p^2\right)\,. \tag{B.20}$$

The denominator of **the coefficient** B is,

$$\mathrm{Dm}(B) = \langle p/\tau_R P_1^0 P_1^0 \rangle_{\mathrm{eq}} \,, \tag{B.21}$$

$$= \left(\rho^{\mathrm{eq}}_{1-\Lambda,0} - 2\frac{\rho^{\mathrm{eq}}_{1-\Lambda,0}}{\rho^{\mathrm{eq}}_{2-\Lambda,0}} \rho^{\mathrm{eq}}_{2-\Lambda,0} + \left(\frac{\rho^{\mathrm{eq}}_{1-\Lambda,0}}{\rho^{\mathrm{eq}}_{2-\Lambda,0}} \right)^2 \rho^{\mathrm{eq}}_{3-\Lambda,0} \right) / \tau_R^0 \,, \tag{B.22}$$

$$= \left(-\rho^{\mathrm{eq}}_{1-\Lambda,0} + \left(\frac{\rho^{\mathrm{eq}}_{1-\Lambda,0}}{\rho^{\mathrm{eq}}_{2-\Lambda,0}} \right)^2 \rho^{\mathrm{eq}}_{3-\Lambda,0} \right) / \tau_R^0 \,. \tag{B.23}$$

The fourth term

$$\begin{aligned} L_4 &= \int dP p^{n+1-\Lambda} P_{2l}(\cos\theta) p^{\langle\mu\rangle} \,, \\ &= \int dP p^{n+1-\Lambda} P_{2l}(\cos\theta) p^{\langle\mu\rangle} \,, \\ &= \frac{(2l-1)!!}{l!} z_{\langle\mu_1\ldots\mu_l\rangle} \int dP p^{n+1-\Lambda} p^{\langle\mu_1\ldots\mu_l\rangle} p^{\langle\mu\rangle} \,. \end{aligned} \tag{B.24}$$

here we use the identity in [**deBrito:2024vhm**] (Eq.[33]). To compute this, we use the identities [**deBrito:2024vhm**] (Eq.[21b])

$$p^{\langle\mu_1\ldots\mu_l\rangle} p^{\langle\mu_{l+1}\rangle} = p^{\langle\mu_1\ldots\mu_{l+1}\rangle} + \frac{l}{2l+1} \left(\Delta_{\lambda\beta} p^\lambda p^\beta \right) \Delta^{\mu_1\ldots\mu_l}_{\alpha_1\ldots\alpha_l} \Delta^{\alpha_l\mu_{l+1}} p^{\langle\alpha_1\ldots\alpha_{l-1}\rangle}, \tag{B.25}$$

[**deBrito:2024vhm**] (Eq.[17])

$$\int dP p^r p^{\langle\mu_1\ldots\mu_l\rangle} f^{\mathrm{eq}} = 0 \qquad\qquad l > 0 \,, \tag{B.26}$$

and,

$$\left(\Delta_{\lambda\beta} p^\lambda p^\beta \right) = \left((p^0)^2 - m^2 \right) = -p^2 \,. \tag{B.27}$$

Setting $l \to 2l$ for the conformal Bjorken case, we see that the third term contains only odd moments. They are therefore identically zero as f is even in θ.

Simplified collision kernel

Finally, putting all the terms together we get the full collision kernel,

$$C_{n,l,\Lambda} = -\frac{1}{\tau_R^0}\Bigg[\left\{\rho_{n-\Lambda,l} - \delta_{l0}\,\rho^{\text{eq}}_{n-\Lambda,l}\right\} - A\,\delta_{l0}\,\rho^{\text{eq}}_{n-\Lambda,0} - B\,\delta_{l0}\left\{\rho^{\text{eq}}_{n-\Lambda,0} - \frac{\rho^{\text{eq}}_{1-\Lambda,0}}{\rho^{\text{eq}}_{2-\Lambda,0}}\rho^{\text{eq}}_{n-\Lambda+1,0}\right\}\Bigg], \tag{B.28}$$

where

$$A = \frac{\rho_{1-\Lambda,0} - \rho^{\text{eq}}_{1-\Lambda,0}}{\rho^{\text{eq}}_{1-\Lambda,0}}, \tag{B.29}$$

$$B = \frac{\rho_{1-\Lambda,0} - \frac{\rho^{\text{eq}}_{1-\Lambda,0}}{\rho^{\text{eq}}_{2-\Lambda,0}}\rho_{2-\Lambda,0}}{\rho^{\text{eq}}_{3-\Lambda,0}\left(\frac{\rho^{\text{eq}}_{1-\Lambda,0}}{\rho^{\text{eq}}_{2-\Lambda,0}}\right)^2 - \rho^{\text{eq}}_{1-\Lambda,0}}. \tag{B.30}$$

Further simplification can be achieved if we use the equilibrium moment expression,

$$\rho^{\text{eq}}_{n,l}(T,\mu) = e^{\mu/T}\frac{T^{n+2}}{2\pi^2}\Gamma(n+2)\delta_{l0}, \tag{B.31}$$

$$C_{n-1,0} = -\frac{1}{\tau_R}\rho_{n-\Lambda,0}\left[1 - T^{n-1}\frac{\Gamma(n-\Lambda+2)}{\Gamma(1-\Lambda+2)}\frac{\rho_{1-\Lambda,0}}{\rho_{n-\Lambda,0}}\right] + \frac{T^{n-2}}{\tau_R}\rho_{2-\Lambda,0}\left(\frac{\Gamma(n-\Lambda+2)}{\Gamma(2-\Lambda+2)}\right)\left[1 - T\frac{\Gamma(2-\Lambda+2)}{\Gamma(1-\Lambda+2)}\frac{\rho_{1-\Lambda,0}}{\rho_{2-\Lambda,0}}\right]\frac{\left[1 - \frac{\Gamma(1-\Lambda+2)}{\Gamma(2-\Lambda+2)}\frac{\Gamma(n+1-\Lambda+2)}{\Gamma(n-\Lambda+2)}\right]}{\left[1 - \left[\frac{\Gamma(1-\Lambda+2)}{\Gamma(2-\Lambda+2)}\right]^2\frac{\Gamma(3-\Lambda+2)}{\Gamma(1-\Lambda+2)}\right]}. \tag{B.32}$$

By defining the two functions,

$$K(n,m,\Lambda) = \frac{\Gamma(n-\Lambda+2)}{\Gamma(m-\Lambda+2)}, \tag{B.33}$$

$$C(n,\Lambda) = \frac{1 - K(1,n,\Lambda)K(n+1,2,\Lambda)}{1 - K(1,2,\Lambda)K(3,2,\Lambda)}, \tag{B.34}$$

we get the simplified expression,

$$\begin{aligned} C_{n,l,\Lambda} = &- \frac{1}{\tau_R}\Big[\rho_{n-\Lambda,l} \\ &- \delta_{l0}\Big\{T^{n-1}K(n,1,\Lambda)[1-C(n,\Lambda)]\rho_{1-\Lambda,l} \\ &+ T^{n-2}K(n,2,\Lambda)C(n,\Lambda)\rho_{2-\Lambda,l}\Big\}\Big] \,. \end{aligned} \tag{B.35}$$

Note that

$$K(n,n,\Lambda) = \frac{\Gamma(n-\Lambda+2)}{\Gamma(n-\Lambda+2)} = 1\,, \tag{B.36}$$

$$C(1,\Lambda) = \frac{1-K(1,1,\Lambda)K(2,2,\Lambda)}{1-K(1,2,\Lambda)K(3,2,\Lambda)} = 0 \tag{B.37}$$

$$C(2,\Lambda) = \frac{1-K(1,2,\Lambda)K(3,2,\Lambda)}{1-K(1,2,\Lambda)K(3,2,\Lambda)} = 1\,, \tag{B.38}$$

and enforce the conservation laws for energy density $\epsilon = \rho_{2,0}$ and number density $n = \rho_{1,0}$,

$$C_{1,0,\Lambda} = 0\,,$$

$$C_{2,0,\Lambda} = 0\,,$$

independent of the value of Λ.

B.1.1 Moment Closure

We observed that the numerical solution to a naive truncation of the moment equations does give a positive definite collision kernel. We remedy this by using the Grad closure procedure, making use of the momentum expansion of the distribution function. We assume that the distribution function can be expanded in momentum as

$$f(\tau,p,\cos(\theta)) = f^{\text{eq}}\sum_{m=0}^{N}\sum_{k=0}^{L}A_{m,k}(\tau)p^m P_{2k}(\cos\theta). \tag{B.39}$$

The moments $\rho_{n,l}$, then can be expressed as

$$\begin{aligned}\rho_{n+\Lambda,l} &= \sum_{m=0}^{N}\sum_{k=0}^{L} A_{m,k}\frac{1}{(2\pi)^3}\int d\theta \sin\theta d\phi dp\; p^{n+m+1+\Lambda}P_{2l}(\cos\theta)P_{2k}(\cos\theta)f^{\text{eq}}\,,\\ &= \sum_{m=0}^{N}\sum_{k=0}^{L} A_{m,k}\delta_{kl}\frac{e^{\alpha}}{2\pi^2}\frac{T^{n+m+2+\Lambda}}{4k+1}\Gamma(m+n+2+\Lambda)\,,\\ &= \sum_{m=0}^{N} A_{m,l}\frac{e^{\alpha}}{2\pi^2}\frac{T^{n+m+2+\Lambda}}{4l+1}\Gamma(m+n+2+\Lambda)\,. \end{aligned} \tag{B.40}$$

To simplify the expressions, we scale the coefficients by,

$$A_{m,l}\frac{e^{\alpha}}{2\pi^2}\frac{1}{4l+1} \to A_{m,l}\,. \tag{B.41}$$

This reduces the above equation to the form,

$$\rho_{n+\Lambda,l} = \sum_{m=0}^{N} A_{m,l}T^{n+m+2+\Lambda}\Gamma(m+n+2+\Lambda)\,. \tag{B.42}$$

Note that $\rho_{n,l}$ is related to $A_{n,l}$ of the same l. So at each l we get a set of N linear equations relating the moments to the coefficients $A_{m,k}$. To make this explicit, we write the above equation in a matrix form, using the following definitions,

We define a Hankel matrix **H**, vectors $\vec{A}_l$ and $\vec{\rho}_l$ as

$$[\mathbf{H}(T,\Lambda)]_{n,m} = T^{n+m+2+\Lambda}\Gamma(n+m+2+\Lambda), \tag{B.43}$$

$$[\vec{A}_l]_n = A_{n,l}, \tag{B.44}$$

$$[\vec{\rho}_l]_n = \rho_{n,l}. \tag{B.45}$$

Then,

$$[\vec{\rho}_l]_{n+\Lambda} = \sum_m [\mathbf{H}(T,\Lambda)]_{n,m}[\vec{A}_l]_m, \tag{B.46}$$

or

$$\vec{\rho}_l(\Lambda) = \mathbf{H}(T,\Lambda)\vec{A}_l. \tag{B.47}$$

We can first compute the coefficients from the integer moments $\rho_{n,l}(\Lambda = 0)$ by inverting Eq.(B.47) to get

$$\vec{A}_l = \mathbf{H}^{-1}(T, 0)\vec{\rho}_l \,. \tag{B.48}$$

Then from Eq.(B.42) we get,

$$\vec{\rho}_l(-\Lambda) = \mathbf{H}(T, -\Lambda)\mathbf{H}^{-1}(T, 0)\vec{\rho}_l(0). \tag{B.49}$$

B.1.2 Positivity of the collision kernel

The matrix $\mathbf{H}(T, \Lambda)$ has the decomposition

$$\mathrm{H}(T, \Lambda) = T^{2+\Lambda}\, \mathrm{D}(T)\mathrm{H}(1, \Lambda)\mathrm{D}(T), \tag{B.50}$$

where $\mathrm{D}(T) = diag(1, T, T^2, \ldots, T^N)$. So to analyze the features of the matrix M,

$$\mathbf{M}(T, \Lambda) = \mathbf{H}(T, -\Lambda)\mathbf{H}^{-1}(T, 0), \tag{B.51}$$

$$= T^{\Lambda} D(T)\mathbf{H}(1, -\Lambda)\mathbf{H}^{-1}(1, 0)D^{-1}(T). \tag{B.52}$$

We only need to be concerned with the matrix $\mathbf{M}(1, \Lambda) = \mathbf{H}(1, -\Lambda)\mathbf{H}^{-1}(1, 0)$ which is independent of T. Note that the diagonal matrices $D(T)$ simply effects a similarity transformation on $\mathbf{M}(1, \Lambda)$ and therefore do not affect the eigenvalues. As this is a fixed matrix independent of the dynamics, one can verify the positive definiteness by numerically computing its eigenvalues.

For $N = 5$, eigenvalues$(\mathbf{M}(1, 0.5)) \in \{0.234,\ 0.292,\ 0.370,\ 0.489,\ 0.703,\ 1.224,\ 4.575\}$. In Fig. (B.1) we plot the minimum eigenvalue of $M(1, \Lambda)$ for $N = 5$ for varying values of Λ. We see that the eigenvalue is positive but exponentially decays to zero as Λ increases.

To show this analytically, first we prove that $\mathbf{H}(1, \Lambda)$ is positive definite. Consider the

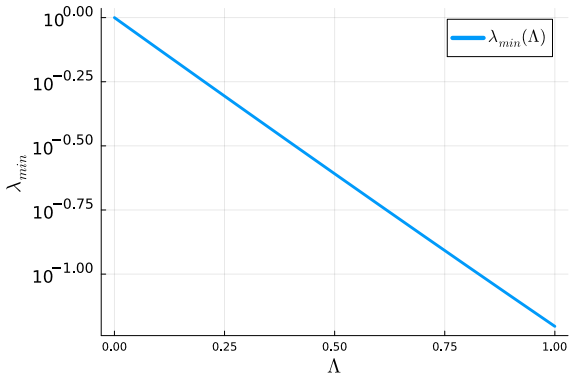

Figure B.1: log plot of the minimum eigenvalue of $M(1,\Lambda)$ for $N = 5$ as a function of Λ

quadratic form $x^T\mathbf{H}(1,\Lambda)x$,

$$\begin{aligned} x^T\mathbf{H}(1,\Lambda)x &= \sum_{n=0}^{N}\sum_{m=0}^{N} x_m x_n \Gamma(n+m+2+\Lambda) \\ &= \sum_{n=0}^{N}\sum_{m=0}^{N} x_m x_n \int_0^\infty dt\; t^{n+m+1+\Lambda} e^{-t} \\ &= \sum_{n=-1}^{N}\sum_{m=-1}^{N} x_m x_n \int_0^\infty dt\; t^{\Lambda} e^{-t} \sum_{n=0,m=0}^{N} x_m x_n t^{n+m+2} \\ &= \int_0^\infty dt\; t^{\Lambda} e^{-t} \left(\sum_{n=-1}^{N} x_n t^{n+1}\right)^2 > 0\,, \end{aligned} \tag{B.53}$$

where we have used the definition of the gamma function. $\mathbf{H}(1,\Lambda)$ is then symmetric and positive definite, which implies that its eigenvalues are positive for all values of Λ. Now the product $\mathbf{M}(1,\Lambda) = \mathbf{H}(1,\Lambda)\mathbf{H}(1,0)$ can be shown to be positive definite by showing that it is similar to a positive definite matrix. For this, multiply both sides of $\mathbf{M}(1,\Lambda)$ by $\sqrt{\mathbf{H}^{-1}(1,0)}$, the principal square root of $\mathbf{H}^{-1}(1,0)$, gives

$$\sqrt{\mathbf{H}^{-1}(1,0)}\mathbf{M}(1,\Lambda)\sqrt{\mathbf{H}^{-1}(1,0)} = \sqrt{\mathbf{H}^{-1}(1,0)}\mathbf{H}(1,\Lambda)\sqrt{\mathbf{H}^{-1}(1,0)}\,. \tag{B.54}$$

Clearly, the new matrix is symmetric.

Now, for two symmetric positive definite matrices A and B, we can show that ABA is also positive definite. Since positive definite matrices are symmetric and invertible, both

A and B satisfy $A^T = A$, $B^T = B$, and $x^T Ax > 0$, $x^T Bx > 0$ for all nonzero vectors x. Consider the matrix $C = ABA$. Then

$$C^T = (ABA)^T = A^T B^T A^T = ABA = C,$$

so C is symmetric. For any nonzero vector x, define $y = Ax$. Because A is invertible, $y \neq 0$. We then have

$$x^T Cx = x^T ABAx = (Ax)^T B(Ax) = y^T By.$$

Since B is positive definite, $y^T By > 0$ for all $y \neq 0$. Therefore $x^T Cx > 0$ for all $x \neq 0$, which shows that $C = ABA$ is positive definite. This completes out proof.

Appendix C

C.1 Formal solution

The Boltzmann equation in the absence of external forces in the relaxation time approximation is given by,

$$p^\mu \partial_\mu f = -\frac{u \cdot p}{\tau_R}(f - f_{\text{eq}}). \tag{C.1}$$

The characteristic curves are given by,

$$\frac{\mathrm{d}x^\mu}{\mathrm{d}s} = p^\mu \qquad \Rightarrow \qquad x^\mu = p^\mu s + c^\mu \,. \tag{C.2}$$

s is the variable that parametrises the characteristic curve and c^μ is the integration constant representing the initial conditions.

We can then write the Boltzmann equation along the characteristic curve as

$$\frac{df(x^\mu(s), p^\mu)}{ds} + \frac{u(x^\mu(s)) \cdot p}{\tau_R(x^\mu(s))} f(x^\mu(s), p^\mu) = \frac{u(x^\mu(s)) \cdot p}{\tau_R(x^\mu(s))} f_{eq}(x^\mu(s), p^\mu) \,. \tag{C.3}$$

This equation is of the form

$$\frac{\mathrm{d}f(s)}{\mathrm{d}s} + \alpha(s) f(s) = g(s), \tag{C.4}$$

and has the solution,

$$f(s) = e^{-\int_0^s \alpha(s')ds'} f(0) + \int_0^s e^{-\int_{s'}^s \alpha(s'')ds''} g(s')ds' \,. \tag{C.5}$$

We can now write a formal solution to Eq.(C.3) as

$$\begin{aligned} f(x^\mu(s), p^\mu) = \exp\left\{ -\int_0^s \frac{u \cdot p}{\tau_R}(x^\mu(s'))ds' \right\} f(x^\mu(0), p^\mu) \\ + \int_0^s ds' \frac{u \cdot p}{\tau_R}(x^\mu(s') \exp\left\{ -\int_{s''}^s \frac{u \cdot p}{\tau_R} ds'' \right\} f_{eq}(x^\mu(s'), p^\mu). \end{aligned} \tag{C.6}$$

Here $x^\mu(0) = c^\mu$. We have from the equation of the characteristic curves,

$$c^\mu = x^\mu - p^\mu s\,. \tag{C.7}$$

Using $x^0 = t$ as the parameter.

$$t = p^0 s + t_0 \qquad \Rightarrow \qquad s = \frac{(t - t_0)}{p^0}, \tag{C.8}$$

$$x^i = \frac{p^i}{p^0}(t - t_0) + c^i \qquad \Rightarrow \qquad c^i = x^i - \frac{p^i}{p^0}(t - t_0). \tag{C.9}$$

also,

$$ds' = \frac{dt'}{p^0}. \tag{C.10}$$

Writing all the parameter dependencies explicitly, we have the formal solution,

$$\begin{aligned} f(x^\mu, p^\mu) = \exp\Big\{ - \int_{t_0}^{t} \frac{u(x^i - v^i(t-t), t') \cdot v}{\tau_R(x^i - v^i(t-t')}, t') dt' \Big\} f_0(x^i - v^i(t - t_0), t_0, p^\mu) \\ + \int_{t_0}^{t} dt' \frac{u(x^i - v^i(t-t'), t') \cdot v}{\tau_R(x^i - v^i(t-t'))} \exp\Big\{ - \int_{t'}^{t} \frac{u(x^i - v^i(t-t''), t'') \cdot v}{\tau_R(x^i - v^i(t-t'')), t'')} dt'' \Big\} f_{eq}(x^i - v^i(t-t'), t' \end{aligned} \tag{C.11}$$

where $v^\mu = p^\mu / p^0$. For brevity, we introduce the notation

$$h(t, t') = h(x^i - v^i(t - t'), t') \tag{C.12}$$

C.1.1 Reparametrization of the integration variable

We define the damping factor

$$\xi(t, t') = \int_{t'}^{t} \frac{u \cdot v}{\tau_R}(t, t'') dt''\,, \tag{C.13}$$

with

$$\frac{\mathrm{d}\xi}{\mathrm{d}t'} = -\frac{u \cdot v}{\tau_R}(t, t')\,. \tag{C.14}$$

We define the damping function,

$$D(t, t') = \exp\{-\xi'\}\,. \tag{C.15}$$

with the property

$$\frac{d}{dt'}D(t,t') = \frac{u\cdot v}{\tau_R}D(t,t')\,. \tag{C.16}$$

We intend to get the time variable t' as a function of the damping factor ξ. For this we Taylor expand t' about t or $\xi = 0$,

$$t'(t,\xi) = e^{\xi\frac{\mathrm{d}}{\mathrm{d}\xi'}}t'(t,\xi')\Big|_{\xi'=0} \tag{C.17}$$

$$= t + \sum_{n=1}^{\infty}\frac{(\xi)^n}{n!}\frac{\mathrm{d}^n}{\mathrm{d}^n\xi'}t'(t,\xi')\Big|_{\xi'=0}\,. \tag{C.18}$$

We now use the relation for invertible functions,

$$\frac{\mathrm{d}t'}{\mathrm{d}\xi} = \left(\frac{\mathrm{d}\xi}{\mathrm{d}t'}\right)^{-1} = -\frac{p^0\tau_R}{u\cdot p}\,, \tag{C.19}$$

and get,

$$\frac{\mathrm{d}^n}{\mathrm{d}\xi^n}t'(t,\xi) = \frac{\mathrm{d}^{n-1}}{\mathrm{d}\xi^{n-1}}\left(-\frac{p^0\tau_R}{u\cdot p}\right)\,. \tag{C.20}$$

So,

$$t'(t,\xi) = t + \sum_{n=1}^{\infty}\frac{(\xi)^n}{n!}\frac{\mathrm{d}^{n-1}}{\mathrm{d}^{n-1}\xi'}\left(-\frac{p^0\tau_R}{u\cdot p}\right)\,. \tag{C.21}$$

As x^μ is independent of ξ, $\frac{\mathrm{d}x^\mu}{\mathrm{d}\xi} = 0$. This implies,

$$e^{\xi\frac{\mathrm{d}}{\mathrm{d}\xi'}}\left(x^\mu\right) = x^\mu\,. \tag{C.22}$$

So we can write,

$$x^\mu - \frac{p^\mu}{p^0}(t-t') = e^{\xi\frac{\mathrm{d}}{\mathrm{d}\xi'}}(x^\mu - \frac{p^\mu}{p^0}(t-t')(\xi'))\Big|_{\xi'=0}\,. \tag{C.23}$$

C.1.2 The Gradient Expansion

Consider the hydrodynamic generator,

$$f_G = \int_0^{\xi_0} d\xi\, f_{eq}(x^\mu - \frac{p^\mu}{p^0}(t-t'(\xi)))\,. \tag{C.24}$$

From Eq.(C.23) we can write,

$$\begin{aligned} f_{eq}(x^\mu - \frac{p^\mu}{p^0}(t-t'(\xi))) &= f_{eq}(e^{\xi\frac{\mathrm{d}}{\mathrm{d}\xi'}}(x^\mu - \frac{p^\mu}{p^0}(t-t'))\Big|_{\xi'=0}) \\ &= e^{\xi\frac{\mathrm{d}}{\mathrm{d}\xi'}} f_{eq}((x^\mu - \frac{p^\mu}{p^0}(t-t')))\Big|_{\xi'=0} \\ &= \sum_{n=0}^{\infty} \frac{(\xi)^n}{n!}\frac{\mathrm{d}^n}{\mathrm{d}^n\xi'} f_{eq}((x^\mu - \frac{p^\mu}{p^0}(t-t')))\Big|_{\xi'=0}, \end{aligned} \tag{C.25}$$

where we have used the commutativity of the Lie series $e^{\xi\frac{\mathrm{d}}{\mathrm{d}\xi'}} f(x) = f(e^{\xi\frac{\mathrm{d}}{\mathrm{d}\xi'}}x)$. The commutativity property of the lie series is equivalent to saying that the Taylor series expansion of the composition of two analytic functions is equal to the composition of their individual Taylor series.

C.1.3 Coordinate transformation and the derivatives

From the chain rule, and Eq.(C.14) we have,

$$\frac{\mathrm{d}}{\mathrm{d}\xi} = -\frac{p^0\tau_R}{u\cdot p}\frac{\mathrm{d}}{\mathrm{d}t'}\,. \tag{C.26}$$

Now consider the function $h \equiv h(x^i - v^i(t-t'), t-(t-t'))$, its derivative

$$\begin{aligned} \frac{\mathrm{d}h}{\mathrm{d}t'} &\equiv \frac{\partial h}{\partial x^i}\frac{\mathrm{d}(x^i - v^i(t-t'))}{\mathrm{d}t'} + \frac{\partial h}{\partial t}\frac{\mathrm{d}(t-(t-t'))}{\mathrm{d}t'} \\ &= v^i\frac{\partial h}{\partial x^i} + \frac{\partial h}{\partial t}\,. \end{aligned} \tag{C.27}$$

At $t' = t$ this reduces to

$$\begin{aligned} \frac{\mathrm{d}h}{\mathrm{d}t'}\Big|_{t'=t} &= v^i\frac{\partial h}{\partial x^i} + \frac{\partial h}{\partial t}\Big|_{t'=t} \\ &= \frac{p^\mu\partial_\mu}{p^0}h(x^i,t)\,. \end{aligned} \tag{C.28}$$

From Eq.(C.26) and Eq.(C.28), we have

$$\frac{\mathrm{d}^n}{\mathrm{d}\xi^n} = \left[-\frac{\tau_R}{u\cdot p}p^\mu\partial_\mu\right]^n. \tag{C.29}$$

This gives

$$f_{eq}(x^\mu - \frac{p^\mu}{p^0}(t - t'(\xi'))) = \sum_{n=0}^{\infty} \frac{(\xi)^n}{n!} \frac{\mathrm{d}^n}{\mathrm{d}^n \xi'} f_{eq}((x^\mu - \frac{p^\mu}{p^0}(t - t'))) \Big|_{\xi=0}$$
$$= \sum_{n=0}^{\infty} \frac{(\xi)^n}{n!} \left[-\frac{\tau_R}{u \cdot p} p^\mu \partial_\mu \right]^n f_{eq}(x^\mu). \tag{C.30}$$

C.2 Solution from integration by parts

We can obtain a series expansion of the hydrodynamic generator f_G in ξ_0 by using integration by parts of

$$f_G = \int_0^{\xi_0} d\xi e^{-\xi} f_{eq}(\xi)\,.$$

The first iteration of integration by parts gives,

$$f_G = (-1)e^{-\xi} f_{eq} \Big|_0^{\xi_0} - \int_0^{\xi_0} d\xi \frac{df_{eq}}{d\xi}(-1)e^{-\xi}\,.$$

Continuing the integration by parts indefinitely we get the series,

$$f_G = \sum_{n=0}^{\infty} e^{-\xi}(-1)\frac{d^n}{d\xi^n}(f_{eq}) \Big|_0^{\xi_0}$$
$$= \sum_{n=0}^{\infty} \left(\frac{d^n}{d\xi^n} f_{eq}(0) - e^{-\xi_0} \frac{d^n}{d\xi^n} f_{eq}(\xi_0) \right). \tag{C.31}$$

In obtaining this we assume that,

$$\lim_{n\to\infty} \int_0^{\xi_0} d\xi \frac{\mathrm{d}^n f_{eq}}{\mathrm{d}^n \xi} e^{-\xi} = 0 \tag{C.32}$$

C.2.1 Equivalace With the Taylor Series Expansion

In this section we show the equivalence between the Taylor expanded gradient series and the one obtained through integration by parts. Consider the second term in Eq.(C.31) and its Taylor expansion about $\xi = 0$. Let

$$g_n(\xi) = \frac{d^n}{d\xi^n} f_{eq}(\xi) \tag{C.33}$$

That is

$$\begin{aligned} g_n(\xi_0) &= \sum_{m=0}^{\infty} \frac{(\xi_0)^m}{m!} \frac{\mathrm{d}^m}{\mathrm{d}\xi^m} \left[g_n(\xi) \right] \Big|_{\xi=0} \\ &= \sum_{m=0}^{\infty} \frac{(\xi_0)^m}{m!} \frac{\mathrm{d}^m}{\mathrm{d}\xi^m} \left[\frac{d^n}{d\xi^n} f_{eq}(\xi) \right] \Big|_{\xi=0} \\ &= \sum_{m=0}^{\infty} \frac{(\xi_0)^m}{m!} \frac{\mathrm{d}^{m+n}}{\mathrm{d}\xi^{m+n}} f_{eq}(\xi) \Big|_{\xi=0} . \end{aligned} \tag{C.34}$$

The sum over all n of g_n gives

$$\sum_{n=0}^{\infty} g_n(\xi_0) = \sum_{n=0}^{\infty} \sum_{m=0}^{\infty} \frac{(\xi_0)^m}{m!} \frac{\mathrm{d}^{m+n}}{\mathrm{d}\xi^{m+n}} f_{eq}(\xi) \Big|_{\xi=0} . \tag{C.35}$$

We now re-parametrise the sum in terms of $m + n$ as

$$\sum_{n=0}^{\infty} g_n(\xi_0) = \sum_{l=m+n=0}^{\infty} e_l(\xi_0) \frac{\mathrm{d}^l}{\mathrm{d}\xi^l} f_{eq}(\xi) \Big|_{\xi=0} \tag{C.36}$$

Where $e_l(\xi_0)$ is the exponential sum function, a polynomial that is the sum of all the coefficients of the derivatives that had $m + n = l$. This polynomial is given by

$$e_l(\xi) = \sum_{m=0}^{l} \frac{\xi^m}{m!}. \tag{C.37}$$

We can see this if we write down the sum as

$$\begin{aligned} \sum_{n=0}^{\infty} g_n(\xi_0) &= \sum_{l=m+n=0}^{\infty} e_l(\xi_0) \frac{\mathrm{d}^l}{\mathrm{d}\xi^l} f_{eq}(\xi) \Big|_{\xi=0} \\ &= f_{eq}(0) \\ &+ \frac{\mathrm{d}^1}{\mathrm{d}\xi^1} f_{eq}(0) + \xi_0 \frac{\mathrm{d}^1}{\mathrm{d}\xi^1} f_{eq}(0) \\ &+ \frac{\mathrm{d}^2}{\mathrm{d}\xi^2} f_{eq}(0) + \xi_0 \frac{\mathrm{d}^2}{\mathrm{d}\xi^2} f_{eq}(0) + \frac{\xi_0^2}{2!} \frac{\mathrm{d}^2}{\mathrm{d}\xi^2} f_{eq}(0) \\ &\vdots \end{aligned} \tag{C.38}$$

$$\sum_{n=0}^{\infty} g_n(\xi_0) = \sum_{l=0}^{\infty} \left(\sum_{k=0}^{l} \frac{\xi^k}{k!} \right) \frac{\mathrm{d}^l}{\mathrm{d}\xi^l} f_{eq}(\xi) \Big|_{\xi=0}$$
$$= \sum_{l=0}^{\infty} \left(\sum_{k=0}^{l} \frac{\xi^k}{k!} \right) \frac{\mathrm{d}^l}{\mathrm{d}\xi^l} f_{eq}(0). \tag{C.39}$$

We get the desired result by renaming the dummy summation index $l \Rightarrow n$ and substituting it in Eq.(C.31).

C.3 Analyticity and convergence

We define the function

$$g(t, \vec{x}) = \frac{u \cdot p}{\tau_R p^0}(t, \vec{x}) \,, \tag{C.40}$$

where $u \cdot p$, τ_R are functions from $\mathbb{R}^{3+1} \to \mathbb{R}$ and p^μ is a parameter ($p^\mu p_\mu = m^2$). As $u \cdot p$ (Energy of the particle in the fluid rest frame) is non-zero and τ_R (the relaxation time) is finite, the function g is non-zero for all $(t, \vec{x})$.

$$\gamma[t'] = (t, \vec{x}) - (p^0, \vec{p}) \frac{(t - t')}{p^0}, \tag{C.41}$$

is a curve from $t' \in [t_0, t] \to \mathbb{R}^{3+1}$. Define,

$$\xi(t') = \int_{t'}^{t} g(\gamma[t'']) dt'' \,. \tag{C.42}$$

If g is an analytic function at $(t, \vec{x})$, then ξ is an analytic function of $(t - t')$ at $t - t' = 0$. Then by Lagrange–Burmann inversion theorem, we have an inverse

$$(t - t'(\xi)) = \sum_{n=1}^{\infty} \frac{a_n}{n!} \xi^n \tag{C.43}$$

where

$$a_n = \lim_{\xi \to 0} \frac{\mathrm{d}^n}{\mathrm{d}t'^n} \left[\frac{(t' - t)}{\xi(t') - \xi(t)} \right] \tag{C.44}$$

and the series is analytic in the neighbourhood of $\xi = 0$. By uniqueness of power series expansion, one can conclude that this is the same as the series obtained through a Taylor series expansion around $\xi = 0$.

The composition of analytic functions is analytic. Therefore, if $f(t, \vec{x})$ is a function from $\mathbb{R}^{3+1} \to \mathbb{R}$ and is analytic at $(t, \vec{x})$, then $f(\gamma(t')) = f(\gamma(t'(\xi)))$ has a series expansion in ξ that is analytic at $\xi = 0 = (t - t')$.

C.4 Generalised Coordinates and Forces

The Boltzmann equation in the presence of external forces can be written as,

$$\left(p^\mu \frac{\partial}{\partial x^\mu} + mK^\mu \frac{\partial}{\partial p^\mu} - \Gamma^\sigma_{\mu\nu} p^\mu p^\nu \frac{\partial}{\partial p^\sigma} \right) f = C(f, f)\,. \tag{C.45}$$

The characteristic equation of Eq.(C.45) will be

$$\frac{\mathrm{d}x^\mu}{\mathrm{d}s} = p^\mu \tag{C.46}$$

$$\frac{\mathrm{d}p^\mu}{\mathrm{d}s} = mK^\mu - \Gamma^\sigma_{\mu\nu} p^\mu p^\nu\,. \tag{C.47}$$

Let $x^\mu(s)$ and $p^\mu(s)$ represent the solutions to the characteristic equations Eq.(C.46). The Boltzmann equation on the characteristic curve in phase space reduces to,

$$\frac{df(x^\mu(s), p^\mu(s))}{ds} + \frac{u(x^\mu(s)) \cdot p}{\tau_R(x^\mu(s))} f(x^\mu(s), p^\mu(s)) = \frac{u(x^\mu(s)) \cdot p}{\tau_R(x^\mu(s))} f_{eq}(x^\mu(s), p^\mu(s))\,. \tag{C.48}$$

The formal solution to this equation follows the same procedure as in the force-free case. A direct re-parametrisation in terms of the time variable $s' \to x^0 = t'$ is not possible. However, this shortcoming doesn't hinder further analysis which follows the same mathematical procedure.

We define the damping factor in terms of the parameter s

$$\xi(s, s') = \int_{s'}^{s} \frac{u \cdot p}{\tau_R}(s, s'') ds''\,. \tag{C.49}$$

The inverse function $s(\xi')$ is obtained as,

$$s'(s,\xi) = s + \sum_{n=1}^{\infty} \frac{(\xi)^n}{n!} \frac{\mathrm{d}^{n-1}}{\mathrm{d}^{n-1}\xi'} \left(-\frac{\tau_R}{u\cdot p} \right) . \tag{C.50}$$

From the chain rule, and Eq.(C.49) we have,

$$\frac{\mathrm{d}}{\mathrm{d}\xi} = -\frac{\tau_R}{u\cdot p}\frac{\mathrm{d}}{\mathrm{d}s'} \tag{C.51}$$

and at at $s' = s$ this reduces to

$$\mathcal{D} \equiv \left.\frac{\mathrm{d}}{\mathrm{d}s'}\right|_{s'=s} \tag{C.52}$$

$$= p^\mu \partial_\mu + \left(mK^\mu - \Gamma^\mu_{\sigma\rho} p^\sigma p^\rho \right) \frac{\partial}{\partial p^\mu} . \tag{C.53}$$

We can expand the equilibrium distribution function in terms of ξ' as,

$$f_{eq}(x^\mu(s), p^\mu(s)) = \sum_{n=0}^{\infty} \frac{(\xi)^n}{n!} \left[-\frac{\tau_R}{p\cdot U}\mathcal{D} \right]^n f_{eq}(x^\mu(s), p^\mu(s)). \tag{C.54}$$

Appendix D

D.1 General Formulas

The Moment Integral

In $0+1$D we define the moments as,

$$\rho_{n,l} = \int \frac{d^3p}{(2\pi)^3}(p^0)^n \left(\frac{p^z}{p^0\tau}\right)^{2l} f\,. \tag{D.1}$$

For the equilibrium distribution function, we have

$$\rho^{eq}_{n,l} = \int \frac{d^3p}{(2\pi)^3}(p^0)^n \left(\frac{p^z}{p^0}\right)^{2l} f^{eq} \tag{D.2}$$

$$= e^{\mu/T}\int \frac{d^3p}{(2\pi)^3}(p^0)^n \left(\frac{p^z}{p^0}\right)^{2l} e^{-p^0/T} \tag{D.3}$$

The final integral is where $(p^0)^2 = |p|^2 + m^2$. Define,

$$y = \frac{p^0}{T}\,, \tag{D.4}$$

$$z = \frac{m}{T} \tag{D.5}$$

We have

$$|p|^2 = T^2(y^2 - z^2) \tag{D.6}$$

So,

$$d|p| = T\frac{y}{\sqrt{y^2-z^2}}dy \tag{D.7}$$

$$\begin{aligned}\rho^{eq}_{n,l}(T,z) &= \frac{e^{\mu/T}}{(2\pi)^3}\int d|p|p^2\sin\theta d\theta d\phi (p^0)^{n-2l}|p|^{2l}\cos^{2l}\theta e^{-p^0/T} \\ &= \frac{e^{\mu/T}}{2\pi^2}\frac{1}{2l+1}\int T^2(y^2-z^2)dy\frac{Ty}{\sqrt{y^2-z^2}}(yT)^{n-2l}T^{2l}(y^2-z^2)^l e^{-y} \\ &= \frac{e^{\mu/T}}{2\pi^2}\frac{T^{n+3}}{2l+1}\int_z^\infty dy y^{n-2l+1}(y^2-z^2)^{l+1/2}e^{-y} \qquad \text{(D.8)}\end{aligned}$$

$$\rho^{eq}_{n,l}(T,z) = \frac{T^{n+3}}{2\pi^2}\frac{G_{n+3,l}(z)}{(2l+1)}e^{\mu/T} \qquad \text{(D.9)}$$

We have

$$\epsilon = \rho^{eq}_{1,0} = \frac{T^4}{2\pi^2}G_{4,l}(z)e^{\mu/T} \qquad \text{(D.10)}$$

$$P = \rho^{eq}_{1,1} = \frac{1}{3}\frac{T^4}{2\pi^2}G_{4,l}(z)e^{\mu/T} \qquad \text{(D.11)}$$

In general we have the relation,

$$\rho^{eq}_{1,l} = \frac{1}{2l+1}\frac{T^4}{2\pi^2}G_{4,l}(z)e^{\mu/T} = \frac{3}{(2l+1)}\frac{G_{4,l}(z)}{G_{4,1}(z)}P \qquad \text{(D.12)}$$

and the conformal limit,

$$\rho^{eq}_{1,l} = \frac{3}{(2l+1)}P \qquad \text{(D.13)}$$

The G-Function

The function $G_{n,l}(z)$ appearing in the equilibrium moment is defined as,

$$G_{n,l}(z) = \int_z^\infty dy y^{n-2l-2}(y^2-z^2)^{l+1/2}e^{-y} \qquad \text{(D.14)}$$

$$\text{(D.15)}$$

For $z=0$, we have

$$\begin{aligned}G_{n,l}(z=0) &= \int_z^\infty dy y^{n-2l-2}(y^2-0^2)^{l+1/2}e^{-y} \\ &= \int_0^\infty dy y^{n-1}e^{-y} \\ &= \Gamma(n) \qquad \text{(D.16)}\end{aligned}$$

D.2 $0+1$D Calculations

D.2.1 Exact solutions to the moment equation

We rewrite the moment equations as

$$\left[\partial_\tau + \left(\frac{2l+1}{\tau}\hat{\mathbf{I}} - \frac{2l-n}{\tau}\hat{\mathbf{S}}\right) + \frac{\hat{\mathbf{I}}}{\tau_R}\right]\rho_n(\tau,l) = \frac{\hat{\mathbf{I}}}{\tau_R}\rho_n^{\text{eq}}(\tau,l) \tag{D.17}$$

where we have defined the shift operator,

$$\hat{\mathbf{S}}\left[h(l)\right] = h(l+1)\,. \tag{D.18}$$

We define the generator of free streaming,

$$\hat{\mathbf{F}} = \frac{2l+1}{\tau}\hat{\mathbf{I}} - \frac{2l-n}{\tau}\hat{\mathbf{S}}\,. \tag{D.19}$$

This essentially encodes the linear matrix algebra of the set of coupled differential equations. But, this allows us to use formal algebraic manipulations to obtain an integral form of the differential equations by considering them as first-order operator differential equations.

To find the propagator of the solutions we define,

$$\hat{\mathcal{M}}_{n,l} = \int_{\tau_0}^{\tau}\left(\frac{2l+1}{\tau}\hat{\mathbf{I}} - \frac{2l-n}{\tau}\hat{\mathbf{S}} + \frac{\hat{\mathbf{I}}}{\tau_R}\right)\,. \tag{D.20}$$

which gives us the integrating(propagator) factor,

$$\exp\left\{\hat{\mathcal{M}}'_{n,l}\right\} = \exp\left\{\int_{\tau'}^{\tau} d\tau'\left(\frac{2l+1}{\tau'}\hat{\mathbf{I}} - \frac{2l-n}{\tau'}\hat{\mathbf{S}} + +\frac{\hat{\mathbf{I}}}{\tau_R}\right)\right\} \tag{D.21}$$

and its inverse

$$\exp\left\{-\hat{\mathcal{M}}'_{n,l}\right\} = \exp\left\{-\int_{\tau'}^{\tau}\left(\frac{2l+1}{\tau}\hat{\mathbf{I}} - \frac{2l-n}{\tau}\hat{\mathbf{S}}\right) + +\frac{\hat{\mathbf{I}}}{\tau_R}\right\}\,. \tag{D.22}$$

Such a manipulation is well defined as

$$[\hat{\mathcal{M}}_{n,l}, \partial_\tau\hat{\mathcal{M}}_{n,l}] = 0\,. \tag{D.23}$$

We now define the operator which is the integral of the generator of Free streaming

$$\hat{\mathbf{K}}_{\tau,\tau'} = \int_{\tau'}^{\tau} \frac{2l+1}{\tau}\hat{\mathbf{I}} - \frac{2l-n}{\tau}\hat{\mathbf{S}}d\tau' \tag{D.24}$$

$$= \log\left(\frac{\tau}{\tau'}\right)\left[(2l+1)\hat{\mathbf{I}} - (2l-n)\hat{\mathbf{S}}_l\right] \tag{D.25}$$

This allows us to write a formal solution,

$$\rho_{n,l}(\tau) = e^{-\xi_0}e^{-\hat{\mathbf{K}}_{\tau,\tau_0}}\rho_{n,l}(\tau_0) \tag{D.26}$$

$$+ \int_{\tau_0}^{\tau} d\tau' \frac{1}{\tau_R} e^{-\xi'}e^{-\hat{\mathbf{K}}_{\tau,\tau'}}\rho^{\text{eq}}_{n,l}(\tau') \tag{D.27}$$

To put this expression in a useful form, we note that if we define the operators,

$$\hat{\mathbf{X}} = -\log\left(\frac{\tau}{\tau'}\right)(2l+1)\,\hat{\mathbf{I}} \tag{D.28}$$

$$\hat{\mathbf{Y}} = \log\left(\frac{\tau}{\tau'}\right)(2l-n)\,\hat{\mathbf{S}}\,, \tag{D.29}$$

They satisfy the commutation relation,

$$[\hat{\mathbf{X}}, \hat{\mathbf{Y}}] = \alpha\hat{\mathbf{Y}}\,. \tag{D.30}$$

where $\alpha = -2\log\left(\frac{\tau}{\tau'}\right)$. For such operators, we have the property [116],

$$e^{\hat{\mathbf{X}}+\hat{\mathbf{Y}}} = e^{\hat{\mathbf{X}}}e^{f(\alpha)\hat{\mathbf{Y}}} \tag{D.31}$$

where

$$f(\alpha) = \frac{1-e^{\alpha}}{\alpha}\,. \tag{D.32}$$

Then we have

$$f(\alpha)\hat{\mathbf{Y}} = -\frac{(2l-n)}{2}\left[1-\left(\frac{\tau'}{\tau}\right)^2\right]\hat{\mathbf{S}} \tag{D.33}$$

Using this we can write

$$e^{-\log\left(\frac{\tau}{\tau'}\right)\left[(2l+1)\hat{\mathbf{I}}-(2l-n)\hat{\mathbf{S}}\right]} = e^{-\log\left(\frac{\tau}{\tau'}\right)(2l+1)\hat{\mathbf{I}}}e^{-\frac{(2l-n)}{2}\left(1-\left(\frac{\tau'}{\tau}\right)^2\right)\hat{\mathbf{S}}}$$

$$= \left(\frac{\tau'}{\tau}\right)^{2l+1}\sum_{k=0}^{\infty}\left[-\frac{(2l-n)}{2}\left(1-\left(\frac{\tau'}{\tau}\right)^2\right)\hat{\mathbf{S}}\right]^k$$

$$= \left(\frac{\tau'}{\tau}\right)^{2l+1}\sum_{k=0}^{\infty}\frac{(-1)^k(2l-n)^{(2k)}}{2^k k!}\left[1-\left(\frac{\tau'}{\tau}\right)^2\right]^k\hat{\mathbf{S}}^k$$

where $(\cdot)^{(k)}$ is the rising poccamer symbol.

We can immediately write down the free streaming solution,

$$\rho_n^{FS}(\tau,l)=\sum_{k=0}^{\infty}\frac{\left(l-\frac{n}{2}\right)^{(k)}}{k!}\left(\frac{\tau_0}{\tau}\right)^{2l+1}\left[\left(\frac{\tau_0}{\tau}\right)^2-1\right]^k\rho_n(\tau_0,l+k) \tag{D.34}$$

The solution to the relaxation equation can be written down as,

$$\begin{aligned}\rho_{n,l}(\tau)=e^{-\xi_0}&\sum_{k=0}^{\infty}\frac{\left(l-\frac{n}{2}\right)^{(k)}}{k!}\left(\frac{\tau_0}{\tau}\right)^{2l+1}\left[\left(\frac{\tau_0}{\tau}\right)^2-1\right]^k\rho_{n,l+k}(\tau_0)\\&+\int_{\tau_0}^{\tau}d\tau'\frac{e^{-\xi'}}{\tau_R}\left(\frac{\tau'}{\tau}\right)^{2l+1}\sum_{k=0}^{\infty}\frac{(l-\frac{n}{2})^{(2k)}}{k!}\left[\left(\frac{\tau'}{\tau}\right)^2-1\right]^k\rho^{\text{eq}}_{n,l+k}(\tau)\,.\end{aligned} \tag{D.35}$$

With the generator of hydrodynamics,

$$\rho^G_{n,l}(\tau)=\int_{\tau_0}^{\tau}d\tau'\sum_{k=0}^{\infty}\frac{\left(l-\frac{n}{2}\right)^{(k)}}{k!}\frac{e^{-\xi'}}{\tau_R}\left(\frac{\tau'}{\tau}\right)^{2l+1}\left[\left(\frac{\tau'}{\tau}\right)^2-1\right]^k\rho^{\text{eq}}_{n,l+k}(\tau') \tag{D.36}$$

We can now use the expression for $\rho^{\text{eq}}_{n,l}$,

$$\rho^G_{n,l}(\tau)=\int_{\tau_0}^{\tau}d\tau'\sum_{k=0}^{\infty}\frac{\left(l-\frac{n}{2}\right)^{(k)}}{k!}\frac{e^{-\xi'}}{\tau_R}\left(\frac{\tau'}{\tau}\right)^{2l+1}\left[\left(\frac{\tau'}{\tau}\right)^2-1\right]^k\frac{T^{n+3}}{2\pi^2}\frac{G_{n+3,l+k}(z)}{(2(l+k)+1)}e^{\mu/T} \tag{D.37}$$

For the conformal case $z=0$, we have $G_{n+3,l+k}(z)=\Gamma(n+3)$ which is independent of l and k. This allows us the simplification,

$$\rho^G_{n,l}(\tau,z=0)=\frac{\Gamma(n+3)}{(2\pi^2)(2l+1)}\int_{\tau_0}^{\tau}d\tau'\frac{e^{-\xi'}}{\tau_R}\left(\frac{\tau'}{\tau}\right)^{2l+1}T^{n+3}\sum_{k=0}^{\infty}\frac{(1+1/2)^{(k)}\left(l-\frac{n}{2}\right)^{(k)}}{(l+3/2)^{(k)}}\frac{1}{k!}\left[\left(\frac{\tau'}{\tau}\right)^2-1\right]^k \tag{D.38}$$

$$=\frac{\Gamma(n+3)}{(2\pi^2)(2l+1)}\int_{\tau_0}^{\tau}d\tau'\frac{e^{-\xi'}}{\tau_R}\left(\frac{\tau'}{\tau}\right)^{2l+1}F(l+\frac{1}{2},l-\frac{n}{2};l+\frac{3}{2};\left(\frac{\tau'}{\tau}\right)^2-1)\,T^{n+3} \tag{D.39}$$

D.2.2 $0+1$D Gradient expansion

Consider the hydrodynamic generator,

$$\rho^G_{n,l}(\tau)=\int_{\tau_0}^{\tau}d\tau'\frac{1}{\tau_R}e^{-\xi'}e^{-\hat{\mathbf{K}}_{\tau,\tau'}}\rho^{\text{eq}}_{n,l}(\tau') \tag{D.40}$$

where $\xi' = \int_{\tau'}^{\tau} d\tau' \frac{1}{\tau_R}$. The free streaming propagator

$$\mathcal{K}_{\tau,\tau'} = e^{-\hat{\mathbf{K}}_{\tau,\tau'}} \tag{D.41}$$

satisfies

$$\partial_{\tau'} \mathcal{K}_{\tau,\tau'} \rho_{n,l}(\tau) = \mathcal{K}_{\tau,\tau'} \left(\partial_{\tau'} + \hat{\mathbf{F}} \right) \rho_{n,l}(\tau') \tag{D.42}$$

Consider the change of variables, $\tau' \to \xi'$. We now expand $e^{-\hat{F}(0,\xi')} \rho^{\text{eq}}_{n,l}(\xi')$ in a Taylor series about $\xi' = 0$ as

$$e^{-\hat{F}(0,\xi')} \rho^{\text{eq}}_{n,l}(\xi') = \sum_{k=0}^{\infty} \frac{(\xi')^k}{k!} \frac{\mathrm{d}^k}{\mathrm{d}\xi'^k} e^{-\hat{F}(0,\xi')} \rho^{\text{eq}}_{n,l}(\xi') \Big|_{\xi'=0} \tag{D.43}$$

$$= \sum_{k=0}^{\infty} \frac{(\xi')^k}{k!} \left[-\tau_R (\partial_{\tau'} + \hat{\mathbf{F}}) \right]^k \rho^{\text{eq}}_{n,l}(\xi') \Big|_{\tau'=\tau} . \tag{D.44}$$

For the ξ' integration we note,

$$\int_{\xi_0}^{0} d\xi' e^{-\xi'} (\xi')^k = \gamma(k+1, \xi_0) \tag{D.45}$$

We now finally get the hydrodynamic generator in terms of the gradients,

$$\rho^{G}_{n,l}(\tau) = \sum_{k=0}^{\infty} \frac{\gamma(k+1,\xi_0)}{k!} \left[-\tau_R (\partial_{\tau} + \hat{\mathbf{F}}) \right]^k \rho^{\text{eq}}_{n,l}(\tau) \tag{D.46}$$

D.2.3 Hydrodynamics

Hydrodynamics in $0+1$D requires us to find the dynamical equations for the energy density ϵ and the two anisotropies, bulk pressure Π and shear pressure π. From energy conservation we get the dynamical equation for energy density ($\epsilon = \rho_{1,1}$),

$$\hat{\mathbf{D}} \rho_{1,0} = \hat{\mathbf{D}} \mathrm{n} = 0 \tag{D.47}$$

$$\hat{\mathbf{D}} \rho_{1,1} = \hat{\mathbf{D}} \epsilon = 0 \tag{D.48}$$

which gives us the familiar energy density and number density evolution equation for Bjorken flow,

$$\partial_\tau \mathrm{n} = -\frac{\mathrm{n}}{\tau} \tag{D.49}$$

$$\partial_\tau \epsilon = -\frac{\epsilon + P_L}{\tau} \tag{D.50}$$

where P_L is the longitudinal pressure $P_L = P + \Pi - \pi$. The equations for the non-equlibrium components,

$$\hat{\mathbf{D}}\pi^G_{n,l} = -\frac{\pi^G_{n,l}}{\tau_R} - \hat{\mathbf{D}}\rho^{eq}_{n,l} \tag{D.51}$$

will give us the evolution equations for the pressure anisotropies. To find this we note the relation between the anisotropic moments and the shear and bulk pressure. The bulk pressure can be computed from the moments using the relations,

$$\pi = P + \Pi - P_L \tag{D.52}$$

$$\Pi = \frac{1}{3}(\epsilon - 3P) - \frac{1}{3}\langle m^2 \rangle \,. \tag{D.53}$$

From this we can infer,

$$\begin{aligned} \Pi &= \frac{1}{3}(\epsilon - 3P) - \frac{1}{3}m^2(\rho^{eq}_{-1,0} + \pi_{-1,0}) \\ &= -\frac{m^2}{3}\pi_{-1,0} \end{aligned} \tag{D.54}$$

$$\pi = \Pi - \pi_{1,1} \tag{D.55}$$

$$= -\frac{m^2}{3}\pi_{-1,0} - \pi_{1,1} \tag{D.56}$$

In the conformal limit

$$\pi = -\pi_{1,1} \tag{D.57}$$

We also need to compute the equilibrium gradient,

$$\hat{\mathbf{D}}\rho^{eq}_{n,l}(\tau) = \partial_\tau \rho^{eq}_{n,l}(\tau) + \frac{(2l+1)}{\tau}\rho^{eq}_{n,l}(\tau) - \frac{(2l-n)}{\tau}\rho^{eq}_{n,l+1}(\tau) \,. \tag{D.58}$$

We can express the time derivative term in terms of the energy derivative,

$$\partial_\tau \rho^{eq}_{n,l}(\tau) = \frac{\partial \rho^{eq}_{n,l}}{\partial \epsilon}\frac{\partial \epsilon}{\partial \tau} + \frac{\partial \rho^{eq}_{n,l}}{\partial n}\frac{\partial n}{\partial \tau} \tag{D.59}$$

$$= -\frac{\partial \rho^{eq}_{n,l}}{\partial \epsilon}\,\frac{(\epsilon + P + \Pi - \pi)}{\tau} - \frac{\partial \rho^{eq}_{n,l}}{\partial \mathrm{n}}\,\frac{\mathrm{n}}{\tau}\,. \tag{D.60}$$

Define

$$c^2_{n,l} = \frac{\partial \rho^{eq}_{n,l}}{\partial \epsilon}\,, \tag{D.61}$$

$$\kappa_{n,l} = n\frac{\partial \rho^{eq}_{n,l}}{\partial \mathrm{n}}\,. \tag{D.62}$$

with the speed of sound $c_s^2 = c^2_{1,1}$ and bulk modulus $\kappa = \kappa_{1,1}$ as $\rho_{1,2} = P$, the equilibrium pressure. Note that any $\hat{\mathbf{D}}^k \rho^{eq}_{n,l}(\tau)$ can be reduced in terms of the hydrodynamic variables ϵ,n,Π and π.

In the Bjorken case we can write,

$$\partial_\tau \rho^{eq}_{n,l}(\tau) = -c^2_{n,l}\frac{(\epsilon + P + \Pi - \pi)}{\tau} - \frac{\kappa_{n,l}}{\tau} \tag{D.63}$$

We then obtain,

$$\hat{\mathbf{D}}P = -c_s^2\frac{(\epsilon + P + \Pi - \pi)}{\tau} - \frac{\kappa}{\tau} + \frac{3P}{\tau} - \frac{\rho^{eq}_{1,2}(\tau)}{\tau} \tag{D.64}$$

$$= -c_s^2\frac{(\Pi - \pi)}{\tau} - \frac{1}{\tau}\left(c_s^2\left[1 + 3\frac{G_{4,0}(z)}{G_{4,1}(z)}\right] + \frac{3}{5}\frac{G_{4,2}(z)}{G_{4,1}(z)} - 3\right)P - \frac{\kappa}{\tau} \tag{D.65}$$

For the conformal case we have the equation of state,

$$\epsilon = 3P \tag{D.66}$$

$$c_s^2 = \frac{1}{3} \tag{D.67}$$

$$\Pi = 0 \tag{D.68}$$

$$\hat{\mathbf{D}}P = -\frac{1}{3}\frac{4P}{\tau} + c_s^2\frac{\pi}{\tau} - \frac{\kappa}{\tau} + \frac{3P}{\tau} - \frac{\rho^{eq}_{1,2}(\tau)}{\tau} \tag{D.69}$$

$$= \frac{5}{3}\frac{P}{\tau} + \frac{1}{3}\frac{\pi}{\tau} - \frac{\kappa}{\tau} - \frac{3}{5}\frac{P}{\tau} \tag{D.70}$$

$$= \frac{16}{15}\frac{P}{\tau} + \frac{1}{3}\frac{\pi}{\tau} - \frac{\kappa}{\tau} \tag{D.71}$$

Evolution of $\pi_{1,1}$

The evolution equation for $\pi_{1,1}$ reads,

$$\hat{\mathbf{D}}\pi_{1,1} = -\frac{\pi_{1,1}}{\tau_R} + c_s^2\frac{(\epsilon + P + \pi_{1,1})}{\tau} + \frac{\kappa}{\tau} - \frac{3P}{\tau} + \frac{\rho^{eq}_{1,2}(\tau)}{\tau} \tag{D.72}$$

$$= -\frac{\pi_{1,1}}{\tau_R} + c_s^2\frac{\pi_{1,1}}{\tau} + c_s^2\frac{(\epsilon + P)}{\tau} + \frac{\kappa}{\tau} - 3\frac{P}{\tau} + \frac{\rho^{eq}_{1,2}(\tau)}{\tau}\,. \tag{D.73}$$

We note that,

$$\hat{\mathbf{D}}\pi_{1,1} = \partial_\tau\pi_{1,1} + (2\cdot 1 + 1)\frac{\pi_{1,1}}{\tau} - (2\cdot 1 - 1)\frac{\pi_{1,2}}{\tau} \tag{D.74}$$

$$= \partial_\tau\pi_{1,1} + 3\frac{\pi_{1,1}}{\tau} - \frac{\pi_{1,2}}{\tau} \tag{D.75}$$

Using this, we get the evolution equation for $\pi_{1,1}$,

$$\partial_\tau\pi_{1,1} + \frac{\pi_{1,1}}{\tau_R} = (c_s^2 - 3)\frac{\pi_{1,1}}{\tau} + c_s^2\frac{(\epsilon + P)}{\tau} + \frac{\kappa}{\tau} + \frac{\rho^{eq}_{1,2}(\tau)}{\tau} - 3\frac{P}{\tau} + \frac{\pi_{1,2}}{\tau} \tag{D.76}$$

Conformal equation,

$$\partial_\tau\pi_{1,1} + \frac{\pi_{1,1}}{\tau_R} = -\frac{4}{3}\frac{1}{\tau}\left(\frac{4P}{5}\right) - \frac{8}{3}\frac{\pi_{1,1}}{\tau} + \frac{\kappa}{\tau} + \frac{\pi_{1,2}}{\tau} \tag{D.77}$$

Evolution of $\pi_{-1,0}$

$$\hat{\mathbf{D}}\pi_{-1,0} = -\frac{\pi_{-1,0}}{\tau_R} - \hat{\mathbf{D}}\rho^{eq}_{-1,0}(\tau) \tag{D.78}$$

We note that $m^2\rho^{eq}_{-1,0}(\tau) = \langle m^2\rangle^{eq} = \epsilon - 3P$ and we get,

$$\begin{aligned}\hat{\mathbf{D}}\rho^{eq}_{-1,0}(\tau) &= \frac{1}{m^2}\hat{\mathbf{D}}(\epsilon - 3P)\\ &= \frac{1}{m^2}\hat{\mathbf{D}}\epsilon - 3\hat{\mathbf{D}}P\\ &= -3\frac{1}{m^2}\hat{\mathbf{D}}P\,,\end{aligned} \tag{D.79}$$

where we have used the nergy conservation relation, $\hat{\mathbf{D}}\epsilon = 0.$ then the evolution equation for $\pi_{-1,0}$ reads,

$$\hat{\mathbf{D}}\pi_{-1,0} = -\frac{\pi_{-1,0}}{\tau_R} + \frac{3}{m^2}\hat{\mathbf{D}}P \tag{D.80}$$

Now,

$$\begin{aligned}\hat{\mathbf{D}}\pi_{-1,0} &= \partial_\tau \pi_{1,1} + (2\cdot 0+1)\frac{\pi_{-1,0}}{\tau} - (2\cdot 0+1)\frac{\pi_{-1,1}}{\tau} \\ &= \partial_\tau \pi_{-1,0} + \frac{\pi_{-1,0}}{\tau} - \frac{\pi_{-1,1}}{\tau}\,. \end{aligned} \tag{D.81}$$

Combining we have

$$\partial_\tau \pi_{-1,0} + \frac{\pi_{-1,0}}{\tau_R} = -\frac{\pi_{-1,0}}{\tau} + \frac{3}{m^2}\left(-c_s^2\frac{(\epsilon+P+\pi_{1,1})}{\tau} - \frac{\kappa}{\tau} + \frac{3P}{\tau} - \frac{\rho^{eq}_{1,2}(\tau)}{\tau}\right) + \frac{\pi_{-1,1}}{\tau} \tag{D.82}$$

Evolution of Π

Multiplying both sides of (D.80) by $-\frac{m^2}{3}$, we get the evolution equation for Π

$$\hat{\mathbf{D}}\Pi = -\frac{\Pi}{\tau_R} - \hat{\mathbf{D}}P \tag{D.83}$$

From (D.82),

$$\partial_\tau \Pi + \frac{\Pi}{\tau_R} = -\frac{\Pi}{\tau} - \left(-c_s^2\frac{(\epsilon+P+\pi_{1,1})}{\tau} - \frac{\kappa}{\tau} + \frac{3P}{\tau} - \frac{\rho^{eq}_{1,2}(\tau)}{\tau}\right) - \frac{m^2}{3}\frac{\pi_{-1,1}}{\tau} \tag{D.84}$$

$$= -\frac{\Pi}{\tau} + c_s^2\frac{(\epsilon+P+\Pi-\pi)}{\tau} + \frac{\kappa}{\tau} - \frac{3P}{\tau} + \frac{\rho^{eq}_{1,2}(\tau)}{\tau} - \frac{m^2}{3}\frac{\pi_{-1,1}}{\tau} \tag{D.85}$$

$$= (1-c_s^2)\frac{\Pi}{\tau} - \frac{\pi}{\tau} + c_s^2\frac{(\epsilon+P)}{\tau} + \frac{\kappa}{\tau} - \frac{3P}{\tau} + \frac{\rho^{eq}_{1,2}(\tau)}{\tau} - \frac{m^2}{3}\frac{\pi_{-1,1}}{\tau} \tag{D.86}$$

D.2.4 Evolution of π

$$\partial_\tau \pi_{1,1} + \frac{\pi_{1,1}}{\tau_R} = -\frac{3\pi_{1,1}}{\tau} - \hat{\mathbf{D}}P + \frac{\pi_{1,2}}{\tau} \tag{D.87}$$

$$\partial_\tau \Pi + \frac{\Pi}{\tau_R} = -\frac{\Pi}{\tau} - \hat{\mathbf{D}}P - \frac{m^2}{3}\frac{\pi_{-1,1}}{\tau} \tag{D.88}$$

We have $\pi_{1,1} = (\pi - \Pi)$. Adding the above two equations we get

$$\partial_\tau(\pi-\Pi) + \frac{(\pi-\Pi)}{\tau_R} = -\frac{3(\pi-\Pi)}{\tau} - \hat{\mathbf{D}}P + \frac{\pi_{1,2}}{\tau} \tag{D.89}$$

$$\partial_\tau \pi - \partial_\tau \Pi + \frac{\pi}{\tau_R} + \frac{-\Pi}{\tau_R} = -\frac{3\pi}{\tau} - \frac{-3\Pi}{\tau} - \hat{\mathbf{D}}P + \frac{\pi_{1,2}}{\tau} \tag{D.90}$$

Adding we get

$$\partial_\tau \pi + \frac{\pi}{\tau_R} = -\frac{3\pi}{\tau} + \frac{2\Pi}{\tau} - 2\,\hat{\mathbf{D}}P + \frac{\pi_{1,2}}{\tau} - \frac{m^2}{3}\frac{\pi_{-1,1}}{\tau} \tag{D.91}$$

$$\hat{\mathbf{D}}P = -c_s^2\frac{\Pi}{\tau} + c_s^2\frac{\pi}{\tau} - c_s^2\frac{(\epsilon+P)}{\tau} + \frac{3P}{\tau} - \frac{\rho_{1,2}^{eq}}{\tau} \tag{D.92}$$

$$\partial_\tau \pi + \frac{\pi}{\tau_R} = -\frac{(3+2c_s^2)\pi}{\tau} + \frac{2(1+c_s^2)\Pi}{\tau} + 2c_s^2\frac{(\epsilon+P)}{\tau} - \frac{6P}{\tau} + 2\frac{\rho_{1,2}^{eq}}{\tau} + \frac{\pi_{1,2}}{\tau} - \frac{m^2}{3}\frac{\pi_{-1,1}}{\tau} \tag{D.93}$$

$$\hat{\mathbf{D}}\pi_{1,1} = -\frac{\pi_{1,1}}{\tau_R} - \hat{\mathbf{D}}P \tag{D.94}$$

Typical structure of second order hydrodynamic equations

$$\dot{\Pi} + \frac{\Pi}{\tau_\Pi} = -\beta_\Pi\theta - \delta_{\Pi\Pi}\theta\,\Pi + \lambda_{\Pi\pi}\sigma_{\mu\nu}\pi^{\mu\nu}\,. \tag{D.95}$$

$$\dot{\pi}^{\mu\nu} + \frac{\pi^{\mu\nu}}{\tau_\pi} = 2\beta_\pi\sigma^{\mu\nu} - \delta_{\pi\pi}\theta\,\pi^{\mu\nu} + \lambda_{\pi\Pi}\Pi\sigma^{\mu\nu} \tag{D.96}$$

$$+ 2\pi_\gamma^{\langle\mu}\omega^{\nu\rangle\gamma} - \tau_{\pi\pi} + 2\pi_\gamma^{\langle\mu}\sigma^{\nu\rangle\gamma}\,. \tag{D.97}$$

D.3 $3+1$D Calculations

The $3+1$D moment equations have the form,

$$\left[\partial_\tau + \hat{\mathbf{L}} + \hat{\boldsymbol{\nu}}_R\right]\vec{\rho} = \hat{\boldsymbol{\nu}}_R\vec{\rho}^{\,\mathrm{eq}}\,. \tag{D.98}$$

Our goal is to construct the propagator $u(\tau,\tau_0)$ for this linear equation. To do so, we employ perturbative techniques familiar from linear differential equations such as the Schrödinger equation, using the interaction picture. In this approach, the operator is decomposed into an exactly solvable part and an interaction term, and the evolution is then expressed in a basis governed by the solvable dynamics.

Here, two operators govern the evolution: the free-streaming Liouville operator $\hat{\mathbf{L}}$ and the collision operator $\hat{\boldsymbol{\nu}}_R$. Either of them may be designated as the interaction, depending on which choice yields the most convenient form for the final expression.

D.3.1 Collision picture

We will choose to decompose the propagator into free streaming and collision part and treat the collision as the interaction. Consider the free streaming equation,

$$\left[\partial_\tau + \hat{\mathbf{L}}\right] = 0 \tag{D.99}$$

with the propagator $\hat{\mathcal{F}}$ satisfying,

$$\partial_\tau \hat{\mathcal{F}}_{\tau,\tau_0} = -\hat{\mathbf{L}}\, \hat{\mathcal{F}}_{\tau,\tau_0} \tag{D.100}$$

We can now define the collision picture operator and variables,

$$\vec{\rho}_c(\tau) = \hat{\mathcal{F}}^{-1}_{\tau,\tau_0} \vec{\rho}(\tau) \tag{D.101}$$

and

$$\hat{\boldsymbol{\nu}}_c = \hat{\mathcal{F}}^{-1}_{\tau,\tau_0}\, \hat{\boldsymbol{\nu}}_R\, \hat{\mathcal{F}}_{\tau,\tau_0} \tag{D.102}$$

Our collision picture with the interaction term equation now reads

$$\left[\partial_\tau + \hat{\boldsymbol{\nu}}_c\right]\ \vec{\rho}_c = 0 \tag{D.103}$$

The propagator for the interaction picture is given by

$$\mathcal{W}_{\tau,\tau_0} = \mathcal{T}\left(e^{-\int_{\tau_0}^{\tau} d\tau' \hat{\boldsymbol{\nu}}_c}\right) \tag{D.104}$$

where $\mathcal{T}$ represents the time ordering. The solution to the interaction picture equation is

$$\vec{\rho}_c(\tau) = \mathcal{W}_{\tau,\tau_0}\rho_c(\tau_0) + \int_{\tau_0}^{\tau} d\tau' \mathcal{W}_{\tau,\tau'}\, \hat{\boldsymbol{\nu}}_c(\tau') \vec{\rho}_c^{\,\mathrm{eq}}(\tau') \tag{D.105}$$

We can therefore write,

$$\int_{\tau_0}^{\tau} d\tau' \mathcal{W}_{\tau,\tau'}\ \hat{\boldsymbol{\nu}}_c(\tau')\vec{\rho}_c^{\,\mathrm{eq}}(\tau') = \int_{\tau_0}^{\tau} d\tau' \partial_{\tau'}\mathcal{W}_{\tau,\tau'}\vec{\rho}_c^{\,\mathrm{eq}}(\tau') \tag{D.106}$$

$$= \mathcal{W}_{\tau,\tau'}\rho_c^{\,\mathrm{eq}}(\tau')\Big|_{\tau_0}^{\tau} - \int_{\tau_0}^{\tau} d\tau' \mathcal{W}_{\tau,\tau'}\partial_{\tau'}\vec{\rho}_c^{\,\mathrm{eq}}(\tau') \tag{D.107}$$

$$= \mathcal{W}_{\tau,\tau'}\rho_c^{\,\mathrm{eq}}(\tau')\Big|_{\tau_0}^{\tau} - \int_{\tau_0}^{\tau} d\tau' \mathcal{W}_{\tau,\tau'}\hat{\boldsymbol{\nu}}_c(\tau')\hat{\boldsymbol{\nu}}_c^{-1}(\tau')\partial_{\tau'}\vec{\rho}_c^{\,\mathrm{eq}}(\tau') \tag{D.108}$$

$$= \sum_{n=0}^{\infty} \mathcal{W}_{\tau,\tau'}\ \left[\hat{\boldsymbol{\nu}}_c^{-1}(\tau')\partial_{\tau'}\right]^k\ \vec{\rho}_c^{\,\mathrm{eq}}(\tau')\Big|_{\tau_0}^{\tau} \tag{D.109}$$

$$= \hat{\mathcal{F}}_{\tau,\tau_0}^{-1}\sum_{n=0}^{\infty}\left[\hat{\boldsymbol{\nu}}^{-1}(\tau)\hat{\mathbf{D}}\right]^k\ \rho^{\,\mathrm{eq}}(\tau) - \mathcal{W}_{\tau,\tau_0}\ \sum_{n=0}^{\infty}\left[\hat{\boldsymbol{\nu}}^{-1}(\tau_0)\hat{\mathbf{D}}\right]^k\ \rho^{\,\mathrm{eq}}(\tau_0) \tag{D.110}$$

where in the last step we used the collision picture definitions. Now we get the solution in the Schrodinger picture

$$\vec{\rho}(\tau) = \hat{\mathcal{F}}_{\tau,\tau_0}\mathcal{W}_{\tau,\tau_0}\rho(\tau_0) + \sum_{n=0}^{\infty}\left[\hat{\boldsymbol{\nu}}^{-1}(\tau)\hat{\mathbf{D}}\right]^k\ \vec{\rho}^{\,\mathrm{eq}}(\tau) - \hat{\mathcal{F}}_{\tau,\tau_0}\mathcal{W}_{\tau,\tau_0}\ \sum_{n=0}^{\infty}\left[\hat{\boldsymbol{\nu}}^{-1}(\tau_0)\hat{\mathbf{D}}\right]^k\ \vec{\rho}^{\,\mathrm{eq}}(\tau_0) \tag{D.111}$$

D.3.2 Free Streaming picture

To derive the gradient expansion in the $3+1$D case, we adopt an alternative approach in which free streaming is treated as a perturbation. Consider the damping equation,

$$\left[\partial_\tau + \hat{\boldsymbol{\nu}}_R\right]\vec{\rho}(\tau) = 0\,. \tag{D.112}$$

with the associated propagator obeying,

$$\partial_\tau \mathcal{W}_{\tau,\tau_0} = -\hat{\boldsymbol{\nu}}_R\,\mathcal{W}_{\tau,\tau_0}\,. \tag{D.113}$$

The propagator has the simple form,

$$\mathcal{W}_{\tau,\tau_0} = e^{-\int_{\tau_0}^{\tau} d\tau'' \frac{1}{\tau_R}}\hat{I}\,. \tag{D.114}$$

We now define the streaming–picture field and operator as,

$$\vec{\rho}_S(\tau) = \mathcal{W}_{\tau,\tau_0}\vec{\rho}(\tau) \tag{D.115}$$

and operator,

$$\hat{\mathbf{L}}_S = \mathcal{W}_{\tau,\tau_0}\hat{\mathbf{L}}\mathcal{W}^{-1}_{\tau,\tau_0} \tag{D.116}$$

We then have the solution,

$$\left[\partial_\tau + \hat{\mathbf{L}}_S\right]\vec{\rho}_S = \partial_\tau\vec{\rho}_S \tag{D.117}$$

The corresponding free–streaming picture propagator is,

$$\hat{\mathcal{F}}_{\tau,\tau_0} = \mathcal{T}e^{-\int_{\tau_0}^{\tau} d\tau\hat{\mathbf{L}}_S} \tag{D.118}$$

which satisfies,

$$\partial_\tau\hat{\mathcal{F}}_{\tau,\tau_0} = -\hat{\mathbf{L}}_S\,\hat{\mathcal{F}}_{\tau,\tau_0} \tag{D.119}$$

The full solution can then be expressed as,

$$\vec{\rho}(\tau) = e^{-\xi_0}\hat{\mathcal{F}}_{\tau,\tau_0}\vec{\rho}(\tau_0) + \int_{\tau_0}^{\tau} d\tau' e^{-\xi'}\hat{\mathcal{F}}_{\tau,\tau'}\frac{\vec{\rho}^{\,\mathrm{eq}}(\tau')}{\tau_R} \tag{D.120}$$

Since ξ does not commute with $\hat{\mathcal{F}}\tau, \tau$', it cannot be treated as a simple scalar integration variable. Instead, we expand $\hat{\mathcal{F}}_{\tau,\tau'}\frac{\vec{\rho}^{\,\mathrm{eq}}(\tau')}{\tau_R}$ in a Taylor series,

$$\begin{aligned}\hat{\mathcal{F}}_{\tau,\tau'}\frac{\vec{\rho}^{\,\mathrm{eq}}(\tau')}{\tau_R} &= \sum_{n=0}^{\infty}\frac{(t-t')^n}{n!}\partial^n_{\tau'}\left(\hat{\mathcal{F}}_{\tau,\tau'}\frac{\vec{\rho}^{\,\mathrm{eq}}(\tau')}{\tau_R}\right)\Bigg|_{\tau'=\tau} \\ &= \sum_{n=0}^{\infty}\frac{(t-t')^n}{n!}\left[\partial_\tau + \hat{\mathbf{F}}\right]^n\frac{\vec{\rho}^{\,\mathrm{eq}}(\tau')}{\tau_R}\,.\end{aligned} \tag{D.121}$$

Define the function

$$g_n(\tau,\tau_0) = \int_{\tau_0}^{\tau} d\tau' e^{-\xi'}(t-t')^n \tag{D.122}$$

The hydrodynamic generator can then be expressed in terms of the gradients as,

$$\vec{\rho}^{G}(\tau) = \int_{\tau_0}^{\tau} d\tau' e^{-\xi'} \hat{\mathcal{F}}_{\tau,\tau'} \frac{\vec{\rho}^{\,\mathrm{eq}(\tau')}}{\tau_R} \tag{D.123}$$

$$= \sum_{n=0}^{\infty} \frac{g_n(\tau,\tau_0)}{n!} \left[\partial_\tau + \hat{\mathbf{F}}\right]^n \frac{\vec{\rho}^{\,\mathrm{eq}}(\tau')}{\tau_R} \,. \tag{D.124}$$

Although this expansion does not take exactly the same form as in the commuting case, it can still be reorganized in terms of gradient operators appearing in the gradient expansion, even though a compact closed-form expression remains out of reach. Note that

$$\left[\partial_\tau + \hat{\mathbf{F}}\right]^n \frac{\vec{\rho}^{\,\mathrm{eq}}(\tau')}{\tau_R} = (-1)^n \left[\frac{-\tau_R}{\tau_R}\left(\partial_\tau + \hat{\mathbf{F}}\right)\right]^n \frac{\vec{\rho}^{\,\mathrm{eq}}(\tau')}{\tau_R} \tag{D.125}$$

$$= \sum_{k=0}^{n} h_{n,k}(-\tau_R, \hat{\mathbf{D}}\tau_R) \left[\tau_R \hat{\mathbf{D}}\right]^n \vec{\rho}^{\,\mathrm{eq}} \tag{D.126}$$

where $h_{n,k}(\tau_R, \hat{\mathbf{D}})$ is a function of τ_R and its derivatives $\hat{\mathbf{D}}\tau_R$. We then get the copact expression,

$$\vec{\rho}^{G}(\tau) = \sum_{n=0}^{\infty} \frac{g_n(\tau,\tau_0)}{n!} \sum_{k=0}^{n} h_{n,k}(\tau_R, \hat{\mathbf{D}}\tau_R) \left[-\tau_R \hat{\mathbf{D}}\right]^k \vec{\rho}^{\,\mathrm{eq}} \tag{D.127}$$

$$= \sum_{n=0}^{\infty} \left(\sum_{k=n}^{\infty} \frac{g_k(\tau,\tau_0)}{n!} h_{k,n}(\tau_R, \hat{\mathbf{D}}\tau_R) \right) \left[-\tau_R \hat{\mathbf{D}}\right]^n \vec{\rho}^{\,\mathrm{eq}} \tag{D.128}$$